REGULATION OF ADIPOSE TISSUE FUNCTION AND METABOLIC HOMEOSTASIS

by

Guoxiao Wang

A dissertation submitted in partial fulfillment
of the requirements for the degree of
Doctor of Philosophy
(Cellular and Molecular Biology)
in the University of Michigan
2014

Doctoral committee:
Associate Professor Jiandie D. Lin, Chair
Associate Professor Peter Dempsey
Professor Ormond MacDougald
Professor Liangyou Rui
Professor Alan R. Saltiel

2014

DEDICATION

To my parents and my husband,
for their unconditional love

ACKNOWLEDGEMENTS

I would like to give special thanks to my mentor Jiandie Lin, who inspires confidence, enhances criticism and drives me forward. He bears all the virtues of a good mentor, always available to students despite the tremendous demands on his time. By actively doing research himself, he led us from the front and served as a role model. He has created a lab that is scientifically intense yet nurturing. He celebrates everybody's success and respects individual difference, allowing us to "smell the rose". I also would like to thank Siming Li, senior research staff in our lab, who has provided tremendous help from the start of my rotation and throughout my thesis research.

I want to thank all my labmates, for the help I receive and friendship I enjoy. Thank you Xuyun Zhao and Zhuoxian Meng for help on our collaborative projects. Thank you Zhimin Chen and Yuanyuan Xiao for sharing resources and ideas that moves my project forward. Thank you Zoharit Cozacov for being such a terrific technician. And thank you Qi Yu and Lin Wang for providing common reagents to allow the lab to run smoothly. I would also like to thank past lab members Di Ma and Matthew Molusky for sharing their experiences as senior graduate students. Thank Carlos Hernandez for advices on adipocyte related studies, and thank Fang Fang (as well as all the Lin lab members) for timely help during my pregnancy.

I would like to thank my thesis committee members Peter Dempsey, Ormond MacDougald, Liangyou Rui and Alan Saltiel, for giving me guidance, feedbacks and sharing reagents over the years, all those assistance are immeasurable!

I would like to acknowledge my collaborators Kaewon Cho, Maeran Uhm (in addition to those warm hugs and listening to my weal and woes), Chun-Rui Hu, Ji-Xin Cheng, Carey N. Lumeng, Matthias Kern, Arne Dietrich, Dequan Zhou, Adewole L. Okunade, Xiong Su, Matthias Blüher. I wouldn't be able to finish my thesis without any of you.

I would like to thank my friends in Ann Arbor especially Yue Shao, Chenxi Shen, Qi Xiao and Xiao-Wei Chen, for giving me rides, accompany me shopping and inviting me to dinner when my husband is not around. To Xiao-Wei, also thank you for sharing reagents and offering scientific advices which helped a lot in my thesis research.

I would also like to thank my CMB/LSI fellow graduate students, especially Elizabeth Adam, Sarah Kampert, Hanxiao Wang, Tamar Feinberg and Derek Jason, for making CMB such a nice program to stay and adding colors to the research life at LSI.

TABLE OF CONTENTS

LIST OF FIGURES

CHAPTER 1 INTRODUCTION

1. 1 Adipose tissues and their role in regulating metabolic homeostasis

Metabolic syndrome is emerging as a global epidemic. Approximately 1 in 4 or 5 adults, depending on the ethnic origin, has one or all of its characteristics (Grundy, 2008), such as abdominal obesity, insulin resistance/glucose intolerance, dyslipidemia, fatty liver, proinflammatory and prothrombotic state and increased risk for cardiovascular disease (Grundy et al., 2004). Adipose tissues play important roles in regulating metabolic homeostasis, and their dysfunction contributes significantly to the progression of metabolic diseases.

1.1.1 Different adipose tissues

In general, adipose tissues can be divided into three subtypes depending on their morphology and thermogenic function: white, brown and beige. White adipose tissues (WAT) contain unilocular adipocytes and mainly serve as a fuel storage depot. Rather than being an inert organ, it undergoes active lipid synthesis and lipolysis in response to different nutritional and hormonal signals. Excessive accumulation of WAT resulting from chronic overnutrition and reduced physical activity alters adipocyte function, leading to excess fatty acid release, increased production of inflammatory cytokines, and abnormal adipocyte hormone signaling. All of these contributes to obesity associated metabolic disorder.

Brown adipose tissue (BAT) contains multilocular, mitochondria-rich brown adipocytes. The high iron content in mitochondria and dense vasculature give the adipocyte a brownish color (Enerback, 2009). The main function of BAT is to generate heat. It is activated when environmental temperature is lower than the organism's thermoneutral point. This adaptive thermogenesis aims at producing heat for defense against cold, and is under the control of norepinephrine, released from sympathetic nerves (Klingenspor, 2003). Norepinephrine binds to adrenergic receptors and activates the cAMP signaling pathway, leading to transcriptional activation of UCP1, a mitochondria carrier protein specific to BAT. It discharges the proton gradient generated in oxidative phosphorylation and therefore uncouples the respiratory chain, allowing for robust fuel oxidation with a low rate of ATP production, thus dissipating most of the energy produced as heat (Cannon and Nedergaard, 2004). For decades, BAT in humans was thought to only exist in the newborn, yet recent discovery of brown fat in adult humans (Cypess et al., 2009; Nedergaard et al., 2007; van Marken Lichtenbelt et al., 2009; Virtanen et al., 2009) raises an intriguing possibility to tackle obesity-related metabolic disorders through activating its thermogenic function.

The third-type of adipocyte, recently identified and named beige/brite or inducible brown fat (Cypess et al., 2013; Jespersen et al., 2013; Petrovic et al., 2010; Wu et al., 2012), resembles white adipocyte at basal level characterized by a unilocular lipid droplet and low levels of UCP1 expression. However, upon activation (e.g. through norepinephrine released from sympathetic nerve terminal), beige adipocytes markedly activate UCP1 expression and transform into adipocytes with multilocular morphology.

1.1.2 Developmental origin and metabolic function of different adipocytes

Adipose tissue is a heterogeneous organ, with WAT scattered in different locations of the body and brown adipocytes residing in WAT (Sanchez-Gurmaches and Guertin, 2013). A certain degree of plasticity has also been found in adipose tissues using lineage tracing to mark the cold-induced beige adipocytes in inguinal WAT. In this study, researchers showed that the labeled cold induced beige adipocytes regained "WAT" characteristics in warmer temperature and the same white adipocytes can be reconverted to beige adipocytes upon subsequent cold challenge, thus demonstrating a bi-directional inter-conversion between beige and white adipocytes (Rosenwald et al., 2013). A couple of studies have identified cell surface markers which made it possible to isolate beige precursors in adult mice, examples are CD137, and platelet derived growth factor receptor alpha (PDGFRα). Precursor cells isolated based on these markers exhibit bi-potentiality in differentiation as they differentiate into white adipocytes at basal condition and become brown adipocytes under stimulations like Irisin or β3-adrenoceptor agonist (Lee et al., 2012; Uezumi et al., 2010; Wu et al., 2012).

Unlike beige adipocytes, the classical brown adipocytes seem to have a distinct developmental origin compared to white adipocytes, sharing the same mesenchymal progenitors with skeletal muscle, labeled positive for myf5 (Seale et al., 2008; Timmons et al., 2007). Although white adipocytes in the epididymal WAT mainly comes from $Myf5^-$ progenitors, white adipocytes from the interscapular and retroperitoneal WAT can also rise from $myf5^+$ precursors (Sanchez-Gurmaches et al., 2012).

The primary function of WAT is energy storage. In general, subcutaneous WAT plays an important role in buffering dietary lipid intake, and therefore protects other tissues from lipotoxicity. On the other hand, visceral fat is more lipolytically active, contributing more to plasma free fatty acid levels and strongly associates with metabolic disease (Bjorndal et al., 2011). In addition to that, WAT also functions as an endocrine organ secreting hormones and cytokines such as leptin and adiponectin to regulate feeding and metabolism (Galic et al., 2010; Ouchi et al., 2011; Waki and Tontonoz, 2007).

In contrast to WAT, BAT plays a catabolic role in metabolic regulation, it is not only activated during adaptive thermogenesis but also by high fat diet feeding, and oxidizes free fatty acids taken up from the plasma (Cannon and Nedergaard, 2004). BAT ablation through UCP1 promoter driven diphtheria toxin A expression resulted in marked obesity associated with insulin resistance in rodents (Hamann et al., 1998). Similar phenotype was observed in mice lacking all three β adrenergic receptors (Bachman et al., 2002). In humans, a negative correlation between BAT activity and BMI/body fat percentage has been observed (van Marken Lichtenbelt et al., 2009; Vijgen et al., 2011). And activation of BAT through cold acclimation has been shown to correct hypertriglyceridemia, increase energy expenditure and reduce adiposity (Bartelt et al., 2011; Yoneshiro et al., 2013). Because beige fat resembles classical brown fat upon activation, and the BAT in humans has similar gene expression signatures compared to beige fat rather than classical BAT (Wu et al., 2012), activating beige fat also provides a promising therapeutic to alleviate metabolic syndrome.

1.1.3 Adipose tissue inflammation in obesity related metabolic disease

Perhaps the earliest evidence suggesting obesity and diabetes as chronic low-grade inflammation comes from the fact that high doses of the anti-inflammatory drug salicylate (or Asprin) reduces blood glucose levels in people with type 2 diabetes (T2D) (Williamson, 1901). The mechanism was unclear until decades later, when Kopp et al. and colleagues discovered that salicylate improves insulin sensitivity through inhibiting the IKKβ/NFκB pathway (Kopp and Ghosh, 1994; Yin et al., 1998; Yuan et al., 2001). Activation of IKKβ/NFκB was found in insulin responsive tissues of obese individuals, and haploinsufficiency of IKKβ alone is able to greatly improve glycemic control in diabetic conditions (Hundal et al., 2002; Yuan et al., 2001). Moreover, epidemiology studies revealed that T2D associates with increased levels of markers and mediators of inflammation. Examples are fibrinogen, C-reactive protein, IL-6, plasminogen activator inhibitor, and TNFα (Shoelson et al., 2006). In experimental models, TNFα directly caused insulin resistance through impairing insulin receptor and insulin receptor substrate 1 (IRS1) phosphorylation (Feinstein et al., 1993), while its neutralization significantly increased peripheral tissue glucose uptake (Hotamisligil et al., 1993). Adipose tissues contribute significantly to plasma content of those inflammatory mediators due to the dramatic remodeling during obesity (Cildir et al., 2013; Tateya et al., 2013).

In addition to lipid filled mature adipocytes held together by a network of collagen fibers, adipose tissues also contain the stromal vascular cells, including preadipocytes, fibroblasts, endothelial cells and cells of the immune system such as leukocytes, macrophages and T cells. As obesity progresses, either induced by high fat diet or due to genetic mutations, large numbers of macrophages start to infiltrate the adipose tissue, which secretes proinflammatory cytokines.

These changes are known to occur even before a significant increase in circulating insulin level (Xu et al., 2003).

Macrophages can be categorized into two phenotypes depending on their responsiveness to inflammatory stimuli: classically activated (M1) macrophages and alternatively activated (M2) macrophages. M1 macrophages participates in destroying foreign organism and tumor cells, while M2 macrophages are thought to play an important role in scavenging debris, wound healing and angiogenesis (Ho and Sly, 2009; Lawrence and Natoli, 2011; Martinez et al., 2008). Pro-inflammatory mediators such as lipopolysaccharide (LPS), TNFα and IFN-γ leads to M1 macrophages activation, while IL-4/IL-13 leads to M2 polarization (Sica and Mantovani, 2012).

In 2007, Lumeng et al. discovered that in addition to increased macrophage number, the polarity of adipose tissue macrophages also changes during obesity progression (Lumeng et al., 2007a; Lumeng et al., 2008; Lumeng et al., 2007b). It is now believed that M2 macrophages contribute to maintain insulin sensitivity during the lean state, while M1 macrophages are recruited to obese adipose tissues to enhance insulin resistance through secretion of inflammatory cytokines. As such, drugs that block the effect of proinflammatory cytokines such RS504393, a CCL2 antagonist, and anakinra, a recombinant human IL-1R antagonist, greatly reduced systemic inflammation and improved glycemic control in obese/diabetic rodents/patients (Kang et al., 2010; Larsen et al., 2009; Larsen et al., 2007). Amlexanox, an inhibitor of the noncanonical IκB kinases IKK-ε and TBK1, also showed similar beneficial effect (Reilly et al., 2013).

Other than macrophages, higher number of T cells have also been found in adipose tissues from obese, insulin resistant mice than in the lean controls (Wu et al., 2007). And their composition undergoes significant change as obesity progress, with increased infiltration of $CD8^+$ cytotoxic T cells and decreased presence of regulatory T (Treg) cells (Nishimura et al., 2009). These changes precede infiltration of macrophages and it is now considered that IFNγ secreted from Type1 T helper cells triggers M1 activation (Sica and Mantovani, 2012), while in the lean state, Treg and type 2 T helper cells help to induce macrophage M2 polarization by expressing IL-4 and IL-13 (Martinez et al., 2008; Tateya et al., 2013; Tiemessen et al., 2007).

1.2. Adipose tissue as an endocrine organ

1.2.1 WAT as an endocrine organ

For centuries people believed that the central role of WAT was triglyceride storage during energy consumption and fatty acid release during starvation. It is after the discovery of leptin (Zhang et al., 1994) that people began to recognize WAT as an important endocrine organ. Leptin, product of the Ob gene, is almost exclusively expressed in mature adipocytes of the WAT (Fain et al., 2004). It functions by binding to the leptin receptor encoded by the Db gene that locates to a different chromosome (Tartaglia et al., 1995). Both leptin deficient ob/ob and the leptin receptor deficient db/db mice are characterized by severe obesity, hyperphagia, diabetes, reduced physical activity and infertility (Galic et al., 2010). These identical syndromes were later explained by parabiosis experiments (Coleman, 2010), suggesting the existence of a circulating hormone that is absent in the ob/ob mouse and present but ineffective in db/db mice. In 1995,

Tartaglia et al. analyzed leptin receptor expression profile and found that it is expressed in the brain, particularly hypothalamus, as well as several peripheral tissues such as kidney, lung, liver and skeletal muscle (Tartaglia et al., 1995). In the same year, Campfield et al. showed that leptin exerts its anorexigenic effect through directly acting on the central nerve system (Campfield et al., 1995). Using the Cre-Loxp system, researchers further mapped out POMC neurons of the arcuate nucleus and SF-1 positives neurons at ventromedial hypothalamus to be critical for leptin's action (Balthasar et al., 2004; Bingham et al., 2008; Dhillon et al., 2006). Although leptin administration in ob/ob mice is able to rapidly reverse obesity through reducing caloric intake and increasing basal metabolic rate (Harris et al., 1998), its application in treating human obesity remains in doubt, as serum levels of leptin positively correlates with percentage of body fat (Considine et al., 1996).

The classical leptin signaling pathway involves recruitment of receptor associated kinases of the Janus family, particularly JAK2, which then phosphorylates STAT3, resulting in their dimerization and nuclear translocation. In the hypothalamus, activated STAT3 dimers suppress orexigenic gene expression (Yang and Barouch, 2007). Other than STAT3, JAK2 phosphorylation also activates MAPK, AMPK and the PI3K pathway. Both impaired JAK2 signaling and reduced blood-brain leptin transfer accounts for leptin resistance observed in obese/diabetic individuals (Sahu, 2011; Yang and Barouch, 2007).

Besides leptin, another relatively well studied adipokine is adiponectin. Adiponectin is exclusively expressed in mature adipocytes from adipose tissue and its expression decreases in obese mice and humans (Hu et al., 1996). Adiponectin circulates in plasma as biochemically

distinct and stable multimers ranging from a high-molecular-weight (HMW) species to low molecular weight hexamers and trimmers (Schraw et al., 2008). The HMW complex is suggested as the most active form since its serum level is significantly lower in patients with coronary heart disease than control and increases during weight loss of obese people (Kobayashi et al., 2004). In mice, adiponectin deficiency leads to severe diet-induced insulin resistance (Maeda et al., 2002) while acute increase in circulating adiponectin levels by two fold significantly lowered hepatic glucose production (Combs et al., 2001). These effects seem to be AMPK dependent, as adiponectin is no longer able to suppress increased hepatic glucose output and glucose intolerance in mice with liver specific AMPK-α2 KO or adenovirus mediated dominant negative AMPK expression (Andreelli et al., 2006; Yamauchi et al., 2002). Again through AMPK, adiponectin stimulates fatty acid oxidation and glucose uptake in skeletal muscle (Yamauchi et al., 2002), and regulates energy expenditure through acting on the hypothalamus (Kubota et al., 2007). Interestingly, adiponectin also exerts AMPK-independent effect through activating receptor associated ceramidase and modulating plasma ceramide levels (Holland et al., 2011).

With the concept of adipose tissue as an endocrine organ becoming more and more prevalent, a cascade of adipokines has been identified, including resistin, the infusion of which leads to hyperglycemia largely by increasing hepatic glucose production (Banerjee et al., 2004), retinol binding protein-4 (RBP4), which induces liver PEPCK expression and impairs insulin signaling in muscle (Yang et al., 2005), and serum amyloid A, Zinc-α2-glycoprotein (ZAG), Apelin, Vaspin, etc. whose target tissues and underlining mechanism are less well defined but all showed association with metabolic disease progression, either having deleterious or beneficial effects (Leal Vde and Mafra, 2013). Moreover, adipose tissues from obese individuals produce

inflammatory cytokines such as TNFα, MCP1 and IL-6, these cytokines are also considered adipokines even though some of them are mainly secreted by infiltrated immune cells.

1.2.2 Endocrine role for BAT

Compared to WAT, role of BAT as an endocrine organ is poorly investigated. The main adipokines released by WAT, such as leptin and adiponectin, are only expressed in brown adipocytes under conditions of inactivity and atrophy, activation of BAT can decrease their expression down to undetectable levels (Cannon and Nedergaard, 2004). Yet observations that mice with genetic ablation of BAT developed much more severe metabolic disorders than merely knocking out UCP1 suggests that BAT is more than just a thermogenic organ for metabolite oxidation (Enerback et al., 1997; Hamann et al., 1996; Lowell et al., 1993). Thyroid hormone may be the only recognized "batokine" hitherto, as type II thyrosine 5'-deiodinase (Dio2) which converts thyrosine to triiodothyrosine (T3) is specifically expressed in BAT and strongly induced during BAT activation (Silva and Larsen, 1983), yet the fact that mice with targeted ablation of Dio2 suffered hypothermia during cold exposure despite normal plasma T3 levels indicated that active T3 generated from BAT functions more like an autocrine factor rather than an endocrine one (de Jesus et al., 2001). The most compelling evidence suggesting BAT may release endocrine signals comes from recent transplantation studies: Subcutaneous transplantation of embryonic BAT corrects Type1 Diabetes in streptozotocin treated mice, possibly due to increased serum levels of IGF-1 (Gunawardana and Piston, 2012). Transplantation of BAT also confers resistance to HFD induced obesity through enhanced sympathetic activity, although the potential endocrine factor that increases sympathetic drive in the recipient mice remains unknown (Zhu et al., 2013). In the same year Stanford et al. found that BAT transplantation

improved metabolic parameters in a “dose”-dependent manner, and such beneficial effect requires IL-6 expression from the BAT used for transplantation (Stanford et al., 2013). All these evidence indicates BAT may play an endocrine function yet exactly how the system works awaits further research.

1.3 STAT family and signaling

The signal transducer and activator of transcription (STAT) proteins family contains 7 members: STAT1, STAT2, STAT3, STAT4, STAT5a, STAT5b and STAT6, all of them participate in relaying signals downstream of cytokine receptors. In general, ligand binding to cytokine receptors triggers receptor dimerization, closing up the distance between receptor associated Janus kinases (JAK), thus enabling them to transphosphorylate each other. Activated JAK in turn phosphorylates carboxy-terminal tails of the receptors, providing docking sites for SH2 domain containing STAT proteins. Once docked on the receptor, STAT proteins undergo tyrosine phosphorylation by JAK and form antiparallel homo- or heterodimers before translocating into the nucleus, where they bind to specific enhancer sequences and induce target gene expression (Levy and Darnell, 2002).

JAK-STAT signaling is characterized by rapid onset and subsequent decay. Two protein-tyrosine phosphatases: SHP-2 and TC-PTP have been found to dephosphorylate STATs in the nucleus, resulting in their nuclear export (Schindler et al., 2007). In addition, activated STATs also induce expression of suppressors of cytokine signaling (SOCS), which bind to phosphorylated cytokine receptors at the STAT docking site and prevent further STAT activation. SOCS proteins can also recruit components of E3 ubiquitin ligases to phosphorylated JAKs, leading to their

polyubiquitination and subsequent proteasomal degradation (Alexander and Hilton, 2004). Each STAT protein has its distinctive C-terminal transcriptional activation domain (TAD) (Kisseleva et al., 2002), which determines the specificity of its target genes. Different STATs also display different preferences for upstream cytokine receptors.

Both STAT1 and STAT2 transduce signals from interferon (IFN) receptors, and their deficiency renders mice more susceptible to bacteria and virus infections, similar to the IFNγ knockout mice (Park et al., 2000; Schindler et al., 2007). An overwhelming body of literature has documented the proinflammatory nature of the IFNγ/STAT1 pathway, the activation of which induces expression of a variety of proinflammatory cytokines/mediators such as IL-12 (Ma et al., 1996), TNFα (Hayes et al., 1995), inducible nitric oxide synthase (iNOS) (Xie et al., 1993) and caspase-1 (Tamura et al., 1996). Moreover, synergistic activation of the proinflammatory transcription factor NFκB can also be induced by IFNγ and TNFα co-treatment (Cheshire and Baldwin, 1997). Accordingly, bioactivity of IFNγ/STAT1 has been involved in many inflammation associated pathologies such as ischemia, atherosclerosis and T2D (de Prati et al., 2005), whereas tissue inflammation can be substantially attenuated in their absence (Chen et al., 2001; Jaruga et al., 2004; O'Rourke et al., 2012; Rocha et al., 2008). In addition to its pro-inflammatory effect, STAT1 activation is also anti-proliferative, when treated with chemical carcinogens, both STAT1 and IFNγ receptor deficient mice developed tumors more rapidly and with greater frequency (Kaplan et al., 1998).

STAT3 transduces signals from the whole IL-6 family of cytokines as well as several growth factors such as granulocyte colony stimulating factor and epidermal growth factor. In contrast to STAT1, STAT3 activation is anti-inflammatory and pro-proliferative (Schindler et al., 2007). Overexpression of STAT3 promotes cell survival and inhibits apoptosis. In accordance with this, constitutively active STAT3 has been found in many types of human cancers and is required for transformation (Bromberg et al., 1999). Moreover, unlike the viable STAT1 and STAT2 knockout mice, STAT3 deficient mice die at E6.5-7.5, demonstrating its essential role in early embryogenesis (Takeda et al., 1997).

STAT4 directs the biological response to the IL-12 family of cytokines including IL-12, IL-23 and IL-27 (Hunter, 2005). STAT4 knockout mice phenolcopies IL-12 deficient mice, revealing that it is required for IL-12 stimulated differentiation of $CD4^+$ T helper1 lymphocytes (Gately et al., 1998; Kaplan et al., 1996b). Whereas STAT6 is required for IL-4/IL-13 dependent T helper2 lymphocyte differentiation (Kaplan et al., 1996a).

STAT5a and STAT5b are two genes localized to the same chromosome and encode proteins that are 96% identical (Kisseleva et al., 2002). Some redundancy in their function has been observed in regulating female ovarian development, as STAT5a/b double knockout results in female infertility while neither single knockout mice showed this defect (Teglund et al., 1998). Despite the structural similarity, STAT5a and STAT5b single knockout mice displayed quite distinct phenotypes: $STAT5a^{-/-}$ mice failed to lactate after parturition due to incomplete terminal differentiation of mammary gland, reminiscent the phenotype of prolactin receptor deficient mice

(Liu et al., 1997; Ormandy et al., 1997). Whereas STAT5b$^{-/-}$ mice are shorter and have reduced male specific liver gene expression, mimicking the growth hormone resistant phenotype in humans (Udy et al., 1997). Other than prolactin and growth hormone, STAT5a/b also transduces signals from the IL3 family and IL2 family of cytokines, as well as from erythropoietin and thrombopoietin (Kisseleva et al., 2002). Pertinent to the thesis, ErbB4 activation by neuregulins (see 1.4 for detail) which leads to STAT5a activation (Olayioye et al., 1999) is also required for mammary gland terminal differentiation, as ErbB4$^{-/-}$ mice rescued from heart defects through transgenic expression of ErbB4 under cardiac specific myosin promoter showed similar lactation defects to that observed in STAT5a$^{-/-}$ mice (Tidcombe et al., 2003).

1.4 Neuregulin-ErbB4 signaling

1.4.1 The Neuregulin family

Neuregulins (NRGs) are a family of proteins containing an epidermal growth factor (EGF)-like motif that distinguishes them from rest of the EGF family members. To date, four different neuregulin genes have been identified (Nrg1-4) with at least 3 of them showing multiple splicing isoforms and only those with EGF-like (EGFL) domain are biologically active (Buonanno and Fischbach, 2001; Hayes et al., 2007). The EGFL domain contains around 52 amino acids. It is characterized by 3 disulfide bonds formed between 6 cysteine residues whose relative positions are conserved within the neuregulin family. Neuregulins are often synthesized as transmembrane precursors, the EGFL domain locates extracellularly and N-terminal to the transmembrane domain (Figure 1.1 and (Guma et al., 2010)). Between the EGFL domain and the transmembrane domain is a cleavage site that can be recognized by the ADAM family of metalloproteases,

especially ADAM17/TACE and ADAM19 (Montero et al., 2000; Seals and Courtneidge, 2003). Cleavage results in shedding of the N terminal fragment that activates the ErbB family of membrane-associated tyrosine kinases.

NRGs are mainly expressed in cells of endothelial, mesenchymal and neuronal origin. Different NRGs play distinctive roles regulating growth, differentiation, survival and migration of cells in the epithelium (Wen et al., 1992), nerve system (Meyer and Birchmeier, 1995), cardiac (Zhao et al., 1998) and skeletal muscle (Florini et al., 1996), depending on their temporal and spatial expression patterns. NRG-1 is the most extensively studied neuregulin, it is expressed in both embryonic and adult brain, heart, as well as in liver, stomach, lung, kidney, spleen and skin (Wen et al., 1994). Pan NRG-1 knockout mice die midway through embryogenesis (E10.5) mainly due to defects in cardiac development (Meyer and Birchmeier, 1995). Other than that malformation of Schwann cells, cranial ganglia, sympathetic neurons and neuromuscular synapse also contribute to embryonic lethality (Britsch et al., 1998; Meyer and Birchmeier, 1995; Schmidt et al., 2011). NRG-2 is expressed mostly in central nervous system and heart (Buonanno and Fischbach, 2001), whereas NRG-3 expression is confined to the nervous system and embryonic mammary gland (Howard et al., 2005; Zhang et al., 1997). In contrast to NRG-1 deficient mice, NRG-2 mutant mice are viable and only displayed a mild phenotype, with early growth retardation and reduced reproductive capacity (Britto et al., 2004). NRG-3 has been shown to promote oligodendrocyte survival (Carteron et al., 2006) and regulate embryonic mammary differentiation (Kogata et al., 2013). Whether NRG-3 is absolutely required for these processes remains unknown. In 1999, Harari et al. identified NRG-4 and detected its expression in adult pancreas and skeletal muscle but not in neurons (Harari et al., 1999). Our group revisited this

issue through quantitative PCR (qPCR) and found that NRG-4 is highly enriched in BAT, with WAT being the 2nd largest reservoir, but low elsewhere (Figure3.1B). Pro-NRG-4 consists of 115 amino acids. Like other neuregulins, it has an extracellular EGFL domain N terminal to the transmembrane region, yet it does not have an N-terminal Ig-G like domain and its cytoplasmic tail is significantly shortened (Figure 1.1 and (Buonanno and Fischbach, 2001; Harari et al., 1999)). As predicted, NRG-4 is a secreted protein and the broad-spectrum matrix metalloprotease inhibitor GM6001 significantly inhibited shedding of its EGFL domain (Hayes et al., 2008).

1.4.2 ErbB family and signaling

The ErbB receptor tyrosine kinase (RTK) family consists of four cell surface receptors: ErbB1 (EGFR), ErbB2, ErbB3 and ErbB4. They were named as such (v-erb-b2 avian erythroblastic leukemia viral oncogene homology 1/2/3/4) due to their high homology to the oncogenic protein kinase v-ERBB, an aberrant form of human EGFR encoded by the avian erythroblastosis virus (Yarden and Sliwkowski, 2001).

All four ErbBs are single transmembrane (TM) proteins with the TM domain separating equal sized extra- and cytoplasmic domain. The extracellular domain contains two highly conserved cysteine-rich regions flanked by two leucine-rich domains that are responsible for ligand interaction. The cytoplasmic domain contains a juxtamembrane region, a tyrosine kinase domain and a carboxyterminal domain (Wieduwilt and Moasser, 2008). Activation of the ErbB RTK is initiated by binding of a ligand to the extracellular regions of these receptors, which causes receptor dimerization and transduces the signal to the intracellular region. The cytoplasmic

tyrosine kinase domain then phosphorylates several tyrosine residues in the C-terminal tail of the receptor, which recruits PTB and SH2 domain containing adaptor proteins such as Shc, Src, Grb2, JAK and the p85 subunit of PI-3 kinase (Bose and Zhang, 2009; Yarden and Sliwkowski, 2001). Interaction with Shc predicts activation of the MAPK pathway, PI-3K recruitment leads to Akt phosphorylation and increased cell survival, while activation of the JAK/STAT pathway results in transcriptional regulation (Figure 1.2).

ErbB2 and ErbB3 are two exceptions with regard to their molecular structures within the ErbB RTK family. ErbB3 lacks observable intrinsic kinase activity due to mutations in its tyrosine kinase domain (Guy et al., 1994), whereas ErbB2 doesn't bind to any known ligand (Klapper et al., 1999). Consequently, neither ErbB2 nor ErbB3 alone supports linear signaling and heterodimerization with each other or with other ErbB family receptors is required for their activation. In fact, ErbB2 is a preferred dimerization partner when cotransfected with any other ErbBs and the ErbB2 containing heterodimer prolongs and enhances downstream signaling and outputs when compared to the respective ErbB homodimers (Yarden and Sliwkowski, 2001).

Besides ligand-mediated receptor dimerization and relaying of phosphorylation signals, the ErbB receptors can also be cleaved by different proteases either shedding the dominant-negative extra-cellular domain (Ghedini et al., 2010), or setting free the cytoplasmic fragment that translocates into the nucleus and functions as a transcription cofactor (Ni et al., 2001). Take ErbB4 as an example, its extracellular domain can be cleaved by metalloproteases, producing a 100 kDa shed fragment and a membrane-anchored 80 kDa fragment (Vecchi and Carpenter, 1997; Zhou and

Carpenter, 2000). This 80 kDa fragment is cleaved further by γ-secretase to liberate the cytoplasmic domain (Ni et al., 2001), which subsequently translocates into the nucleus and has been shown to potentiate STAT5 induced gene expression (Williams et al., 2004).

Ligands of the ErbB family receptors are polypeptides with a consensus EGFL domain. Specific ErbB receptors have their preferential ligands depending on affinity and dimerization partners and one ligand may selectively bind to only 1 or 2 of the ErbB receptors (Figure 1.3). For instance, EGF only binds to ErbB1, while heparin binding EGFL growth factor (HB-EGF) binds to both ErbB1 and EbB4. In the case of neuregulin, ErbB3 and ErbB4 are the direct receptors while ErbB1 and ErbB2 function as coreceptors as they do not bind to neuregulins on their own (Burden and Yarden, 1997). Specific binding between NRGs and the ErbB receptors are also reflected by the phenotype of their respective knockout mice. Like the NRG-1 null mice, whole body ErbB4 and ErbB2 deficiency also led to embryonic lethality at E10.5 due to heart trabeculation failure while ErbB3 knockout mice die from abnormal endocardial cushion at E13.5 (Gassmann et al., 1995; Guma et al., 2010), indicating NRG-1 signaling through ErbB4/ErbB2 dimer is critical for embryonic heart development.

1.4.3 Metabolic functions of ErbBs and their ligands

Other than affecting neuronal and cardiovascular development, ErbB receptors and their ligands are also involved in metabolic regulation. First of all, recombinant NRG-1 isoform heregulin-β1 dose and time dependently stimulated glucose uptake both in L6E9 muscle cells and in *ex vivo* cultured soleus muscle (Suarez et al., 2001). In a chronic setting, picomolars of heregulin-β1 that

are non-myogenic was shown to increase skeletal muscle mitochondria biogenesis through activating PGC-1α and PPARδ. Insulin sensitivity was also improved through enhanced Glut4 expression (Canto et al., 2007). In 2003, Lebrasseur et al. noticed that muscle contraction activated all NRG receptors and induced expression of multiple NRGs (Lebrasseur et al., 2003). Muscle contraction activates ErbB4 through Ca^{2+} induced cleavage of NRG-1 and increases Glut4 translocation; as such, blockage of ErbB4 signaling significantly impaired contraction coupled muscle glucose uptake (Canto et al., 2006). On the whole organism level, muscle specific overexpression of heparin-binding EGF like growth factor (HB-EGF), a known ligand of ErbB4 (Elenius et al., 1997), protected mice from diet induced obesity and improved insulin sensitivity through activating the PI3K-Akt pathway (Fukatsu et al., 2009).

Besides muscle, two other vital metabolic organs are adipose tissue and liver. While ErbB3 and ErbB4 are undetectable in adipocytes, ErbB1 and ErbB2 have been found to decrease during 3T3-L1 adipocyte differentiation (Pagano and Calvo, 2003) and in one study ErbB1 abundance dropped in adipose tissues of insulin resistant/diabetic women (Rogers et al., 2012). As for liver, ErbB1 and ErbB3 dominate from embryonic day 19 and throughout adulthood. ErbB2 is expressed in embryonic liver and in neonatal mice, but virtually disappears after p21, whereas ErbB4 is only detected in trace amount by some authors including our group (Carver et al., 2002). The ErbB1 ligand EGF has been shown to regulate both basal and glucagon induced gluconeogenesis in isolated hepatocytes depending on the redox state of the substrate, suppressing it when the main substrate is lactate, and enhancing it when the main substrate is pyruvate (Soler et al., 1991).

Both ErbB1 and ErbB3 displayed circadian variation in protein expression in adult liver, with the latter exhibiting a larger amplitude (Carver et al., 2002). In addition to that, insulin significantly suppressed ErbB3 expression and impaired its binding to NRG-1β in cultured hepatocytes in a PI3K dependent manner, as two PI3K inhibitors, wortmannin and LY294002, completely relieved those inhibitory effects (Carver et al., 1996; K et al., 1997). The inhibition of ErbB3 expression by insulin correlated with its rhythmic expression pattern, reaching nadir at 8:00a.m, when plasma insulin is highest in postprandial mice, and peaking at 8:00p.m when the starved mice just started to eat (Carver et al., 2002).

1.5 Regulation of hepatic lipid metabolism

Non-alcoholic fatty liver disease (NAFLD) is currently the most common form of chronic liver disease and is strongly associated with obesity, type 2 diabetes and insulin resistance. The prevalence of US-defined NAFLD (5.5% or more fat in the liver) in the general population ranges from 9.3 to 29% in Asia, 16% in Mexico, 23% in Italy, 30% in Israel and 31% in the United States (Lazo and Clark, 2008). Moreover, a much higher prevalence of NAFLD has been found among people with type 2 diabetes, ranging from 40% to 69.5% (Lazo and Clark, 2008). NAFLD is caused by an imbalance between liver lipid availability and disposal. Dietary fat from the intestine, non-esterified fatty acids (NEFA) released from adipose tissue, and *de novo* lipogenesis in the liver are three main contributors to liver lipid content. While fatty acid β-oxidation, and very low density lipoprotein (VLDL) secretion are the two ways liver clears up its triglyceride content (Lavoie and Gauthier, 2006). Pertinent to the thesis, the following sections will focus on *de novo* lipogenesis, which contributes to 26% of liver fat (Ferre and Foufelle, 2010).

De novo lipogenesis is the enzymatic pathway for converting dietary carbohydrate into fat. It starts with citrate, the intermediate metabolite in tricarboxylic acid cycle generated in mitochondria. After being transported into cytosol, citrate is converted into Acetyl-CoA by ATP citrate lyase (ACL). Through the action of acetyl-CoA carboxylase (ACC), acetyl-CoA is converted into malonyl-CoA, which is converted further into NEFA by fatty acid synthase (FASN). Fatty acids generated in this way are saturated, yet through the action of stearoyl-CoA desaturase 1 (SCD1), monounsaturated fatty acids are made. These saturated and unsaturated fatty acids are then esterified with glycerol-3 phosphate to form triglycerides catalyzed by enzymes such as GPAT and DGAT (Ferre and Foufelle, 2007).

Full activation of abovementioned lipogenic enzymes requires both high insulin and high glucose concentrations, and a number of studies have shown that insulin action on this family of genes is mediated by a transcription factor called sterol regulatory element binding protein-1c (SREBP1c), while the effect of glucose on lipogenic gene expression is shown to be mediated through carbohydrate response element binding protein (CHREBP) (Ferre and Foufelle, 2007).

To date, three SREBP isoforms have been identified and characterized: SREBP1a, SREBP1c and SREBP2 (Jeon and Osborne, 2012). SREBP1a and 1c are transcribed from the same gene but by a different promoter. Whereas SREBP1a and SREBP2 tend to regulate cholesterol biosynthesis, SREBP1c has a greater role in regulating fatty acid synthesis than cholesterol synthesis (Horton et al., 1998; Shimano et al., 1997a; Shimano et al., 1999).

SREBP1c is synthesized as a precursor embedded in the endoplasmic reticulum (ER), where it interacts with SREBP cleavage-activating protein (SCAP), SCAP again interacts with insulin induced gene (INSIG), which sequesters the whole complex in the ER. Insulin not only leads to transcriptional increase of SREBP1c precursor expression, but also dissociates SCAP from INSIG, resulting in Golgi transfer of the SREBP1c-SCAP complex. Inside Golgi apparatus, SREBP1c undergoes double cleavage by the proteases S1P and S2P, and the resulting mature protein translocates into the nucleus to carry out transcriptional regulation function (Ferre and Foufelle, 2010).

Other than insulin, SREBP1c is also regulated by liver X receptors (LXR). LXR belongs to the nuclear hormone receptor superfamily, its endogenous ligands are oxysterols and it obligately dimerize with retinoid X receptors (RXR) to regulate transcriptional activation of target genes, through binding to their LXR-element (LXRE), which has been found in the 5' flanking region of SREBP1c (Repa et al., 2000). Both LXR agonist T0901317 and RXR agonist LG268 significantly induced liver SREBP1c expression as well as nuclear translocation, while in mice lacking LXR, liver expression of SREBP1c and its target lipogenic genes are significantly decreased (Repa et al., 2000; Schultz et al., 2000).

Through promoting fatty acid synthesis and lipid deposition, SREBP1c has been implicated in the development of metabolic disorders such as insulin resistance and type 2 diabetes. Loss of function studies on SREBP1c is relatively limited since SREBP1c knockout mice only showed modest phenotype due to compensatory increase of SREBP1a and SREBP2 (Liang et al., 2002), and knock-out of both SREBP1c and SREBP1a is virtually lethal (Shimano et al., 1997b).

However, bypassing the compensation issue of SREBP1c single KO and lethality of SREBP1c/1a double KO, Tang et al. found that a small molecule inhibitor of SREBP1c called betulin significantly improved hyperglycemia and insulin resistance (Tang et al., 2011). Following her study Moon et al. found that SCAP deletion, which significantly decreased expression levels of all SREBPs, rescued fatty liver phenotype in the leptin deficient ob/ob mice (Moon et al., 2012). On the other hand, liver steatosis resulting from increased SREBP1c expression has been found in both genetic and diet induced insulin resistant mouse models (Ferre and Foufelle, 2007). And liver specific SREBP1c overexpression alone, leads to increased hepatic triglyceride content and hyperinsulinemia (Knebel et al., 2012). All these evidences suggest that NAFLD, associated with increased SREBP1c expression, contributes to insulin resistance.

Figure 1.1 Neuregulin (NRG) structure
NRG gene products share a characteristic signature for the epidermal growth factor (EGF) domain, which is located in the extracellular region that differentiates this subfamily from other members of the EGF family. NRG-1 isoforms have been classified in types I–VI on the basis of differences in the N-terminal distal region. NRG3 and NRG4 are the two simplest NRGs that do not contain the N-terminal IgG like domain. Many of the NRGs are glycosylated extracellularly and red arrow designates the potential metalloprotease cleavage site.

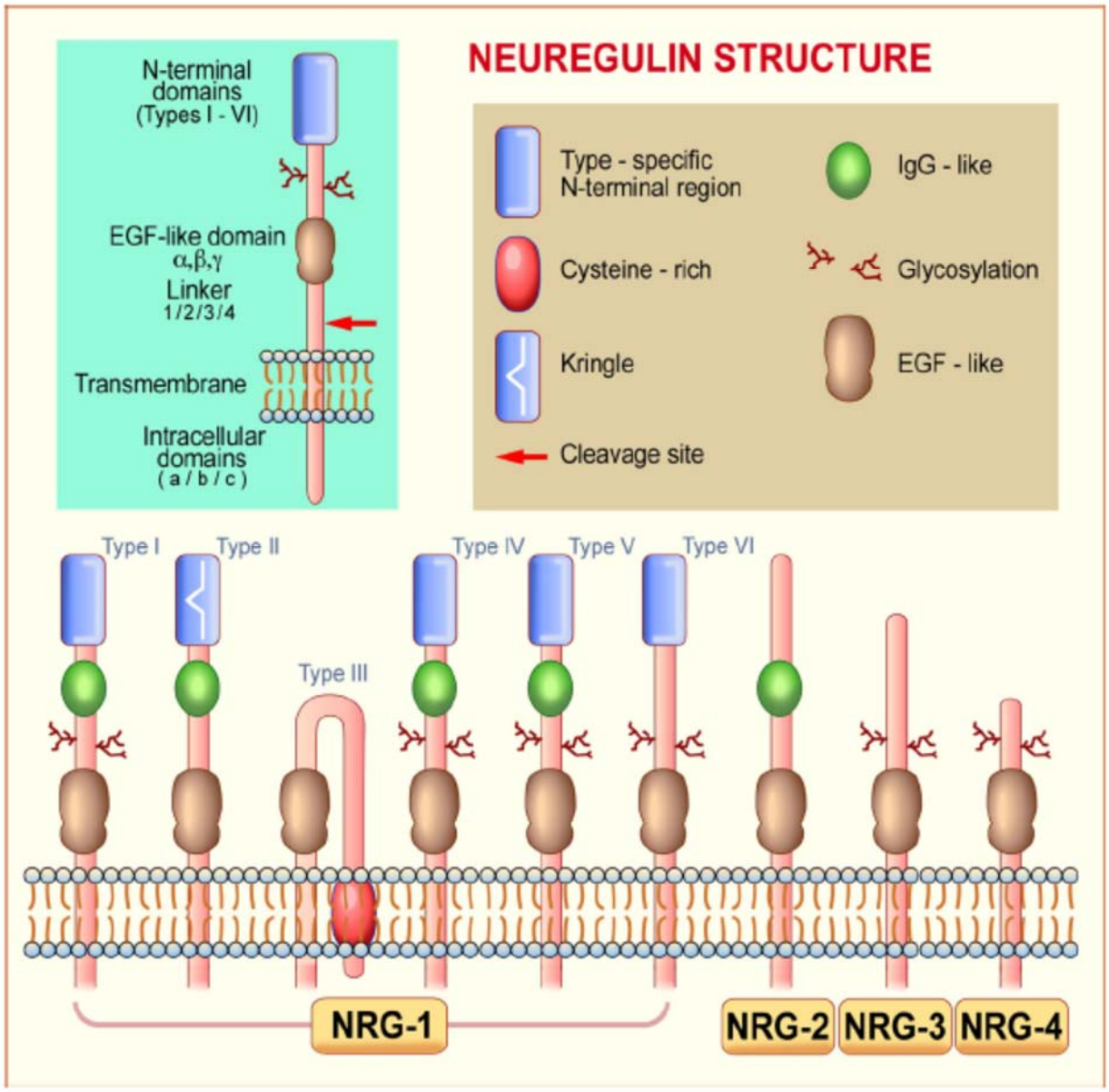

(© Guma et al. 2009)

Figure 1.2 ErbB signaling network
Ligand induced ErbB receptor dimerization leads to tyrosine phosphorylation at the C-terminals of the receptors, thus providing docking site for SH2 and PTB domain containing proteins such as PI3K, Shc and STAT5. Activation of these proteins relays signals downstream, resulting in Akt, MAPK activation and STAT5 target gene expression, respectively.

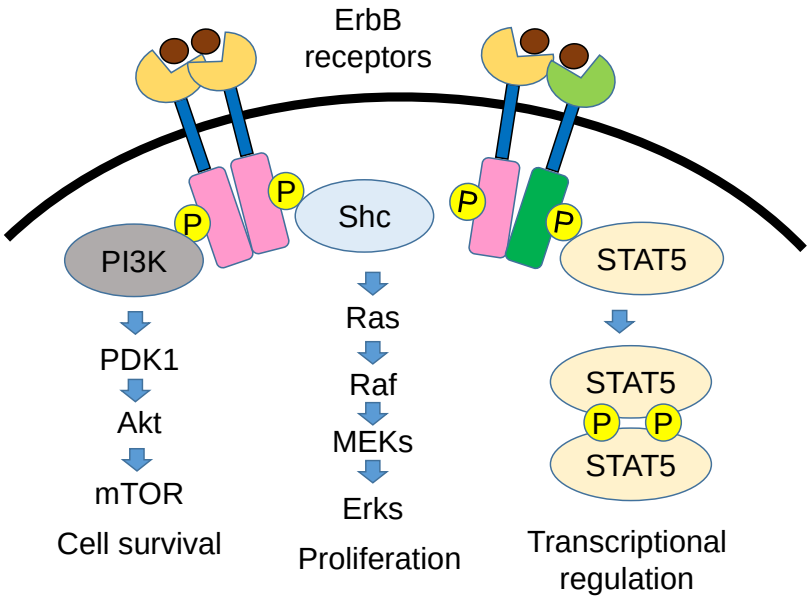

Figure 1.3 ErbB receptors and ligand specificity
Ligands that bind to individual ErbB receptors are listed above each receptor. ErbB2 is an orphan receptor while ErbB3 lacks intrinsic kinase activity.

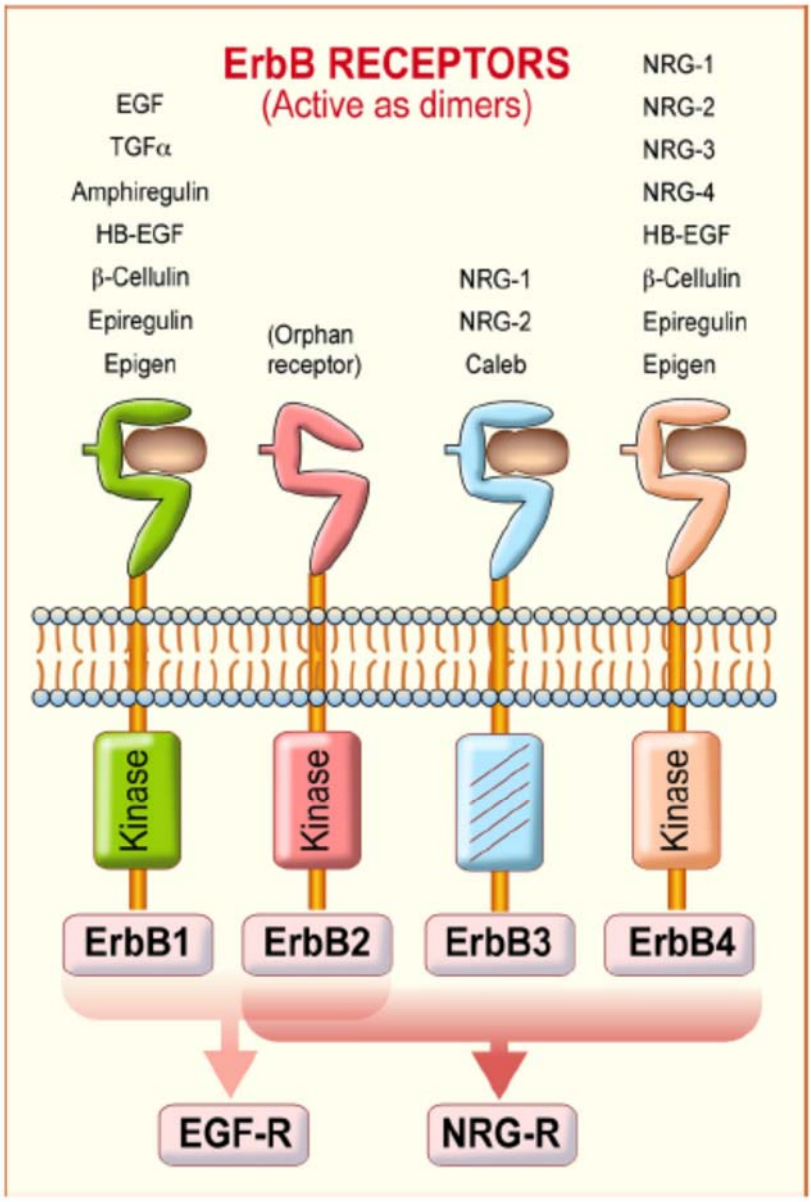

(© Guma et al. 2009)

1.6 References

Alexander, W.S., and Hilton, D.J. (2004). The role of suppressors of cytokine signaling (SOCS) proteins in regulation of the immune response. Annu Rev Immunol *22*, 503-529.

Andreelli, F., Foretz, M., Knauf, C., Cani, P.D., Perrin, C., Iglesias, M.A., Pillot, B., Bado, A., Tronche, F., Mithieux, G., *et al.* (2006). Liver adenosine monophosphate-activated kinase-alpha2 catalytic subunit is a key target for the control of hepatic glucose production by adiponectin and leptin but not insulin. Endocrinology *147*, 2432-2441.

Bachman, E.S., Dhillon, H., Zhang, C.Y., Cinti, S., Bianco, A.C., Kobilka, B.K., and Lowell, B.B. (2002). betaAR signaling required for diet-induced thermogenesis and obesity resistance. Science *297*, 843-845.

Balthasar, N., Coppari, R., McMinn, J., Liu, S.M., Lee, C.E., Tang, V., Kenny, C.D., McGovern, R.A., Chua, S.C., Jr., Elmquist, J.K., *et al.* (2004). Leptin receptor signaling in POMC neurons is required for normal body weight homeostasis. Neuron *42*, 983-991.

Banerjee, R.R., Rangwala, S.M., Shapiro, J.S., Rich, A.S., Rhoades, B., Qi, Y., Wang, J., Rajala, M.W., Pocai, A., Scherer, P.E., *et al.* (2004). Regulation of fasted blood glucose by resistin. Science *303*, 1195-1198.

Bartelt, A., Bruns, O.T., Reimer, R., Hohenberg, H., Ittrich, H., Peldschus, K., Kaul, M.G., Tromsdorf, U.I., Weller, H., Waurisch, C., *et al.* (2011). Brown adipose tissue activity controls triglyceride clearance. Nat Med *17*, 200-205.

Bingham, N.C., Anderson, K.K., Reuter, A.L., Stallings, N.R., and Parker, K.L. (2008). Selective loss of leptin receptors in the ventromedial hypothalamic nucleus results in increased adiposity and a metabolic syndrome. Endocrinology *149*, 2138-2148.

Bjorndal, B., Burri, L., Staalesen, V., Skorve, J., and Berge, R.K. (2011). Different adipose depots: their role in the development of metabolic syndrome and mitochondrial response to hypolipidemic agents. J Obes *2011*, 490650.

Bose, R., and Zhang, X. (2009). The ErbB kinase domain: structural perspectives into kinase activation and inhibition. Exp Cell Res *315*, 649-658.

Britsch, S., Li, L., Kirchhoff, S., Theuring, F., Brinkmann, V., Birchmeier, C., and Riethmacher, D. (1998). The ErbB2 and ErbB3 receptors and their ligand, neuregulin-1, are essential for development of the sympathetic nervous system. Genes Dev *12*, 1825-1836.

Britto, J.M., Lukehurst, S., Weller, R., Fraser, C., Qiu, Y., Hertzog, P., and Busfield, S.J. (2004). Generation and characterization of neuregulin-2-deficient mice. Mol Cell Biol *24*, 8221-8226.

Bromberg, J.F., Wrzeszczynska, M.H., Devgan, G., Zhao, Y., Pestell, R.G., Albanese, C., and Darnell, J.E., Jr. (1999). Stat3 as an oncogene. Cell *98*, 295-303.

Buonanno, A., and Fischbach, G.D. (2001). Neuregulin and ErbB receptor signaling pathways in the nervous system. Curr Opin Neurobiol *11*, 287-296.

Burden, S., and Yarden, Y. (1997). Neuregulins and their receptors: a versatile signaling module in organogenesis and oncogenesis. Neuron *18*, 847-855.

Campfield, L.A., Smith, F.J., Guisez, Y., Devos, R., and Burn, P. (1995). Recombinant mouse OB protein: evidence for a peripheral signal linking adiposity and central neural networks. Science *269*, 546-549.

Cannon, B., and Nedergaard, J. (2004). Brown adipose tissue: function and physiological significance. Physiol Rev *84*, 277-359.

Canto, C., Chibalin, A.V., Barnes, B.R., Glund, S., Suarez, E., Ryder, J.W., Palacin, M., Zierath, J.R., Zorzano, A., and Guma, A. (2006). Neuregulins mediate calcium-induced glucose transport during muscle contraction. J Biol Chem *281*, 21690-21697.

Canto, C., Pich, S., Paz, J.C., Sanches, R., Martinez, V., Orpinell, M., Palacin, M., Zorzano, A., and Guma, A. (2007). Neuregulins increase mitochondrial oxidative capacity and insulin sensitivity in skeletal muscle cells. Diabetes *56*, 2185-2193.

Carteron, C., Ferrer-Montiel, A., and Cabedo, H. (2006). Characterization of a neural-specific splicing form of the human neuregulin 3 gene involved in oligodendrocyte survival. J Cell Sci *119*, 898-909.

Carver, R.S., Sliwkowski, M.X., Sitaric, S., and Russell, W.E. (1996). Insulin regulates heregulin binding and ErbB3 expression in rat hepatocytes. J Biol Chem *271*, 13491-13496.

Carver, R.S., Stevenson, M.C., Scheving, L.A., and Russell, W.E. (2002). Diverse expression of ErbB receptor proteins during rat liver development and regeneration. Gastroenterology *123*, 2017-2027.

Chen, E.S., Greenlee, B.M., Wills-Karp, M., and Moller, D.R. (2001). Attenuation of lung inflammation and fibrosis in interferon-gamma-deficient mice after intratracheal bleomycin. Am J Respir Cell Mol Biol *24*, 545-555.

Cheshire, J.L., and Baldwin, A.S., Jr. (1997). Synergistic activation of NF-kappaB by tumor necrosis factor alpha and gamma interferon via enhanced I kappaB alpha degradation and de novo I kappaBbeta degradation. Mol Cell Biol *17*, 6746-6754.

Cildir, G., Akincilar, S.C., and Tergaonkar, V. (2013). Chronic adipose tissue inflammation: all immune cells on the stage. Trends Mol Med *19*, 487-500.

Coleman, D.L. (2010). A historical perspective on leptin. Nat Med *16*, 1097-1099.

Combs, T.P., Berg, A.H., Obici, S., Scherer, P.E., and Rossetti, L. (2001). Endogenous glucose production is inhibited by the adipose-derived protein Acrp30. J Clin Invest *108*, 1875-1881.

Considine, R.V., Sinha, M.K., Heiman, M.L., Kriauciunas, A., Stephens, T.W., Nyce, M.R., Ohannesian, J.P., Marco, C.C., McKee, L.J., Bauer, T.L., *et al.* (1996). Serum immunoreactive-leptin concentrations in normal-weight and obese humans. N Engl J Med *334*, 292-295.

Cypess, A.M., Lehman, S., Williams, G., Tal, I., Rodman, D., Goldfine, A.B., Kuo, F.C., Palmer, E.L., Tseng, Y.H., Doria, A., *et al.* (2009). Identification and importance of brown adipose tissue in adult humans. N Engl J Med *360*, 1509-1517.

Cypess, A.M., White, A.P., Vernochet, C., Schulz, T.J., Xue, R., Sass, C.A., Huang, T.L., Roberts-Toler, C., Weiner, L.S., Sze, C., *et al.* (2013). Anatomical localization, gene expression profiling and functional characterization of adult human neck brown fat. Nat Med *19*, 635-639.

de Jesus, L.A., Carvalho, S.D., Ribeiro, M.O., Schneider, M., Kim, S.W., Harney, J.W., Larsen, P.R., and Bianco, A.C. (2001). The type 2 iodothyronine deiodinase is essential for adaptive thermogenesis in brown adipose tissue. J Clin Invest *108*, 1379-1385.

de Prati, A.C., Ciampa, A.R., Cavalieri, E., Zaffini, R., Darra, E., Menegazzi, M., Suzuki, H., and Mariotto, S. (2005). STAT1 as a new molecular target of anti-inflammatory treatment. Curr Med Chem *12*, 1819-1828.

Dhillon, H., Zigman, J.M., Ye, C., Lee, C.E., McGovern, R.A., Tang, V., Kenny, C.D., Christiansen, L.M., White, R.D., Edelstein, E.A., *et al.* (2006). Leptin directly activates SF1 neurons in the VMH, and this action by leptin is required for normal body-weight homeostasis. Neuron *49*, 191-203.

Elenius, K., Paul, S., Allison, G., Sun, J., and Klagsbrun, M. (1997). Activation of HER4 by heparin-binding EGF-like growth factor stimulates chemotaxis but not proliferation. EMBO J *16*, 1268-1278.

Enerback, S. (2009). The origins of brown adipose tissue. N Engl J Med *360*, 2021-2023.

Enerback, S., Jacobsson, A., Simpson, E.M., Guerra, C., Yamashita, H., Harper, M.E., and Kozak, L.P. (1997). Mice lacking mitochondrial uncoupling protein are cold-sensitive but not obese. Nature *387*, 90-94.

Fain, J.N., Madan, A.K., Hiler, M.L., Cheema, P., and Bahouth, S.W. (2004). Comparison of the release of adipokines by adipose tissue, adipose tissue matrix, and adipocytes from visceral and subcutaneous abdominal adipose tissues of obese humans. Endocrinology *145*, 2273-2282.

Feinstein, R., Kanety, H., Papa, M.Z., Lunenfeld, B., and Karasik, A. (1993). Tumor necrosis factor-alpha suppresses insulin-induced tyrosine phosphorylation of insulin receptor and its substrates. J Biol Chem *268*, 26055-26058.

Ferre, P., and Foufelle, F. (2007). SREBP-1c transcription factor and lipid homeostasis: clinical perspective. Horm Res *68*, 72-82.

Ferre, P., and Foufelle, F. (2010). Hepatic steatosis: a role for de novo lipogenesis and the transcription factor SREBP-1c. Diabetes Obes Metab *12 Suppl 2*, 83-92.

Florini, J.R., Samuel, D.S., Ewton, D.Z., Kirk, C., and Sklar, R.M. (1996). Stimulation of myogenic differentiation by a neuregulin, glial growth factor 2. Are neuregulins the long-sought muscle trophic factors secreted by nerves? J Biol Chem *271*, 12699-12702.

Fukatsu, Y., Noguchi, T., Hosooka, T., Ogura, T., Kotani, K., Abe, T., Shibakusa, T., Inoue, K., Sakai, M., Tobimatsu, K., *et al.* (2009). Muscle-specific overexpression of heparin-binding epidermal growth factor-like growth factor increases peripheral glucose disposal and insulin sensitivity. Endocrinology *150*, 2683-2691.

Galic, S., Oakhill, J.S., and Steinberg, G.R. (2010). Adipose tissue as an endocrine organ. Mol Cell Endocrinol *316*, 129-139.

Gassmann, M., Casagranda, F., Orioli, D., Simon, H., Lai, C., Klein, R., and Lemke, G. (1995). Aberrant neural and cardiac development in mice lacking the ErbB4 neuregulin receptor. Nature *378*, 390-394.

Gately, M.K., Renzetti, L.M., Magram, J., Stern, A.S., Adorini, L., Gubler, U., and Presky, D.H. (1998). The interleukin-12/interleukin-12-receptor system: role in normal and pathologic immune responses. Annu Rev Immunol *16*, 495-521.

Ghedini, G.C., Ciravolo, V., Tortoreto, M., Giuffre, S., Bianchi, F., Campiglio, M., Mortarino, M., Figini, M., Coliva, A., Carcangiu, M.L., *et al.* (2010). Shed HER2 extracellular domain in HER2-mediated tumor growth and in trastuzumab susceptibility. J Cell Physiol *225*, 256-265.

Grundy, S.M. (2008). Metabolic syndrome pandemic. Arterioscler Thromb Vasc Biol *28*, 629-636.

Grundy, S.M., Brewer, H.B., Jr., Cleeman, J.I., Smith, S.C., Jr., and Lenfant, C. (2004). Definition of metabolic syndrome: Report of the National Heart, Lung, and Blood

Institute/American Heart Association conference on scientific issues related to definition. Circulation *109*, 433-438.

Guma, A., Martinez-Redondo, V., Lopez-Soldado, I., Canto, C., and Zorzano, A. (2010). Emerging role of neuregulin as a modulator of muscle metabolism. Am J Physiol Endocrinol Metab *298*, E742-750.

Gunawardana, S.C., and Piston, D.W. (2012). Reversal of type 1 diabetes in mice by brown adipose tissue transplant. Diabetes *61*, 674-682.

Guy, P.M., Platko, J.V., Cantley, L.C., Cerione, R.A., and Carraway, K.L., 3rd (1994). Insect cell-expressed p180erbB3 possesses an impaired tyrosine kinase activity. Proc Natl Acad Sci U S A *91*, 8132-8136.

Hamann, A., Flier, J.S., and Lowell, B.B. (1996). Decreased brown fat markedly enhances susceptibility to diet-induced obesity, diabetes, and hyperlipidemia. Endocrinology *137*, 21-29.

Hamann, A., Flier, J.S., and Lowell, B.B. (1998). Obesity after genetic ablation of brown adipose tissue. Z Ernahrungswiss *37 Suppl 1*, 1-7.

Harari, D., Tzahar, E., Romano, J., Shelly, M., Pierce, J.H., Andrews, G.C., and Yarden, Y. (1999). Neuregulin-4: a novel growth factor that acts through the ErbB-4 receptor tyrosine kinase. Oncogene *18*, 2681-2689.

Harris, R.B., Zhou, J., Redmann, S.M., Jr., Smagin, G.N., Smith, S.R., Rodgers, E., and Zachwieja, J.J. (1998). A leptin dose-response study in obese (ob/ob) and lean (+/?) mice. Endocrinology *139*, 8-19.

Hayes, M.P., Freeman, S.L., and Donnelly, R.P. (1995). IFN-gamma priming of monocytes enhances LPS-induced TNF production by augmenting both transcription and MRNA stability. Cytokine *7*, 427-435.

Hayes, N.V., Blackburn, E., Smart, L.V., Boyle, M.M., Russell, G.A., Frost, T.M., Morgan, B.J., Baines, A.J., and Gullick, W.J. (2007). Identification and characterization of novel spliced variants of neuregulin 4 in prostate cancer. Clin Cancer Res *13*, 3147-3155.

Hayes, N.V., Newsam, R.J., Baines, A.J., and Gullick, W.J. (2008). Characterization of the cell membrane-associated products of the Neuregulin 4 gene. Oncogene *27*, 715-720.

Ho, V.W., and Sly, L.M. (2009). Derivation and characterization of murine alternatively activated (M2) macrophages. Methods Mol Biol *531*, 173-185.

Holland, W.L., Miller, R.A., Wang, Z.V., Sun, K., Barth, B.M., Bui, H.H., Davis, K.E., Bikman, B.T., Halberg, N., Rutkowski, J.M., *et al.* (2011). Receptor-mediated activation of ceramidase activity initiates the pleiotropic actions of adiponectin. Nat Med *17*, 55-63.

Horton, J.D., Shimomura, I., Brown, M.S., Hammer, R.E., Goldstein, J.L., and Shimano, H. (1998). Activation of cholesterol synthesis in preference to fatty acid synthesis in liver and adipose tissue of transgenic mice overproducing sterol regulatory element-binding protein-2. J Clin Invest *101*, 2331-2339.

Hotamisligil, G.S., Shargill, N.S., and Spiegelman, B.M. (1993). Adipose expression of tumor necrosis factor-alpha: direct role in obesity-linked insulin resistance. Science *259*, 87-91.

Howard, B., Panchal, H., McCarthy, A., and Ashworth, A. (2005). Identification of the scaramanga gene implicates Neuregulin3 in mammary gland specification. Genes Dev *19*, 2078-2090.

Hu, E., Liang, P., and Spiegelman, B.M. (1996). AdipoQ is a novel adipose-specific gene dysregulated in obesity. J Biol Chem *271*, 10697-10703.

Hundal, R.S., Petersen, K.F., Mayerson, A.B., Randhawa, P.S., Inzucchi, S., Shoelson, S.E., and Shulman, G.I. (2002). Mechanism by which high-dose aspirin improves glucose metabolism in type 2 diabetes. J Clin Invest *109*, 1321-1326.

Hunter, C.A. (2005). New IL-12-family members: IL-23 and IL-27, cytokines with divergent functions. Nat Rev Immunol *5*, 521-531.

Jaruga, B., Hong, F., Kim, W.H., and Gao, B. (2004). IFN-gamma/STAT1 acts as a proinflammatory signal in T cell-mediated hepatitis via induction of multiple chemokines and adhesion molecules: a critical role of IRF-1. Am J Physiol Gastrointest Liver Physiol *287*, G1044-1052.

Jeon, T.I., and Osborne, T.F. (2012). SREBPs: metabolic integrators in physiology and metabolism. Trends Endocrinol Metab *23*, 65-72.

Jespersen, N.Z., Larsen, T.J., Peijs, L., Daugaard, S., Homoe, P., Loft, A., de Jong, J., Mathur, N., Cannon, B., Nedergaard, J., *et al.* (2013). A classical brown adipose tissue mRNA signature partly overlaps with brite in the supraclavicular region of adult humans. Cell Metab *17*, 798-805.

K, S.R., Rubakhin, S.S., Szucs, A., Hughes, T.K., and Stefano, G.B. (1997). Opposite effects of interleukin-2 and interleukin-4 on GABA-induced inward currents of dialysed Lymnaea neurons. Gen Pharmacol *29*, 73-77.

Kang, Y.S., Lee, M.H., Song, H.K., Ko, G.J., Kwon, O.S., Lim, T.K., Kim, S.H., Han, S.Y., Han, K.H., Lee, J.E.*, et al.* (2010). CCR2 antagonism improves insulin resistance, lipid metabolism, and diabetic nephropathy in type 2 diabetic mice. Kidney Int *78*, 883-894.

Kaplan, D.H., Shankaran, V., Dighe, A.S., Stockert, E., Aguet, M., Old, L.J., and Schreiber, R.D. (1998). Demonstration of an interferon gamma-dependent tumor surveillance system in immunocompetent mice. Proc Natl Acad Sci U S A *95*, 7556-7561.

Kaplan, M.H., Schindler, U., Smiley, S.T., and Grusby, M.J. (1996a). Stat6 is required for mediating responses to IL-4 and for development of Th2 cells. Immunity *4*, 313-319.

Kaplan, M.H., Sun, Y.L., Hoey, T., and Grusby, M.J. (1996b). Impaired IL-12 responses and enhanced development of Th2 cells in Stat4-deficient mice. Nature *382*, 174-177.

Kisseleva, T., Bhattacharya, S., Braunstein, J., and Schindler, C.W. (2002). Signaling through the JAK/STAT pathway, recent advances and future challenges. Gene *285*, 1-24.

Klapper, L.N., Glathe, S., Vaisman, N., Hynes, N.E., Andrews, G.C., Sela, M., and Yarden, Y. (1999). The ErbB-2/HER2 oncoprotein of human carcinomas may function solely as a shared coreceptor for multiple stroma-derived growth factors. Proc Natl Acad Sci U S A *96*, 4995-5000.

Klingenspor, M. (2003). Cold-induced recruitment of brown adipose tissue thermogenesis. Exp Physiol *88*, 141-148.

Knebel, B., Haas, J., Hartwig, S., Jacob, S., Kollmer, C., Nitzgen, U., Muller-Wieland, D., and Kotzka, J. (2012). Liver-specific expression of transcriptionally active SREBP-1c is associated with fatty liver and increased visceral fat mass. PLoS One *7*, e31812.

Kobayashi, H., Ouchi, N., Kihara, S., Walsh, K., Kumada, M., Abe, Y., Funahashi, T., and Matsuzawa, Y. (2004). Selective suppression of endothelial cell apoptosis by the high molecular weight form of adiponectin. Circ Res *94*, e27-31.

Kogata, N., Zvelebil, M., and Howard, B.A. (2013). Neuregulin 3 and erbb signalling networks in embryonic mammary gland development. J Mammary Gland Biol Neoplasia *18*, 149-154.

Kopp, E., and Ghosh, S. (1994). Inhibition of NF-kappa B by sodium salicylate and aspirin. Science *265*, 956-959.

Kubota, N., Yano, W., Kubota, T., Yamauchi, T., Itoh, S., Kumagai, H., Kozono, H., Takamoto, I., Okamoto, S., Shiuchi, T.*, et al.* (2007). Adiponectin stimulates AMP-activated protein kinase in the hypothalamus and increases food intake. Cell Metab *6*, 55-68.

Larsen, C.M., Faulenbach, M., Vaag, A., Ehses, J.A., Donath, M.Y., and Mandrup-Poulsen, T. (2009). Sustained effects of interleukin-1 receptor antagonist treatment in type 2 diabetes. Diabetes Care *32*, 1663-1668.

Larsen, C.M., Faulenbach, M., Vaag, A., Volund, A., Ehses, J.A., Seifert, B., Mandrup-Poulsen, T., and Donath, M.Y. (2007). Interleukin-1-receptor antagonist in type 2 diabetes mellitus. N Engl J Med *356*, 1517-1526.

Lavoie, J.M., and Gauthier, M.S. (2006). Regulation of fat metabolism in the liver: link to non-alcoholic hepatic steatosis and impact of physical exercise. Cell Mol Life Sci *63*, 1393-1409.

Lawrence, T., and Natoli, G. (2011). Transcriptional regulation of macrophage polarization: enabling diversity with identity. Nat Rev Immunol *11*, 750-761.

Lazo, M., and Clark, J.M. (2008). The epidemiology of nonalcoholic fatty liver disease: a global perspective. Semin Liver Dis *28*, 339-350.

Leal Vde, O., and Mafra, D. (2013). Adipokines in obesity. Clin Chim Acta *419*, 87-94.

Lebrasseur, N.K., Cote, G.M., Miller, T.A., Fielding, R.A., and Sawyer, D.B. (2003). Regulation of neuregulin/ErbB signaling by contractile activity in skeletal muscle. Am J Physiol Cell Physiol *284*, C1149-1155.

Lee, Y.H., Petkova, A.P., Mottillo, E.P., and Granneman, J.G. (2012). In vivo identification of bipotential adipocyte progenitors recruited by beta3-adrenoceptor activation and high-fat feeding. Cell Metab *15*, 480-491.

Levy, D.E., and Darnell, J.E., Jr. (2002). Stats: transcriptional control and biological impact. Nat Rev Mol Cell Biol *3*, 651-662.

Liang, G., Yang, J., Horton, J.D., Hammer, R.E., Goldstein, J.L., and Brown, M.S. (2002). Diminished hepatic response to fasting/refeeding and liver X receptor agonists in mice with selective deficiency of sterol regulatory element-binding protein-1c. J Biol Chem *277*, 9520-9528.

Liu, X., Robinson, G.W., Wagner, K.U., Garrett, L., Wynshaw-Boris, A., and Hennighausen, L. (1997). Stat5a is mandatory for adult mammary gland development and lactogenesis. Genes Dev *11*, 179-186.

Lowell, B.B., V, S.S., Hamann, A., Lawitts, J.A., Himms-Hagen, J., Boyer, B.B., Kozak, L.P., and Flier, J.S. (1993). Development of obesity in transgenic mice after genetic ablation of brown adipose tissue. Nature *366*, 740-742.

Lumeng, C.N., Bodzin, J.L., and Saltiel, A.R. (2007a). Obesity induces a phenotypic switch in adipose tissue macrophage polarization. J Clin Invest *117*, 175-184.

Lumeng, C.N., DelProposto, J.B., Westcott, D.J., and Saltiel, A.R. (2008). Phenotypic switching of adipose tissue macrophages with obesity is generated by spatiotemporal differences in macrophage subtypes. Diabetes *57*, 3239-3246.

Lumeng, C.N., Deyoung, S.M., Bodzin, J.L., and Saltiel, A.R. (2007b). Increased inflammatory properties of adipose tissue macrophages recruited during diet-induced obesity. Diabetes *56*, 16-23.

Ma, X.J., Chow, J.M., Gri, G., Carra, G., Gerosa, F., Wolf, S.E., Dzialo, R., and Trinchieri, G. (1996). The interleukin 12 p40 gene promoter is primed by interferon gamma in monocytic cells. J Exp Med *183*, 147-157.

Maeda, N., Shimomura, I., Kishida, K., Nishizawa, H., Matsuda, M., Nagaretani, H., Furuyama, N., Kondo, H., Takahashi, M., Arita, Y.*, et al.* (2002). Diet-induced insulin resistance in mice lacking adiponectin/ACRP30. Nat Med *8*, 731-737.

Martinez, F.O., Sica, A., Mantovani, A., and Locati, M. (2008). Macrophage activation and polarization. Front Biosci *13*, 453-461.

Meyer, D., and Birchmeier, C. (1995). Multiple essential functions of neuregulin in development. Nature *378*, 386-390.

Montero, J.C., Yuste, L., Diaz-Rodriguez, E., Esparis-Ogando, A., and Pandiella, A. (2000). Differential shedding of transmembrane neuregulin isoforms by the tumor necrosis factor-alpha-converting enzyme. Mol Cell Neurosci *16*, 631-648.

Moon, Y.A., Liang, G., Xie, X., Frank-Kamenetsky, M., Fitzgerald, K., Koteliansky, V., Brown, M.S., Goldstein, J.L., and Horton, J.D. (2012). The Scap/SREBP pathway is essential for developing diabetic fatty liver and carbohydrate-induced hypertriglyceridemia in animals. Cell Metab *15*, 240-246.

Nedergaard, J., Bengtsson, T., and Cannon, B. (2007). Unexpected evidence for active brown adipose tissue in adult humans. Am J Physiol Endocrinol Metab *293*, E444-452.

Ni, C.Y., Murphy, M.P., Golde, T.E., and Carpenter, G. (2001). gamma -Secretase cleavage and nuclear localization of ErbB-4 receptor tyrosine kinase. Science *294*, 2179-2181.

Nishimura, S., Manabe, I., Nagasaki, M., Eto, K., Yamashita, H., Ohsugi, M., Otsu, M., Hara, K., Ueki, K., Sugiura, S.*, et al.* (2009). CD8+ effector T cells contribute to macrophage recruitment and adipose tissue inflammation in obesity. Nat Med *15*, 914-920.

O'Rourke, R.W., White, A.E., Metcalf, M.D., Winters, B.R., Diggs, B.S., Zhu, X., and Marks, D.L. (2012). Systemic inflammation and insulin sensitivity in obese IFN-gamma knockout mice. Metabolism *61*, 1152-1161.

Olayioye, M.A., Beuvink, I., Horsch, K., Daly, J.M., and Hynes, N.E. (1999). ErbB receptor-induced activation of stat transcription factors is mediated by Src tyrosine kinases. J Biol Chem *274*, 17209-17218.

Ormandy, C.J., Binart, N., and Kelly, P.A. (1997). Mammary gland development in prolactin receptor knockout mice. J Mammary Gland Biol Neoplasia *2*, 355-364.

Ouchi, N., Parker, J.L., Lugus, J.J., and Walsh, K. (2011). Adipokines in inflammation and metabolic disease. Nat Rev Immunol *11*, 85-97.

Pagano, E., and Calvo, J.C. (2003). ErbB2 and EGFR are downmodulated during the differentiation of 3T3-L1 preadipocytes. J Cell Biochem *90*, 561-572.

Park, C., Li, S., Cha, E., and Schindler, C. (2000). Immune response in Stat2 knockout mice. Immunity *13*, 795-804.

Petrovic, N., Walden, T.B., Shabalina, I.G., Timmons, J.A., Cannon, B., and Nedergaard, J. (2010). Chronic peroxisome proliferator-activated receptor gamma (PPARgamma) activation of epididymally derived white adipocyte cultures reveals a population of thermogenically competent, UCP1-containing adipocytes molecularly distinct from classic brown adipocytes. J Biol Chem *285*, 7153-7164.

Reilly, S.M., Chiang, S.H., Decker, S.J., Chang, L., Uhm, M., Larsen, M.J., Rubin, J.R., Mowers, J., White, N.M., Hochberg, I.*, et al.* (2013). An inhibitor of the protein kinases TBK1 and IKK-varepsilon improves obesity-related metabolic dysfunctions in mice. Nat Med *19*, 313-321.

Repa, J.J., Liang, G., Ou, J., Bashmakov, Y., Lobaccaro, J.M., Shimomura, I., Shan, B., Brown, M.S., Goldstein, J.L., and Mangelsdorf, D.J. (2000). Regulation of mouse sterol regulatory element-binding protein-1c gene (SREBP-1c) by oxysterol receptors, LXRalpha and LXRbeta. Genes Dev *14*, 2819-2830.

Rocha, V.Z., Folco, E.J., Sukhova, G., Shimizu, K., Gotsman, I., Vernon, A.H., and Libby, P. (2008). Interferon-gamma, a Th1 cytokine, regulates fat inflammation: a role for adaptive immunity in obesity. Circ Res *103*, 467-476.

Rogers, C., Moukdar, F., McGee, M.A., Davis, B., Buehrer, B.M., Daniel, K.W., Collins, S., Barakat, H., and Robidoux, J. (2012). EGF receptor (ERBB1) abundance in adipose tissue is reduced in insulin-resistant and type 2 diabetic women. J Clin Endocrinol Metab *97*, E329-340.

Rosenwald, M., Perdikari, A., Rulicke, T., and Wolfrum, C. (2013). Bi-directional interconversion of brite and white adipocytes. Nat Cell Biol *15*, 659-667.

Sahu, A. (2011). Intracellular leptin-signaling pathways in hypothalamic neurons: the emerging role of phosphatidylinositol-3 kinase-phosphodiesterase-3B-cAMP pathway. Neuroendocrinology *93*, 201-210.

Sanchez-Gurmaches, J., and Guertin, D.A. (2013). Adipocyte lineages: Tracing back the origins of fat. Biochim Biophys Acta.

Sanchez-Gurmaches, J., Hung, C.M., Sparks, C.A., Tang, Y., Li, H., and Guertin, D.A. (2012). PTEN loss in the Myf5 lineage redistributes body fat and reveals subsets of white adipocytes that arise from Myf5 precursors. Cell Metab *16*, 348-362.

Schindler, C., Levy, D.E., and Decker, T. (2007). JAK-STAT signaling: from interferons to cytokines. J Biol Chem *282*, 20059-20063.

Schmidt, N., Akaaboune, M., Gajendran, N., Martinez-Pena y Valenzuela, I., Wakefield, S., Thurnheer, R., and Brenner, H.R. (2011). Neuregulin/ErbB regulate neuromuscular junction development by phosphorylation of alpha-dystrobrevin. J Cell Biol *195*, 1171-1184.

Schraw, T., Wang, Z.V., Halberg, N., Hawkins, M., and Scherer, P.E. (2008). Plasma adiponectin complexes have distinct biochemical characteristics. Endocrinology *149*, 2270-2282.

Schultz, J.R., Tu, H., Luk, A., Repa, J.J., Medina, J.C., Li, L., Schwendner, S., Wang, S., Thoolen, M., Mangelsdorf, D.J., *et al.* (2000). Role of LXRs in control of lipogenesis. Genes Dev *14*, 2831-2838.

Seale, P., Bjork, B., Yang, W., Kajimura, S., Chin, S., Kuang, S., Scime, A., Devarakonda, S., Conroe, H.M., Erdjument-Bromage, H., *et al.* (2008). PRDM16 controls a brown fat/skeletal muscle switch. Nature *454*, 961-967.

Seals, D.F., and Courtneidge, S.A. (2003). The ADAMs family of metalloproteases: multidomain proteins with multiple functions. Genes Dev *17*, 7-30.

Shimano, H., Horton, J.D., Shimomura, I., Hammer, R.E., Brown, M.S., and Goldstein, J.L. (1997a). Isoform 1c of sterol regulatory element binding protein is less active than isoform 1a in livers of transgenic mice and in cultured cells. J Clin Invest *99*, 846-854.

Shimano, H., Shimomura, I., Hammer, R.E., Herz, J., Goldstein, J.L., Brown, M.S., and Horton, J.D. (1997b). Elevated levels of SREBP-2 and cholesterol synthesis in livers of mice homozygous for a targeted disruption of the SREBP-1 gene. J Clin Invest *100*, 2115-2124.

Shimano, H., Yahagi, N., Amemiya-Kudo, M., Hasty, A.H., Osuga, J., Tamura, Y., Shionoiri, F., Iizuka, Y., Ohashi, K., Harada, K., *et al.* (1999). Sterol regulatory element-binding protein-1 as a key transcription factor for nutritional induction of lipogenic enzyme genes. J Biol Chem *274*, 35832-35839.

Shoelson, S.E., Lee, J., and Goldfine, A.B. (2006). Inflammation and insulin resistance. J Clin Invest *116*, 1793-1801.

Sica, A., and Mantovani, A. (2012). Macrophage plasticity and polarization: in vivo veritas. J Clin Invest *122*, 787-795.

Silva, J.E., and Larsen, P.R. (1983). Adrenergic activation of triiodothyronine production in brown adipose tissue. Nature *305*, 712-713.

Soler, C., Poveda, B., Pastor-Anglada, M., and Soley, M. (1991). Effect of epidermal growth factor (EGF) on gluconeogenesis in isolated rat hepatocytes. Dependency on the red-ox state of the substrate. Biochim Biophys Acta *1091*, 193-196.

Stanford, K.I., Middelbeek, R.J., Townsend, K.L., An, D., Nygaard, E.B., Hitchcox, K.M., Markan, K.R., Nakano, K., Hirshman, M.F., Tseng, Y.H., *et al.* (2013). Brown adipose tissue regulates glucose homeostasis and insulin sensitivity. J Clin Invest *123*, 215-223.

Suarez, E., Bach, D., Cadefau, J., Palacin, M., Zorzano, A., and Guma, A. (2001). A novel role of neuregulin in skeletal muscle. Neuregulin stimulates glucose uptake, glucose transporter translocation, and transporter expression in muscle cells. J Biol Chem *276*, 18257-18264.

Takeda, K., Noguchi, K., Shi, W., Tanaka, T., Matsumoto, M., Yoshida, N., Kishimoto, T., and Akira, S. (1997). Targeted disruption of the mouse Stat3 gene leads to early embryonic lethality. Proc Natl Acad Sci U S A *94*, 3801-3804.

Tamura, T., Ueda, S., Yoshida, M., Matsuzaki, M., Mohri, H., and Okubo, T. (1996). Interferon-gamma induces Ice gene expression and enhances cellular susceptibility to apoptosis in the U937 leukemia cell line. Biochem Biophys Res Commun *229*, 21-26.

Tang, J.J., Li, J.G., Qi, W., Qiu, W.W., Li, P.S., Li, B.L., and Song, B.L. (2011). Inhibition of SREBP by a small molecule, betulin, improves hyperlipidemia and insulin resistance and reduces atherosclerotic plaques. Cell Metab *13*, 44-56.

Tartaglia, L.A., Dembski, M., Weng, X., Deng, N., Culpepper, J., Devos, R., Richards, G.J., Campfield, L.A., Clark, F.T., Deeds, J., *et al.* (1995). Identification and expression cloning of a leptin receptor, OB-R. Cell *83*, 1263-1271.

Tateya, S., Kim, F., and Tamori, Y. (2013). Recent advances in obesity-induced inflammation and insulin resistance. Front Endocrinol (Lausanne) *4*, 93.

Teglund, S., McKay, C., Schuetz, E., van Deursen, J.M., Stravopodis, D., Wang, D., Brown, M., Bodner, S., Grosveld, G., and Ihle, J.N. (1998). Stat5a and Stat5b proteins have essential and nonessential, or redundant, roles in cytokine responses. Cell *93*, 841-850.

Tidcombe, H., Jackson-Fisher, A., Mathers, K., Stern, D.F., Gassmann, M., and Golding, J.P. (2003). Neural and mammary gland defects in ErbB4 knockout mice genetically rescued from embryonic lethality. Proc Natl Acad Sci U S A *100*, 8281-8286.

Tiemessen, M.M., Jagger, A.L., Evans, H.G., van Herwijnen, M.J., John, S., and Taams, L.S. (2007). CD4+CD25+Foxp3+ regulatory T cells induce alternative activation of human monocytes/macrophages. Proc Natl Acad Sci U S A *104*, 19446-19451.

Timmons, J.A., Wennmalm, K., Larsson, O., Walden, T.B., Lassmann, T., Petrovic, N., Hamilton, D.L., Gimeno, R.E., Wahlestedt, C., Baar, K.*, et al.* (2007). Myogenic gene expression signature establishes that brown and white adipocytes originate from distinct cell lineages. Proc Natl Acad Sci U S A *104*, 4401-4406.

Udy, G.B., Towers, R.P., Snell, R.G., Wilkins, R.J., Park, S.H., Ram, P.A., Waxman, D.J., and Davey, H.W. (1997). Requirement of STAT5b for sexual dimorphism of body growth rates and liver gene expression. Proc Natl Acad Sci U S A *94*, 7239-7244.

Uezumi, A., Fukada, S., Yamamoto, N., Takeda, S., and Tsuchida, K. (2010). Mesenchymal progenitors distinct from satellite cells contribute to ectopic fat cell formation in skeletal muscle. Nat Cell Biol *12*, 143-152.

van Marken Lichtenbelt, W.D., Vanhommerig, J.W., Smulders, N.M., Drossaerts, J.M., Kemerink, G.J., Bouvy, N.D., Schrauwen, P., and Teule, G.J. (2009). Cold-activated brown adipose tissue in healthy men. N Engl J Med *360*, 1500-1508.

Vecchi, M., and Carpenter, G. (1997). Constitutive proteolysis of the ErbB-4 receptor tyrosine kinase by a unique, sequential mechanism. J Cell Biol *139*, 995-1003.

Vijgen, G.H., Bouvy, N.D., Teule, G.J., Brans, B., Schrauwen, P., and van Marken Lichtenbelt, W.D. (2011). Brown adipose tissue in morbidly obese subjects. PLoS One *6*, e17247.

Virtanen, K.A., Lidell, M.E., Orava, J., Heglind, M., Westergren, R., Niemi, T., Taittonen, M., Laine, J., Savisto, N.J., Enerback, S.*, et al.* (2009). Functional brown adipose tissue in healthy adults. N Engl J Med *360*, 1518-1525.

Waki, H., and Tontonoz, P. (2007). Endocrine functions of adipose tissue. Annu Rev Pathol *2*, 31-56.

Wen, D., Peles, E., Cupples, R., Suggs, S.V., Bacus, S.S., Luo, Y., Trail, G., Hu, S., Silbiger, S.M., Levy, R.B.*, et al.* (1992). Neu differentiation factor: a transmembrane glycoprotein containing an EGF domain and an immunoglobulin homology unit. Cell *69*, 559-572.

Wen, D., Suggs, S.V., Karunagaran, D., Liu, N., Cupples, R.L., Luo, Y., Janssen, A.M., Ben-Baruch, N., Trollinger, D.B., Jacobsen, V.L.*, et al.* (1994). Structural and functional aspects of the multiplicity of Neu differentiation factors. Mol Cell Biol *14*, 1909-1919.

Wieduwilt, M.J., and Moasser, M.M. (2008). The epidermal growth factor receptor family: biology driving targeted therapeutics. Cell Mol Life Sci *65*, 1566-1584.

Williams, C.C., Allison, J.G., Vidal, G.A., Burow, M.E., Beckman, B.S., Marrero, L., and Jones, F.E. (2004). The ERBB4/HER4 receptor tyrosine kinase regulates gene expression by functioning as a STAT5A nuclear chaperone. J Cell Biol *167*, 469-478.

Williamson, R.T. (1901). On the Treatment of Glycosuria and Diabetes Mellitus with Sodium Salicylate. Br Med J *1*, 760-762.

Wu, H., Ghosh, S., Perrard, X.D., Feng, L., Garcia, G.E., Perrard, J.L., Sweeney, J.F., Peterson, L.E., Chan, L., Smith, C.W.*, et al.* (2007). T-cell accumulation and regulated on activation, normal T cell expressed and secreted upregulation in adipose tissue in obesity. Circulation *115*, 1029-1038.

Wu, J., Bostrom, P., Sparks, L.M., Ye, L., Choi, J.H., Giang, A.H., Khandekar, M., Virtanen, K.A., Nuutila, P., Schaart, G.*, et al.* (2012). Beige adipocytes are a distinct type of thermogenic fat cell in mouse and human. Cell *150*, 366-376.

Xie, Q.W., Whisnant, R., and Nathan, C. (1993). Promoter of the mouse gene encoding calcium-independent nitric oxide synthase confers inducibility by interferon gamma and bacterial lipopolysaccharide. J Exp Med *177*, 1779-1784.

Xu, H., Barnes, G.T., Yang, Q., Tan, G., Yang, D., Chou, C.J., Sole, J., Nichols, A., Ross, J.S., Tartaglia, L.A.*, et al.* (2003). Chronic inflammation in fat plays a crucial role in the development of obesity-related insulin resistance. J Clin Invest *112*, 1821-1830.

Yamauchi, T., Kamon, J., Minokoshi, Y., Ito, Y., Waki, H., Uchida, S., Yamashita, S., Noda, M., Kita, S., Ueki, K.*, et al.* (2002). Adiponectin stimulates glucose utilization and fatty-acid oxidation by activating AMP-activated protein kinase. Nat Med *8*, 1288-1295.

Yang, Q., Graham, T.E., Mody, N., Preitner, F., Peroni, O.D., Zabolotny, J.M., Kotani, K., Quadro, L., and Kahn, B.B. (2005). Serum retinol binding protein 4 contributes to insulin resistance in obesity and type 2 diabetes. Nature *436*, 356-362.

Yang, R., and Barouch, L.A. (2007). Leptin signaling and obesity: cardiovascular consequences. Circ Res *101*, 545-559.

Yarden, Y., and Sliwkowski, M.X. (2001). Untangling the ErbB signalling network. Nat Rev Mol Cell Biol *2*, 127-137.

Yin, M.J., Yamamoto, Y., and Gaynor, R.B. (1998). The anti-inflammatory agents aspirin and salicylate inhibit the activity of I(kappa)B kinase-beta. Nature *396*, 77-80.

Yoneshiro, T., Aita, S., Matsushita, M., Kayahara, T., Kameya, T., Kawai, Y., Iwanaga, T., and Saito, M. (2013). Recruited brown adipose tissue as an antiobesity agent in humans. J Clin Invest *123*, 3404-3408.

Yuan, M., Konstantopoulos, N., Lee, J., Hansen, L., Li, Z.W., Karin, M., and Shoelson, S.E. (2001). Reversal of obesity- and diet-induced insulin resistance with salicylates or targeted disruption of Ikkbeta. Science *293*, 1673-1677.

Zhang, D., Sliwkowski, M.X., Mark, M., Frantz, G., Akita, R., Sun, Y., Hillan, K., Crowley, C., Brush, J., and Godowski, P.J. (1997). Neuregulin-3 (NRG3): a novel neural tissue-enriched protein that binds and activates ErbB4. Proc Natl Acad Sci U S A *94*, 9562-9567.

Zhang, Y., Proenca, R., Maffei, M., Barone, M., Leopold, L., and Friedman, J.M. (1994). Positional cloning of the mouse obese gene and its human homologue. Nature *372*, 425-432.

Zhao, Y.Y., Sawyer, D.R., Baliga, R.R., Opel, D.J., Han, X., Marchionni, M.A., and Kelly, R.A. (1998). Neuregulins promote survival and growth of cardiac myocytes. Persistence of ErbB2 and ErbB4 expression in neonatal and adult ventricular myocytes. J Biol Chem *273*, 10261-10269.

Zhou, W., and Carpenter, G. (2000). Heregulin-dependent trafficking and cleavage of ErbB-4. J Biol Chem *275*, 34737-34743.

Zhu, Z., Spicer, E.G., Gavini, C.K., Goudjo-Ako, A.J., Novak, C.M., and Shi, H. (2013). Enhanced sympathetic activity in mice with brown adipose tissue transplantation (transBATation). Physiol Behav *125C*, 21-29.

CHAPTER 2 OTOPETRIN1 PROTECTS MICE FROM OBESITY-ASSOCIATED METABOLIC DYSFUNCTION THROUGH ATTENUATING ADIPOSE TISSUE INFLAMMATION

2.1 Abstract

Chronic low-grade inflammation is emerging as a pathogenic link between obesity and metabolic disease. Persistent immune activation in white adipose tissue (WAT) impairs insulin sensitivity and systemic metabolism in part through the actions of proinflammatory cytokines. Whether obesity activates an adaptive mechanism to counteract chronic inflammation in adipose tissues has not been elucidated. Here we identified Otopetrin 1 (Otop1) as a component of a counter-inflammatory pathway that is induced in WAT during obesity. Otop1 expression is markedly increased in obese mouse WAT and is stimulated by TNFα in cultured adipocytes. Otop1 mutant mice respond to high-fat diet with pronounced insulin resistance and hepatic steatosis, accompanied by augmented adipose tissue inflammation. Otop1 attenuates interferon γ (IFNγ) signaling through physical interaction with and downregulation of the transcription factor STAT1. Thus, Otop1 defines a unique target of cytokine signaling that attenuates obesity-induced adipose tissue inflammation and plays an adaptive role in maintaining metabolic homeostasis in obesity.

2.2 Introduction

Obesity poses significant risk to patient health due to its associated metabolic disorders. White adipose tissue (WAT) stores the bulk of body fat and also plays an important role in endocrine metabolic signaling (Tontonoz and Spiegelman, 2008; Trujillo and Scherer, 2006), whereas brown adipose tissue (BAT) defends against cold and obesity through uncoupled mitochondrial respiration (Brakenhielm et al., 2004; Lowell and Spiegelman, 2000). Obesity is associated with chronic low-grade inflammation in adipose tissues (Gregor and Hotamisligil, 2011; Lumeng and Saltiel, 2011; Odegaard and Chawla, 2013; Osborn and Olefsky, 2012; Sun et al., 2012). The pathogenic role of the persistent activation of inflammatory signaling in metabolic disease has been demonstrated in numerous mouse models. An emerging view suggests that attenuating the proinflammatory response may provide significant metabolic benefits in obesity. While therapeutic development targeting inflammation remains in its early stage in humans, several candidates have shown promise, including salsalate, a prodrug of salicylate (Goldfine et al., 2008), and IL-1 receptor antagonists (Larsen et al., 2007). In addition, the beneficial effects of PPARγ agonists have at least in part been attributed to their anti-inflammatory activities (Hevener et al., 2007; Pascual et al., 2005).

The molecular and cellular events that lead to the engagement and sustained activation of the innate immune system in obesity are complex and remain to be unraveled. In adipose tissues, obesity-induced inflammation is associated with a robust shift of adipose tissue macrophages from alternatively activated (M2) to classically activated (M1) subtypes (Aron-Wisnewsky et al., 2009; Lumeng et al., 2007a). This shift toward proinflammatory macrophage polarization coincides with the development of insulin resistance and has been proposed as an early event underlying metabolic dysregulation (Lumeng et al., 2007b). A parallel shift from anti-

inflammatory regulatory T cells to $CD4^+$ helper and $CD8^+$ cytotoxic T cells also occurs in WAT during obesity (Feuerer et al., 2009; Nishimura et al., 2009; Winer et al., 2009). The latter produces proinflammatory cytokines such as tumor necrosis factor α (TNFα), a prototypical cytokine associated with obesity (Hotamisligil et al., 1993), and interferon γ (IFNγ), which contribute to chronic inflammation in adipose tissues. Several pathways downstream of cytokine receptors have been shown to play a role in obesity-induced inflammation and its metabolic consequences, including IKKβ, NF-κB, JNK, IKKε, and inflammasome activation (Arkan et al., 2005; Cai et al., 2005; Chiang et al., 2009; Hirosumi et al., 2002; Stienstra et al., 2010; Vandanmagsar et al., 2011). The activation of these signaling pathways impairs insulin signaling in adipocytes. As such, genetic and pharmacological inhibition of these pathways leads to attenuation of inflammatory signaling and improved insulin sensitivity. While key components of proinflammatory signaling have been elucidated, whether obesity activates adaptive pathways that counteract inflammation and the extent to which they contribute to metabolic homeostasis remain largely unknown.

Otopetrin 1 (Otop1) is a member of the otopetrin domain protein family that is highly conserved in species ranging from nematodes to vertebrates (Hughes et al., 2008b; Hurle et al., 2011). Otop1 is predicted to contain 12 transmembrane domains and has been demonstrated to localize to the plasma membrane (Hughes et al., 2007a). Mice harboring *tilted* mutation (A151E, $Otop1^{tlt}$) have impaired otoconia development (Hurle et al., 2003), likely as a consequence of altered cellular calcium in vestibular supporting cells (Hughes et al., 2007a; Kim et al., 2011a). Importantly, Otop1 knockout mice develop similar defects in otoconia formation (Kim et al., 2010), suggesting that $Otop1^{tlt}$ mutant represents a *bona fide* loss-of-function allele. Whether

Otop1 is expressed in peripheral tissues and regulates other physiological processes remains unknown. In this study, we found that Otop1 is induced in white adipose tissues during obesity and counteracts obesity-associated adipose tissue inflammation. Otop1 defines a novel adaptive mechanism that maintains metabolic homeostasis through attenuating chronic inflammation.

2.3 Results

2.3.1 Otop1 is expressed in BAT but dispensable for cold-induced adaptive thermogenesis

Brown adipose tissue (BAT) is responsible for non-shivering thermogenesis in response to cold exposure in rodents and may contribute to energy balance in humans. We analyzed the transcriptional profile of diverse mouse tissues and cell lines (GSE10246) to identify putative molecular markers of brown adipocytes. These analyses uncovered Otop1 as a gene that shares tissue distribution with uncoupling protein 1 (Ucp1), a known brown fat marker. Quantitative realtime PCR (qPCR) analysis indicated that Otop1 mRNA was abundantly expressed in brown adipose tissue (Figure 2.1A). To determine whether Otop1 expression is regulated during adipogenesis, we immortalized brown preadipocytes from neonatal brown fat and induced differentiation in culture using a previously described protocol (Klein et al., 1999). Similar to Ucp1, Otop1 mRNA expression was strongly induced during brown adipocyte differentiation (Figure 2.1B). In contrast, Otop1 mRNA was nearly undetectable in 3T3-L1 adipocytes (data not shown). The brown fat gene program is highly responsive to environmental temperature. Acute cold exposure stimulates mitochondrial biogenesis and thermogenic gene expression through activation of the sympathetic nervous system, whereas chronic cold acclimation results in the expansion of brown fat mass and augmentation of thermogenic capacity (Brakenhielm et al., 2004; Gesta et al., 2007). As expected, Ucp1 mRNA expression was stimulated by both acute

and chronic cold exposure (Figure 2.1C-D). On the contrary, Otop1 mRNA expression remained largely unchanged in response to acute cold exposure, whereas it was markedly increased in BAT following cold acclimation.

To determine whether Otop1 is required for cold-induced adaptive thermogenesis, we subjected wild type (WT) and Otop1^{tlt} mutant mice to cold exposure at 4ºC and measured their core body temperature using a rectal probe. While rectal body temperature dropped slightly following cold exposure, no significant difference was observed between the two groups (Figure 2.1E). H&E staining revealed that Otop1 mutant brown fat appeared nearly indistinguishable from control before and after cold exposure (Figure 2.1F). The expression of Ucp1 and genes involved in mitochondrial oxidative phosphorylation and fatty acid β-oxidation was similar between WT and mutant groups (Figure 2.1G). Protein levels for NADH dehydrogenase 1β subcomplex 8 (NDUFB8, complex I), succinate dehydrogenase subunit b (SDHB, complex II), and ubiquinol cytochrome c reductase core protein 2 (UQCRC2, complex III) were also similar (Figure 2.1H). Interestingly, PGC-1α mRNA level was elevated in Otop1 mutant brown fat. Together, these data suggest that, while Otop1 expression is enriched in brown fat, its function is dispensable for cold-induced adaptive thermogenesis.

2.3.2 Otop1 is induced in obese white adipose tissue in response to proinflammatory signaling

Adipose tissue inflammation is emerging as a pathogenic link between obesity and metabolic disorders. The sustained chronic inflammation is associated with a phenotypic switch of resident immune cells from anti-inflammatory to proinflammatory subtypes in adipose tissues (Feuerer et

al., 2009; Lumeng et al., 2007a). Whether obesity also activates adaptive mechanisms to counteract inflammation caused by chronic overnutrition remains largely unexplored. Otop1 mRNA expression is present in BAT, but nearly undetectable in epididymal WAT (eWAT) from lean mice. Interestingly, Otop1 mRNA level was markedly increased in eWAT following high-fat diet (HFD)-induced obesity (Figure 2.2A). Compared to WT, Otop1 mRNA expression was increased by approximately 80-fold in eWAT from leptin receptor deficient (db/db) mice. Similar increase in Otop1 expression was also observed in inguinal fat from obese mice (data not shown). In contrast, Otop1 mRNA levels in BAT remained similar between lean and obese mice (Figure 2.2B). We did not detect changes in Otop1 mRNA expression by HFD in other tissues, including skeletal muscle and liver (Figure2.2 C-D). To determine whether Otop1 expression in eWAT correlates with the severity of obesity, we fed a cohort of C57BL/6J male mice with HFD for 10 weeks to induce obesity. Mice fed HFD gained variable body weight and exhibited different degree of obesity and insulin resistance. Gene expression analysis in this cohort indicated that eWAT Otop1 expression strikingly correlated with body weight of individual mice (Figure 2.3A). This increase in Otop1 expression in obese eWAT was due to its induction in mature adipocytes, but not other cell types in the stromal vascular fraction (SVF) (Figure 2.3B). Expression of leptin was included as markers for mature adipocytes.

Obesity-associated chronic inflammation is characterized by augmented production of proinflammatory cytokines in adipose tissues, such as TNFα, IFNγ, IL-1β, and IL-6 (Hotamisligil et al., 1993; Rotter et al., 2003; Trujillo and Scherer, 2006). To determine whether Otop1 induction is triggered by proinflammatory cytokines, we treated differentiated 3T3-L1 adipocytes with TNFα, IFNγ, or LPS and examined gene expression using qPCR. Compared to

control treatments, mRNA expression of Otop1 and IL-6, the latter being a known target gene of TNFα, was induced by TNFα in a dose-dependent manner (Figure 2.3C). In contrast, while IFNγ and LPS induced the expression of their respective target genes (Ifih1 and Ccl5) in 3T3-L1 adipocytes, these treatments had modest effects on Otop1 mRNA expression (Figure 2.3 D-E). These results suggest that obesity-associated induction of Otop1 in WAT is likely a direct consequence of heightened adipose tissue inflammation.

2.3.3 Otop1 mutant mice develop more severe diet-induced metabolic disorders

While the deleterious effects of innate immune activation has been well established, whether obesity engages an adaptive response to counteract inflammation in adipose tissues has not been elucidated. We next sought to assess the significance of Otop1 in adipose tissue homeostasis, particularly in the context of obesity. WT and Otop1^{tlt} mutant mice gained similar body weight after 12 weeks of HFD feeding (Figure 2.4A). Plasma concentrations of non-esterified fatty acids (NEFA) and β-hydroxybutyrate, but not triglycerides, were lower in Otop1^{tlt} mutant mice (Figure 2.4B). Despite a lack of difference in body weight gain, fasting blood glucose and insulin levels were significantly elevated in the mutant mice (Figure 2.4C). While blood glucose levels were similar under fed conditions, plasma insulin concentration was elevated in Otop1^{tlt} mutant mice. Further, insulin and glucose tolerance tests indicated that mutant mice developed more severe insulin resistance (Figure 2.4D-E), suggesting that Otop1 is required for maintaining insulin sensitivity in diet-induced obesity. In support of this, basal levels of phosphor-AKT were also reduced in adipose tissues and skeletal muscle. Importantly, insulin-stimulated AKT phosphorylation was markedly blunted in several tissues from HFD-fed Otop1^{tlt} mutant mice, including WAT, BAT, liver, and skeletal muscle (Figure 2.5). We conclude from these studies

that obesity-induced expression of Otop1 in WAT may serve a beneficial role in maintaining metabolic homeostasis in the state of chronic overnutrition.

We performed H&E staining on liver sections from mice fed standard chow or high-fat diet for different periods of time, and found that Otop1^{tlt} mice developed more severe hepatic steatosis after two months on HFD (Figure 2.6A). These histological findings were confirmed by Stimulated Raman Scattering (SRS) microscopy, a label-free imaging method that detects cellular lipids by measuring molecular vibrations of fatty-acyl chains (Folick et al., 2011; Le et al., 2010). As shown in Figure 2.6B, pericentral hepatocytes from Otop1^{tlt} mutant mice had larger lipid droplets compared to control following two and three months of HFD feeding. Measurements of liver triglyceride content after three months of HFD feeding revealed that Otop1^{tlt} mice had approximately 58% higher hepatic triglyceride content than WT control (Figure 2.6C). In addition, liver vs. body weight ratio was significantly higher in the mutant mice. Gene expression analysis indicated that mRNA levels of Fsp27 and Plin4, two lipid droplet proteins, were significantly elevated in Otop1^{tlt} mutant livers (Figure 2.6D). The expression of peroxisomal enoyl-CoA hydratase (Ehhadh) and HMG-CoA synthase 2 (Hmgcs2), genes involved lipid metabolism, but not fibroblast growth factor 21 (Fgf21), was lower in mutant livers. Because Otop1 expression was nearly undetectable in the liver in lean and obese mice, the exacerbation of hepatic steatosis in mutant mice is most likely secondary to altered adipose tissue metabolism and function.

2.3.4 Otop1 mutant mice exhibit more severe adipose tissue inflammation following HFD-feeding

As described above, Otop1 expression was elevated in mouse WAT in obesity and was induced in response to TNFα treatments in cultured adipocytes (Figure 2.3C). To our surprise, Otop1 mutant mice showed exacerbated diet-induced insulin resistance and hepatic steatosis. These findings suggest a plausible mechanism where Otop1 contributes to metabolic homeostasis by counteracting obesity-induced adipose tissue inflammation. In support of this, we found that Otop1^{tlt} mutant mice developed progressively more severe adipose tissue inflammation and increased macrophage infiltration as revealed by H&E and whole-mount immunofluorescence staining (Figure 2.7A-B). Compared to WT, the presence of crown like structures, characteristic of inflamed adipose tissues in obesity, was more pronounced in Otop1^{tlt} mutant eWAT. In contrast, the histological appearance of brown adipose tissues was similar between the two groups (Figure 2.7C). We next analyzed the characteristics of adipose tissue macrophages using flow cytometry with specific cell surface markers. Compared to WT, Otop1^{tlt} mutant eWAT had higher proportion of CD301^{-}CD11c^{+} classically polarized (M1) macrophages, whereas alternatively activated (M2) macrophages (CD301^{+}CD11c^{-}) was significantly lower (Figure 2.7D). Consequently, the M1/M2 ratio was significantly increased in Otop1^{tlt} mutant eWAT. Similar changes in M1/M2 macrophages were also observed in inguinal WAT (iWAT) from Otop1^{tlt} mice (Figure 2.7E), though the differences only achieved borderline significance.

We next performed immunoblotting and qPCR analyses to examine molecular changes in adipose tissues from HFD-fed control and Otop1 mutant mice. Immunoblotting studies revealed that protein levels of IKK epsilon (IKKε), a target of NF-kB recently implicated in obesity-induced adipose tissue inflammation (Chiang et al., 2009; Reilly et al., 2013), were increased in Otop1 mutant eWAT (Figure 2.8A). Consistently, NFkB-p105, phospho-NFkB-p105, and NFkB-

p65 protein levels were elevated in Otop1^{tlt} mutant eWAT. Total TBK1 and phospho-TBK1 protein levels were also higher in Otop1^{tlt} mutant eWAT. mRNA expression of many metabolic genes was similar between two groups, including PPARγ and Srebp1c, key regulators of adipocyte gene expression, hormone-sensitive lipase (Hsl), adipose triglyceride lipase (Atgl), and Ehhadh (Figure 2.8B). Consistent with changes in macrophage subtypes, we found that mRNA expression of macrophage marker F4/80 was elevated, whereas the expression of Arginase 1 (Arg1), a marker for M2 macrophages, was significantly lower in mutant eWAT. The expression levels of Mac2 and Cd68 were also elevated in Otop1 mutant iWAT. In contrast, the expression of TNFα and many interferon γ target genes, including 2'-5' oligoadenylate synthetase like 1 (Oasl1), Oasl2, interferon induced protein 44 (Ifi44), and interferon induced transmembrane protein 3 (Ifitm3), was significantly higher in Otop1^{tlt} eWAT than control. Similar induction of macrophage markers and IFNγ target genes was observed in Otop1^{tlt} mutant mouse iWAT (Figure 2.8B). Because IFNγ expression remained largely unaltered, the induction of its target genes in mutant WAT is likely due to augmented IFNγ signaling in Otop1^{tlt} mutant adipocytes. To directly test this, we treated epididymal fat explants from HFD-fed WT and Otop1^{tlt} mutant mice with IFNγ and examined target gene responses. The induction of several IFNγ target genes, including Oasl2, Ifi44, Ifih1, and interferon regulatory factor 1 (Irf1), was significantly higher in Otop1^{tlt} mutant fat explants than control in response to IFNγ stimulation (Figure 2.8C). Together, these results suggest that Otop1 induction in obese WAT is likely an adaptive homeostatic response that exerts a protective role by counteracting obesity-induced adipose inflammation.

2.3.5 Otop1 interacts with STAT1 and attenuates IFNγ signaling in adipocytes

To explore the molecular mechanisms by which Otop1 modulates IFNγ signaling, we ectopically expressed Flag-HA-tagged Otop1 in 3T3-L1 and immortalized brown preadipocytes and performed immunoaffinity purification of the Otop1 protein complexes. Mass spectrometry and immunoblotting analyses indicated that Otop1 physically interacted with STAT1 (Figure 2.9A,B), a transcription factor that plays a critical role in IFNγ signaling (Stark and Darnell, 2012). The interaction between Otop1 and STAT1 appears to be independent of STAT1 phosphorylation (Figure 2.9B). To determine whether the exacerbation of adipose tissue inflammation in Otop1 mutant mice results from cell-autonomous effects of Otop1 on inflammatory signaling, we first examined the response of WT and Otop1 mutant adipocytes to IFNγ treatments. Because brown adipocytes express endogenous Otop1, we immortalized brown preadipocytes from WT and Otop1 mutant neonates and performed studies following adipocyte differentiation. As expected, IFNγ treatments strongly induced tyrosine phosphorylation of STAT1, STAT3, and STAT5, but only had modest effects on the NFkB and IKKε/TBK1 pathways (Figure 2.9C). Total and phosphorylated STAT3 and STAT5 proteins were comparable between WT and Otop1 mutant adipocytes. In contrast, total STAT1 protein levels were elevated in mutant adipocytes, resulting in more robust tyrosine phosphorylation in response to IFNγ treatments.

We performed microarray studies to identify downstream pathways that were affected by Otop1 mutation. Consistent with the eWAT gene expression profile, the expression of a large number of IFNγ target genes, including Oasl1, Oasl2, Ifi44, Ifitm3, and Ifih1, was significantly elevated in Otop1 mutant adipocytes compared to control (Figure 2.10A). In response to IFNγ treatments, mRNA expression of these target genes was induced to higher levels in Otop1 mutant adipocytes

compared to WT control (Figure 2.10B). These results strongly suggest that Otop1 attenuates IFNγ signaling in adipocytes through its physical interaction with STAT1.

We further assessed whether ectopic overexpression of Otop1 attenuates the IFNγ/STAT1 signaling pathway in adipocytes. We treated differentiated brown adipocytes expressing vector or Otop1 with IFNγ and examined STAT1 protein levels and phosphorylation. Compared to vector, Otop1 overexpression significantly decreased total STAT1 protein levels and phosphorylated STAT1 following IFNγ stimulation (Figure 2.11A). In contrast, protein levels of STAT3, NFkB, and IKKε/TBK1 remained largely unaltered by Otop1. Basal STAT5 phosphorylation is slightly lower in adipocytes overexpressing Otop1, yet the differences disappeared after IFNγ treatment. Consistent with decreased STAT1 levels, basal expression of IFNγ targets such as Ifi44, Oasl1, Oasl2, and Ifih1, was reduced by retroviral-mediated overexpression of Otop1 (Figure 2.11B). Further, the induction of these genes in response to IFNγ was also significantly dampened in Otop1-overexpressing adipocytes. Taken together, we conclude that Otop1 negatively regulates IFNγ signaling in adipocytes and may serve to counteract chronic proinflammatory immune response in obese adipose tissues.

2.4 Discusion

The pathogenic role of chronic inflammation in the development of obesity-associated metabolic disease has been well established. Attenuation of inflammatory signaling generally resulted in improved metabolic profiles in rodent models of obesity. While counter-inflammation has been proposed as a key aspect of homeostatic regulation (Saltiel, 2012), the molecular components of this negative feedback arm remain elusive. In this study, we identified Otop1 as an obesity-

induced target of cytokine signaling in WAT. Otop1 mutant mice develop more severe diet-induced insulin resistance and hepatic steatosis that are accompanied by augmented adipose tissue inflammation. Otop1 interacts with Stat1 and attenuates IFNγ signaling in adipocytes in a cell-autonomous manner. Together, these studies illustrate a novel pathway that counteracts obesity-associated chronic inflammation and preserves metabolic homeostasis in obesity (Figure 2.12).

A remarkable aspect of Otop1 expression in WAT is that it is highly induced during obesity. Thus, mRNA levels of Otop1 in WAT correlate tightly with the degree of HFD-induced obesity. Elevated expression of Otop1 was also observed in white fat depots from db/db mice. While it is possible that the induction of Otop1 expression in obese adipose tissues may result from changes in cell populations in WAT, gene expression analyses in fractionated adipocytes and stromal vascular cells indicated that Otop1 induction occurred exclusively in adipocytes. Otop1 mRNA was nearly undetectable in the stromal vascular fraction. The stimuli that drive obesity-associated induction of Otop1 in adipocytes may be multifaceted in nature. In cultured 3T3-L1 adipocytes, the proinflammatory cytokine TNFα, but not IFNγ and LPS, strongly induced Otop1 expression in a dose-dependent manner, suggesting that Otop1 is likely a target downstream of a subset of proinflammatory signals.

Otop1 mutant mice developed diet-induced obesity at similar pace compared to controls, suggesting that Otop1 does not play a major role in the regulation of whole body energy balance. A surprise here is that the mutant mice developed more severe insulin resistance and hepatic steatosis. Because Otop1 expression was not detected in the liver in lean and obese mice, the

exacerbation of liver fat accumulation in HFD-fed Otop1 mutant mice was most likely secondary to the metabolic perturbations that occurred in mutant adipose tissues. In support of this, we found that the formation of crown-like structures, which are indicative of adipocyte death and inflammatory response, was accelerated in Otop1 mutant adipose tissue. The increase in crown-like structures was accompanied by a shift in macrophage polarization toward a proinflammatory subtype. Accordingly, mRNA and protein markers of inflammatory signaling were also elevated in Otop1 mutant eWAT following HFD-feeding. These observations are consistent with a critical role for Otop1 in attenuating obesity-associated inflammation. This mechanism is apparently distinct from the counterinflammatory actions of noncanonical IKKs, i.e. IKKε and TBK1, which are induced in obesity to sustain chronic inflammation in adipose tissue (Chiang et al., 2009; Reilly et al., 2013). Recent studies have also implicated GPR120 as a sensor for anti-inflammatory fatty acids with insulin-sensitizing effects (Oh et al., 2010). However, GPR120 appears to act primarily in macrophages. As such, concerted activation of counter-inflammation in both adipocytes and immune cells is required for maintaining normal adipose tissue function and metabolic homeostasis.

The mechanisms by which Otop1 exerts its anti-inflammatory effects appear to be mediated, at least in part, by attenuating IFNγ signaling in adipocytes. IFNγ is primarily produced by natural killer and T cells and plays an important role in M1 macrophage activation (Hu and Ivashkiv, 2009). IFNγ also directly activates its receptors on adipocytes and elicits its effects on cytokine expression and metabolism (McGillicuddy et al., 2009; Wada et al., 2011). Interestingly, IFNγ deficient mice have an improved metabolic profile following HFD feeding (O'Rourke et al., 2012; Rocha et al., 2008), suggesting that excess IFNγ signaling may have deleterious effects on

adipose tissue function and systemic metabolism. The expression of a number of IFNγ target genes was elevated in Otop1 mutant eWAT. Importantly, the inhibitory effects of Otop1 on IFNγ target gene expression appears to be cell-autonomous, as Otop1 mutant adipocytes have elevated expression of these genes at baseline. In response to IFNγ treatments, the induction of these genes was further augmented. In contrast, overexpression of Otop1 in adipocytes significantly blunted IFNγ-induced gene expression. These gain- and loss-of-function studies suggest that exacerbated adipose tissue inflammation in Otop1 mutant mice is likely due to augmented proinflammatory cytokine signaling in adipocytes. At the molecular level, Otop1 physically interacts with STAT1, a downstream transcription factor essential for IFNγ signaling, and selectively reduces STAT1 protein expression in adipocytes. The biochemical mechanisms underlying the downregulation of STAT1 by Otop1 remain currently unknown.

Previous studies have established the framework for the involvements of chronic inflammation in the pathogenesis of obesity-related adipose tissue dysfunction and metabolic disease. However, surprisingly little is known about potential activation of anti-inflammatory pathways that may counterbalance excess inflammation in the state of overnutrition. Disruption of the proinflammatory signaling cascades via genetic or pharmacological means has been proven effective in mitigating metabolic disease. As such, it is only logical to speculate that a putative component of the anti-inflammatory arm is itself a target of inflammatory signaling and that the deficiency of this counter-regulatory arm may worsen obesity-induced metabolic disorders. Thus, Otop1 is likely a component of a novel counter-inflammatory signaling pathway that maintains adipose immune homeostasis in obesity. Activation of this adaptive pathway may provide metabolic benefits in obesity.

2.5 Future direction

2.5.1 Detecting endogenous Otop1 at protein level

Although we were able to show Otop1 mRNA expression significantly induced in WAT in obese conditions, it is also important to know to what extend Otop1 expression is increased at protein level, as protein is the ultimate functional form that mediates all the anti-inflammatory effects of Otop1. Generation of good Otop1 antibody is necessary for testing interaction between endogenous Otop1 and endogenous STAT1 in adipose tissues under physiological and pathological conditions. Fasting and feeding, quiescence and inflammation, on the other hand, may provide another layer of regulation on Otop1-STAT1 interaction.

2.5.2 How does Otop1 affect STAT1 expression/phosphorylation

According to Figure 2.9 and Figure 2.11, Otop1 attenuates IFNγ signaling mainly through down-regulating STAT1 protein level. Although absolute phospho-STAT1 at tyr701 is decreased, the ratio between phosphorylated STAT1 and total STAT1 seems unaffected by Otop1 expression. STAT1 is relatively stable, yet it can still be ubiquitinated and targeted to proteasomal degradation (Tanaka et al., 2005). STAT1 also binds to its own promoter to stimulate transcription of itself in a positive feedback loop (Hu et al., 2008). Therefore it is possible that Otop1 overexpression may lead to increased STAT1 ubiquitination, or sequester phosphorylated STAT1 in cytosol to prevent its transcriptional amplification, both providing mechanisms for STAT1 downregulation.

2.5.3 Involvement of Ca^{2+}

Otop1 overexpression has been to shown to reduce Ca^{2+} influx in response to purinergic stimuli (Hughes et al., 2007b). And in the macular cells expressing mutant Otop1 (Otop1^{tlt}), calcium influx peak in response to ATP is significantly increased (Kim et al., 2011b). Taken into account it has 12 transmembrane domains (Hughes et al., 2008a), Otop1 may very likely function as a Ca^{2+} transporter. IFNγ has been shown to elicit Ca^{2+} influx in many cell types (Aas et al., 1998; Chang et al., 2004; Kung et al., 1995). Activation of Ca^{2+} dependent CaMKII potentiates type I IFN stimulated STAT1 activation in macrophages (Wang et al., 2008), while BAPTA-AM, an intracellular Ca^{2+} chelator, completely blocked C-peptide induced STAT1 phosphorylation (Lee et al., 2010). Therefore it is possible that Otop1 overexpression suppresses STAT1 phosphorylation through decreasing intracellular Ca^{2+} levels, while in the Otop1^{tlt} adipocytes, increase in Ca^{2+} influx in response to IFNγ leads to increased STAT1 phosphorylation. One direct way to prove this hypothesis is Ca^{2+} imaging, which is technically challenging due to the difficulty of loading Fura-2-acetoxymethyl ester into the adipocytes. Yet CaMKII inhibitors and Ca^{2+} chelator treatment could give us a clue as for whether Ca^{2+} is involved in Otop1's effects on IFNγ stimulated STAT1 phosphorylation and target gene expression.

2.5.4 Creating fat specific Otop1 transgenic mice

In this chapter we concluded that Otop1 attenuates adipose tissue inflammation based on the *in vivo* observation that the mutant mice had worsened metabolic phenotype due to increased adipose tissue inflammation primed by enhanced response to IFNγ stimuli, and overexpression of Otop1 in cultured adipocytes is able to suppress such response. However, a definitive study on the role of Otop1 in suppressing adipose tissue inflammation requires generation of fat specific otop1 transgenic mice. Moreover, Otop1 overexpression *in vitro* seems to inhibit 3T3-L1

adipogenic differentiation, whether the same thing holds true *in vivo* and whether it contributes to the anti-inflammatory effect of Otop1 still awaits further exploration.

2.6 Material and methods

2.6.1 Animals and animal care

All animal studies were performed following the guideline established by the University Committee on Use and Care of Animals at the University of Michigan. Mice were housed in a specific pathogen-free facility at 77 ºF with a 12-h light, 12-h dark cycle and free access to food and water. For chow diet feeding, male wild-type C57BL/6J mice and Otop1^{tlt} mice were fed with Teklad 5001 lab diet. For HFD feeding, mice were fed with a diet consisting 60% of calories from fat (D12492, Research Diets Inc.) starting at 10 to 12 weeks of age.

2.6.2 Adipocyte isolation and differentiation

Immortalization and differentiation of brown adipocytes were performed as described (Klein et al., 1999). Briefly, SV40 large T antigen-immortalized brown preadipocytes were cultured in DMEM with 10% fetal bovine serum (FBS). Differentiation was induced two days post confluence (day 0) by adding a cocktail containing 0.5mM IBMX, 125μM indomethacin, 1μM dexamethasone to the maintenance media (DMEM supplemented with 10% FBS, 20nM insulin and 1nM T3). Two days after induction, cells were cultured in the maintenance media alone. Total RNA was isolated at different days for gene expression analysis.

3T3-L1 fibroblasts were cultured in DMEM with 10% bovine growth serum (BGS) until two days post confluent. Differentiation was induced by adding a cocktail containing 0.5mM IBMX,

1μM dexamethasone and 1μg/mL insulin to DMEM supplemented with 10% FBS. Three days after induction, cells were cultured in DMEM containing 10% FBS plus 1μg/mL of insulin for two more days followed by maintenance in DMEM supplemented with 10% FBS. TNFα, IFNγ and LPS treatment were carried out in mature adipocytes cultured in the maintenance media.

2.6.3 Adipose tissue explant culture

Epididymal WAT was dissected and transferred to a petri dish with 20mL DMEM, cut into pieces with diameters less than 4mm (about 5-10mg). Tissue pieces were filtered through 200μm nylon mesh, washed once with 10x volume of PBS and then with 10x volume of DMEM, transferred into 6-well plates with serum-free M199 media (1nM insulin, 1nM Dex), and cultured for 2 hrs before IFNγ treatment at 10ng/mL for 4hrs. Following treatments, fat tissues were quickly dried on paper towels and processed for RNA isolation and qPCR gene expression analysis.

2.6.4 Metabolic and gene expression analyses

Plasma concentrations of free glycerol and triglycerides (Sigma), β-hydroxybutyrate (Stanbio Laboratory), and non-esterified fatty acid (Wako Diagnostics) were measured using commercial assay kits. Liver triglyceride was extracted and measured as previously described (Li et al., 2008). Plasma insulin was measured using an ELISA kit (CrystalChem). Glucose and insulin tolerance tests were performed as previously described (Molusky et al., 2012). For insulin signaling studies, mice were fed HFD for 8 weeks before receiving a single dose of intravenous injection of saline or insulin (1.5 U/kg). Tissues were rapidly dissected 10 min after injection for immunoblotting analyses.

For gene expression analysis, total RNA from white adipose tissue was extracted using a commercial kit from Invitrogen. Total RNA from other tissues and cultured cells was extracted using TRIzol method. For quantitative real-time PCR (qPCR) analysis, equal amount of RNA was reverse-transcribed using MMLV-RT followed by quantitative PCR reactions using SYBR Green (Life Technologies). Relative abundance of mRNA was normalized to ribosomal protein 36B4. Adipose tissue and liver gene expression was analyzed using specific primers (Table 2.S1). Statistical significance was determined by Student's t-test.

2.6.5 Immunoblotting analyses

Tissues were homogenized in a lysis buffer containing 50 mM Tris (pH 7.5), 150mM NaCl, 5mM NaF, 25mM β-glycerolphosphate, 1mM sodium orthovanadate, 10% glycerol, 1% tritonX-100, 1 mM dithiothreitol (DTT), and freshly added protease inhibitors. Immunoblotting experiments were performed using specific antibodies and visualized on film using horseradish peroxidase–conjugated secondary antibodies (Sigma and Cell Signaling) and Western Chemiluminescent HRP Substrate (Millipore). Phospho-STAT1 (Y701), phospho-STAT3 (Y705), phospho-STAT5 (Y694), STAT1, STAT3, STAT5, phospho-TBK1 (S172), TBK1, NFκB-p65, phospho-NFκB-p105 (Ser933), NFκB-p105, phospho-Akt (Ser473), phospho-Akt (T308), Akt antibody were purchased from Cell Signaling Technology. Antibodies against PPARγ (Santa Cruz Biotechnology), HA (sc-66181), Flag (Sigma), and tubulin (Sigma) were used.

2.6.6 Affinity purification of Otop1 protein complex

Total cell lysates were prepared from mature brown adipocytes stably express MSCV-vector or MSCV- Flag-HA-Otop1. Sequential steps of affinity purification was performed using anti-HA (Roche) and anti-Flag (Sigma) affinity matrix followed by eluting with 200 μg/ml HA and Flag peptides, respectively. Eluted protein complex was analyzed by SDS-PAGE. Following colloidal blue staining, individual bands were excised for protein identification by mass spectrometry.

2.6.7 FACS analysis

Adipose tissue fractionation, flow cytometry analysis, and whole mount immunofluorescence staining were performed as previously described (Lumeng et al., 2007a; Lumeng et al., 2007b). Blood leukocytes and SVCs were incubated in Fc Block (rat anti-mouse CD16/32; eBioscience) for 10 min and then stained with CD45-e450, CD11b-APC-Cy7, CD11c-PE-Cy7, CD301-APC and F4/80-PE (eBioscience) or appropriate isotype controls for 30 min. Labeled cells were then washed twice with FACS buffer followed by fixation in 1% paraformaldehyde in PBS. Cells were analyzed on FACSCanto II Flow Cytometer (BD Bioscciences) using FlowJo software (Version 9.6; Treestar). For whole mount immunostaining, adipose tissue samples were fixed with 1% paraformaldehyde and stained with anti-caveolin and anti-Mac2 antibodies in PBS-T/BSA. Samples were imaged on an inverted confocal microscope using FluoView software (Olympus).

2.6.8 Statistics

Data were analysed using two-tailed Student's *t*-test for independent groups. A p-value of less than 0.05 was considered statistically significant.

Figure 2.1 Otop1 is dispensable for cold-induced adaptive thermogenesis
(A) qPCR analysis of Otop1 expression in mouse tissues using pooled RNAs from three mice. Data represent mean ± s.e.m. (B) Time-course mRNA expression of Otop1 and Ucp1 during brown adipocyte differentiation. Data represent mean ± s.d. from triplicate wells. (C) qPCR analysis of BAT gene expression in mice exposed to ambient room temperature (RT, n=3) or 4ºC for 6 hrs (cold, n=3). (D) qPCR analysis of BAT gene expression in mice housed at room temperature (RT, n=5) or acclimated to 4ºC (Acc, n=5). (E) Rectal body temperature in WT (open, n=8) and Otop1^{tlt} mice (filled, n=6) during cold exposure. (F) H&E staining of BAT from WT and Otop1^{tlt} mice housed at room temperature (RT) or 4ºC for 6 hrs (Cold). Scale bar indicates 100 μm. (G) qPCR analysis of BAT gene expression in cold-exposed mice in E. Data in panels C-E and G represent mean ± s.e.m. *p<0.05, **p<0.01, cold vs. RT. (H) Immunoblots of total BAT lysates. Tubulin was included as a loading control.

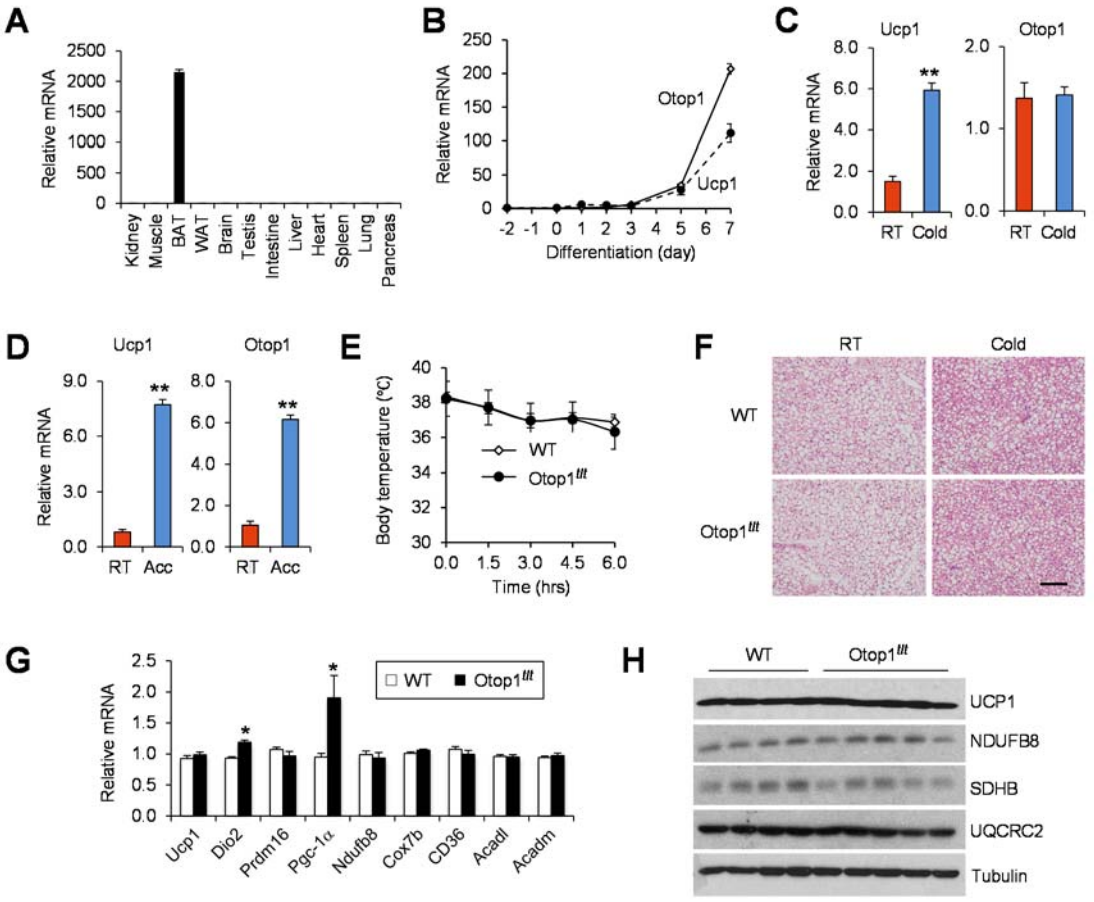

Figure 2.2 Otop1 is induced in obese white adipose tissues
(A) qPCR analysis of Otop1 expression in WAT from WT mice fed chow (n=5) or HFD (n=6) for three months, and from a separate group of WT (n=4) and db/db mice (n=4). (B-D) qPCR analysis of Otop1 expression in BAT, liver and skeletal muscle from above mentioned mice. Data represent mean ± s.e.m. *p<0.01, obese vs. lean.

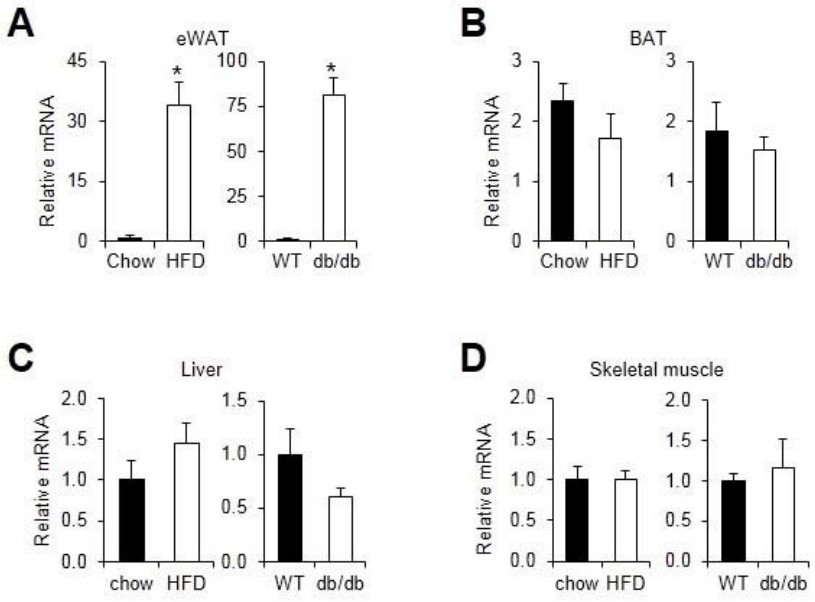

Figure 2.3 Proinflammatory cytokines induce Otop1 expression in obese WAT
(A) Correlation of eWAT Otop1 expression with body weight. Relative Otop1 mRNA levels were plotted against respective body weight. (B) qPCR analysis of stromal vascular (SVF) and mature adipocyte (Adi) fractions isolated from eWAT from mice fed chow (n=3) or HFD (n=3). Data represent mean ± s.e.m. *p<0.01, obese vs. lean. (C) qPCR analysis of 3T3-L1 adipocytes treated with indicated concentrations of TNFα for 6 hrs. (D-E) qPCR analysis of 3T3-L1 adipocytes treated with IFNγ (D) or LPS (E) for 6 hrs. Data in D-F represent mean ± s.d. from one representative study performed in triplicate wells. *p<0.01, vs. saline.

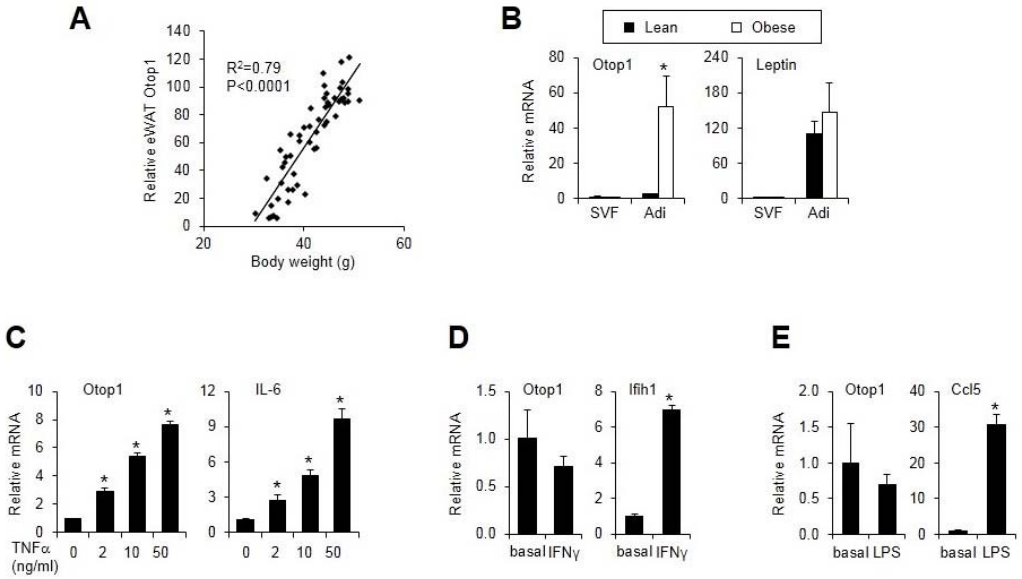

Figure 2.4 Otop1^{tlt} mutant mice develop more severe HFD-induced insulin resistance
(A) Body weight of WT (open diamond, n=8) and Otop1^{tlt} mice (filled circle, n=8) during HFD feeding. (B) Plasma concentrations of β-hydroxybutyrate, NEFA, and triglycerides after overnight fasting. (C) Plasma glucose and insulin levels under fed and fasted conditions. (D) Insulin tolerance test in WT (n=6) and Otop1^{tlt} mice (n=7) in HFD-fed mice. (E) Glucose tolerance test in WT (n=8) and Otop1^{tlt} mice (n=8) 9 weeks after HFD-feeding. Data represent mean ± SEM. *p<0.05, Otop1^{tlt} vs. WT.

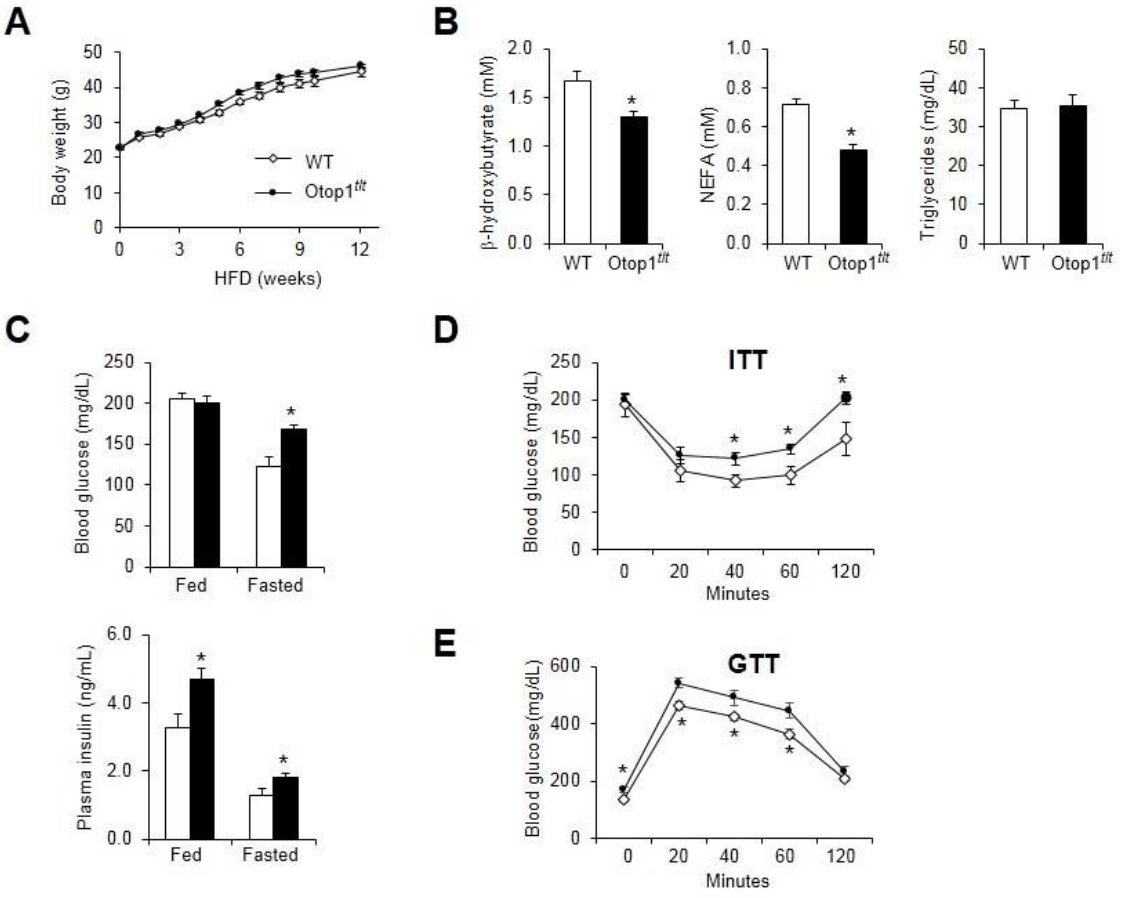

Figure 2.5 Impaired insulin-stimulated AKT phosphorylation in Otop1^{tlt} mouse tissues
8 weeks after HFD feeding, tissues were harvested from WT and Otop1^{tlt} mice 10 minutes after a single intravenous injection of saline or insulin. Immunoblots of total tissue lysates (left). Quantitation of phosphorylated AKT was performed following normalization to total AKT levels (right). *p<0.05, Otop1^{tlt} vs. WT.

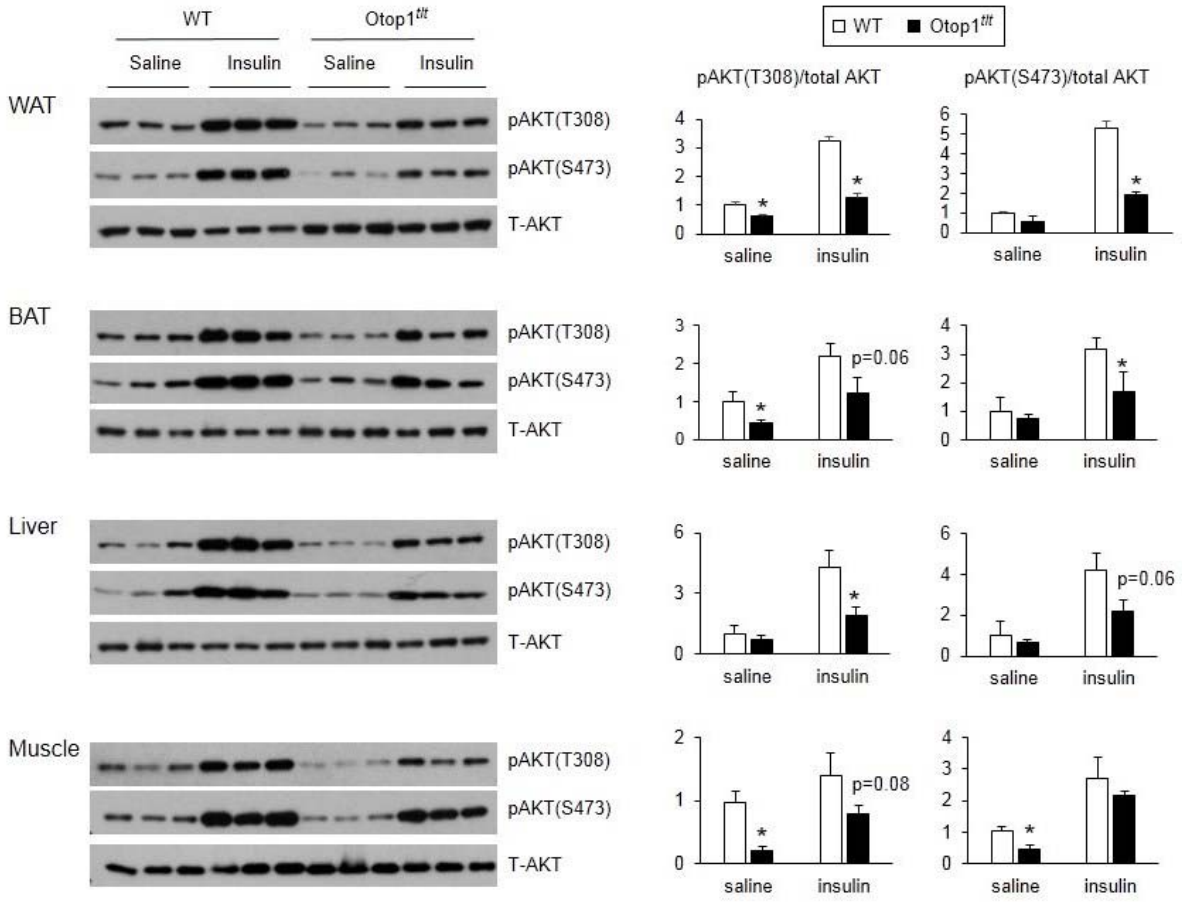

Figure 2.6 Otop1^{tlt} mutant mice develop more severe diet-induced hepatic steatosis
(A) H&E staining of liver sections in WT and Otop1^{tlt} mice fed chow or HFD for different periods of time (scale bar=100 μm). (B) SRS imaging of liver sections. Arrows indicate lipid droplets (scale bar=25 μm). (C) Liver/body weight ratio and liver triglyceride content in WT (open, n=8) and Otop1^{tlt} mice (filled, n=8) after three months HFD feeding. (D) qPCR analysis of hepatic gene expression in WT (open) and Otop1^{tlt} mice (filled). Data in C-D represent mean ± s.e.m. *p<0.05, Otop1^{tlt} vs. WT.

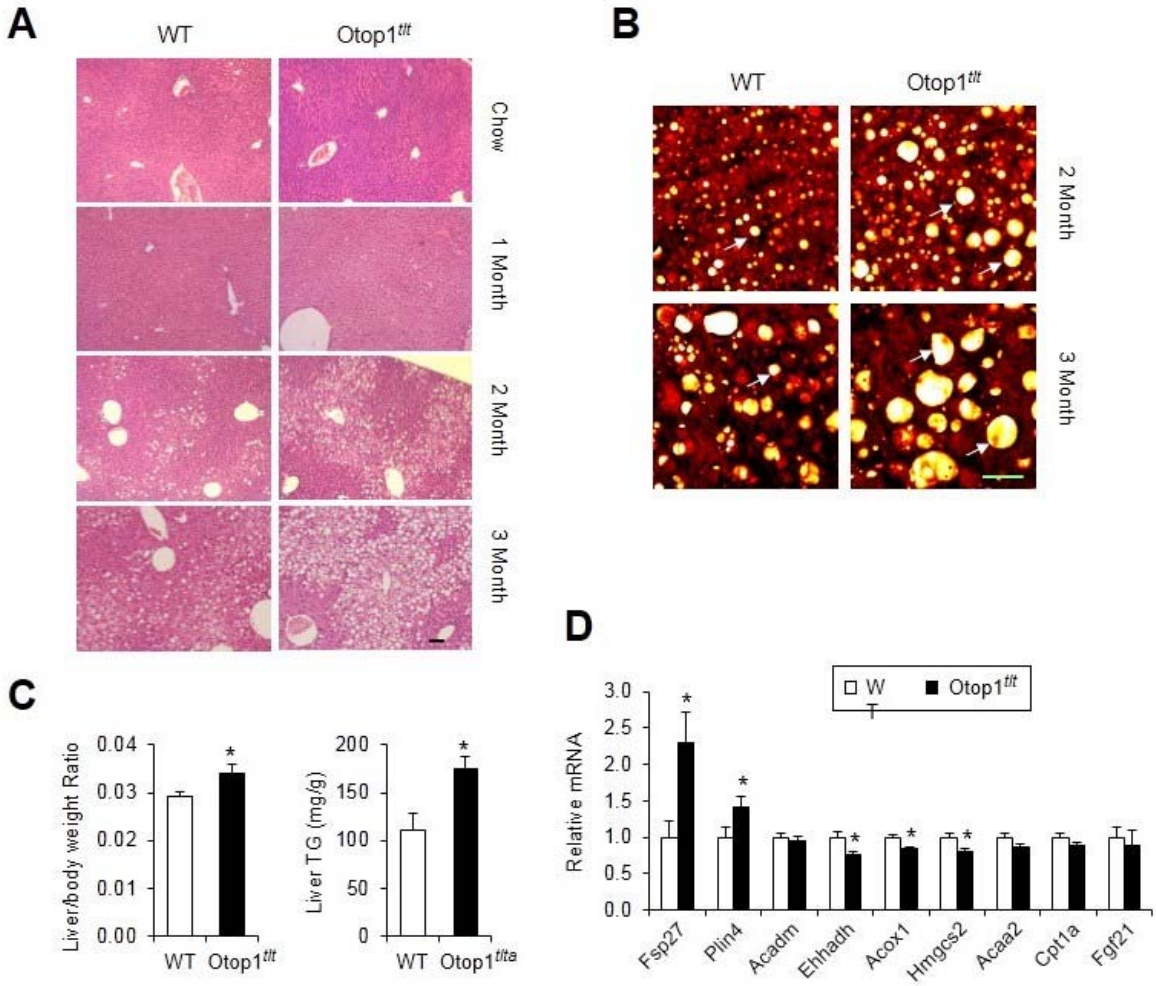

Figure 2.7 Otop1 mutant mice have exacerbated adipose tissue inflammation following HFD-feeding

(A) H&E staining of eWAT from WT and Otop1^{tlt} mice fed chow or HFD for different periods of time. Scale bar indicates 100 μM. (B) Confocal images of eWAT following whole mount immunofluorescence staining using Caveolin (green) and Mac2 (red) antibodies (scale bar=50 μm). (C) H&E staining of BAT from WT and Otop1^{tlt} mice fed with HFD for 3 months. (D) Flow cytometry analyses of adipose tissue macrophages (ATM) in stromal vascular fraction (SVF) of eWAT from HFD-fed WT (open, n=8) and Otop1^{tlt} (filled, n=7) mice. (E) Flow cytometry analyses of adipose tissue macrophage (ATM) in iWAT from mice in (D). Data in D-E represent mean ± s.e.m. *p<0.05, $^{\#}$ p<0.1, Otop1^{tlt} vs. WT.

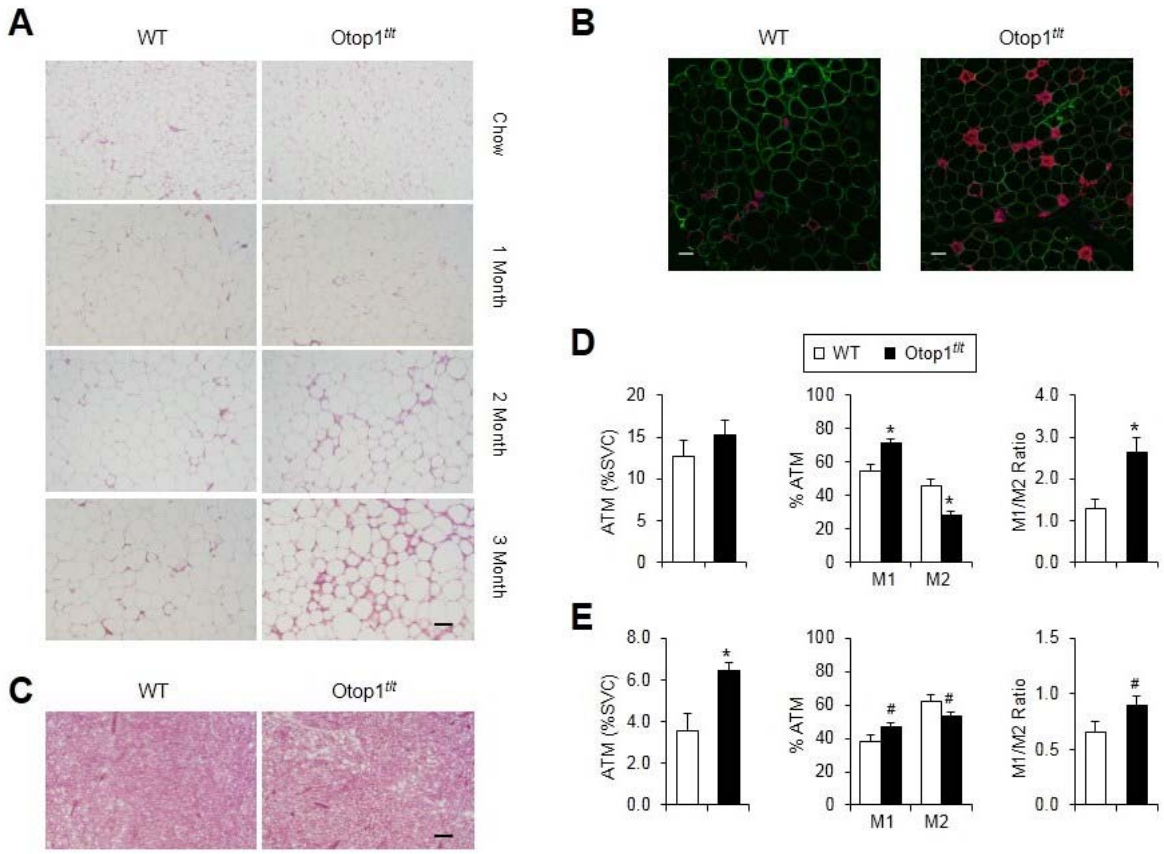

Figure 2.8 Otop1 negatively regulates WAT inflammation and IFNγ response
(A) Immunoblots of inflammation markers in total eWAT lysates from HFD-fed mice. Fold change in Otop1^{tlt} samples was quantitated following normalization to tubulin. *p<0.05, Otop1^{tlt} vs. WT. (B) qPCR analysis of eWAT and iWAT gene expression in HFD-fed WT (open, n=8) and Otop1^{tlt} mice (filled, n=8) for 3 months. Data represent mean ± s.e.m. *p<0.05, Otop1^{tlt} vs. WT. (C) qPCR analysis of epididymal fat explants from HFD fed WT and Otop1^{tlt} mutant mice without or with IFNγ stimulation. Data represent mean ± s.d. from triplicate wells. *p<0.05, Otop1^{tlt} vs. WT.

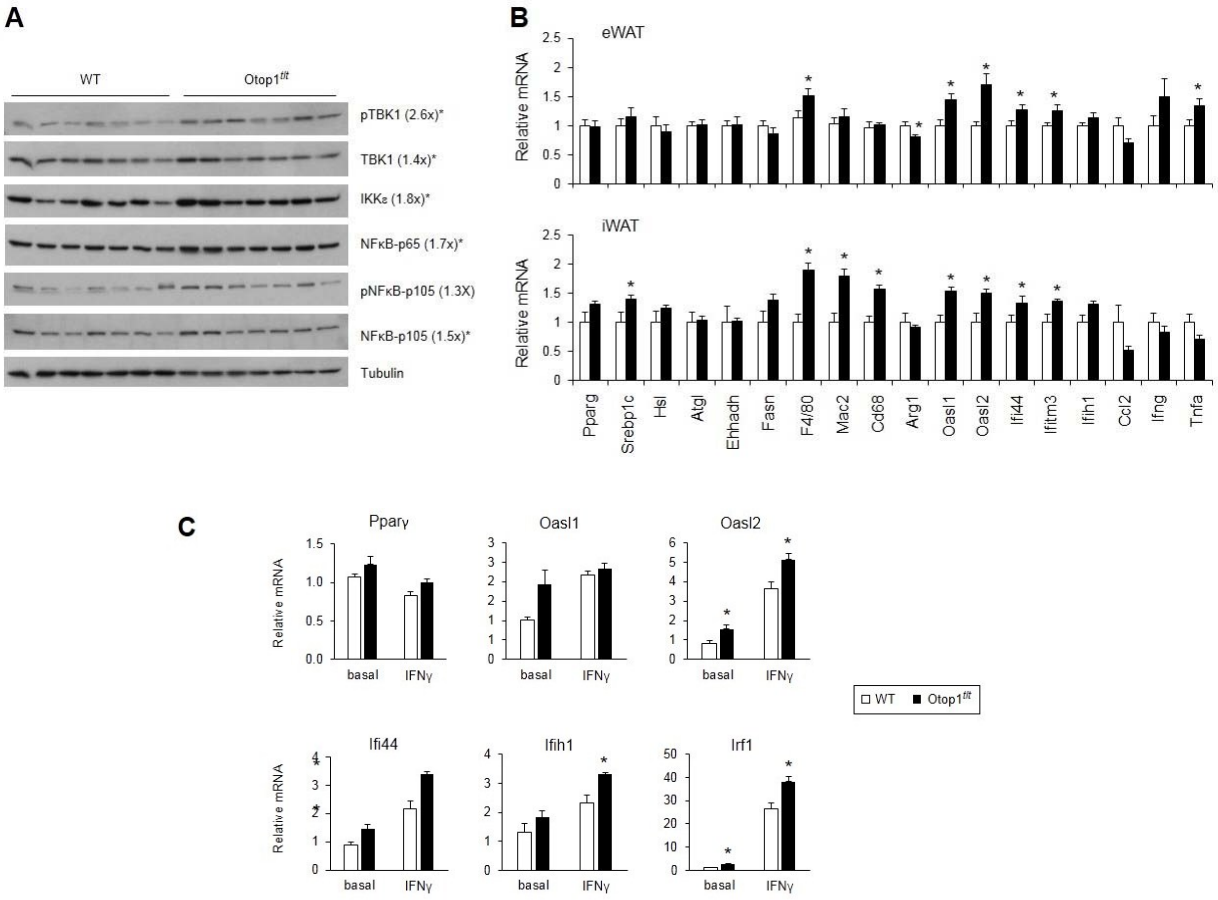

Figure 2.9 Otop1 physically interacts with STAT1 and regulates IFNγ response in adipocytes

(A-B) Immunoblots of total cell lysates and immunoprecipitated proteins (anti-HA) from differentiated 3T3-L1 adipocytes (A) or brown adipocytes (B) stably expressing vector or Flag-HA-tagged Otop1 (FHO) and treated with vehicle or IFNγ. (C) Immunoblots of total cell lysates from brown adipocytes stably expressing vector (Vec) or Otop1 treated with saline (-) or IFNγ for indicated time.

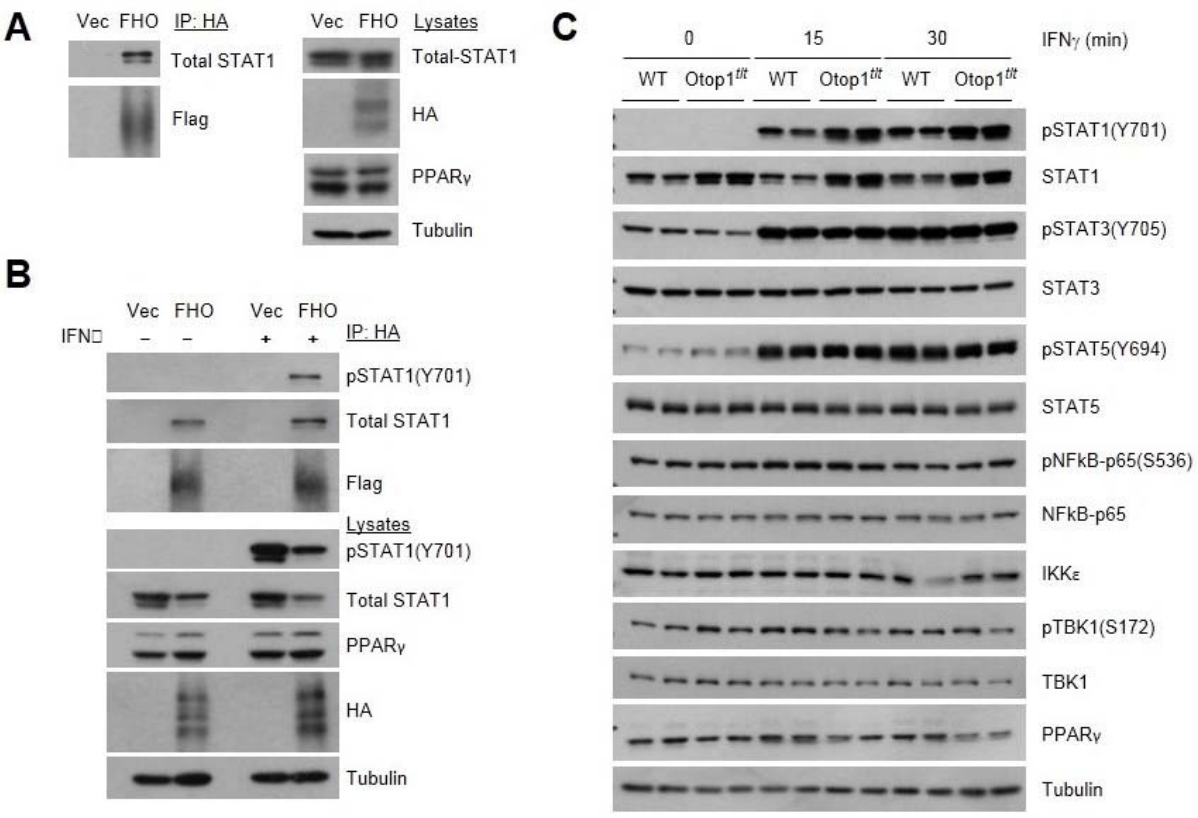

Figure 2.10 IFNγ signaling is augmented in Otop1^{tlt} mutant adipocytes
(A) Clustering analysis of IFNγ target genes in differentiated WT and Otop1^{tlt} brown adipocytes. (B) qPCR analysis of gene expression in differentiated adipocytes treated with saline (-) or 10 ng/mL IFNγ (+) for 4 hrs. Data represent mean ± s.d. from triplicate wells. *p<0.05, Otop1^{tlt} vs. WT.

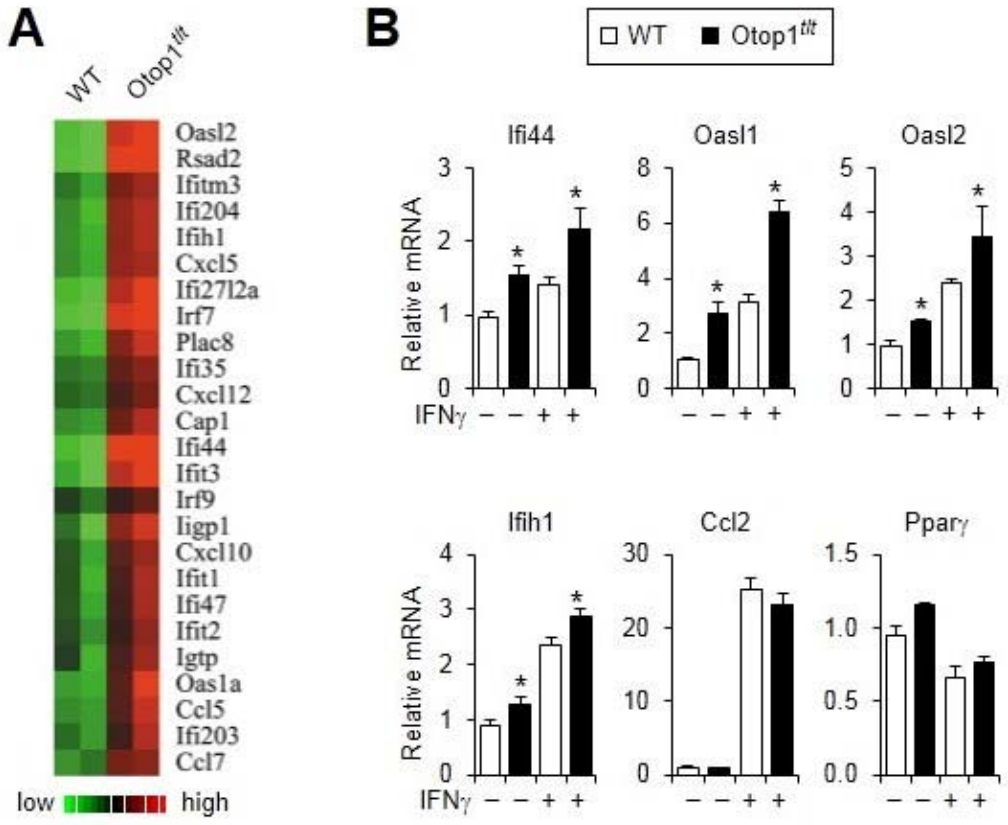

Figure 2.11 Otop1 attenuates IFNγ signaling in adipocytes
(A) Immunoblots of total cell lysates from brown adipocytes stably expressing vector (Vec) or Otop1 treated with saline (-) or IFNγ for 15 or 30 minutes. (B) qPCR analysis of gene expression in differentiated brown adipocytes stably expressing vector (open) or Otop1 (filled) treated with saline or 10 ng/ml IFNγ for 4 hrs. Data represent mean ± s.d. from triplicate wells. *p<0.05, Otop1 vs. vector.

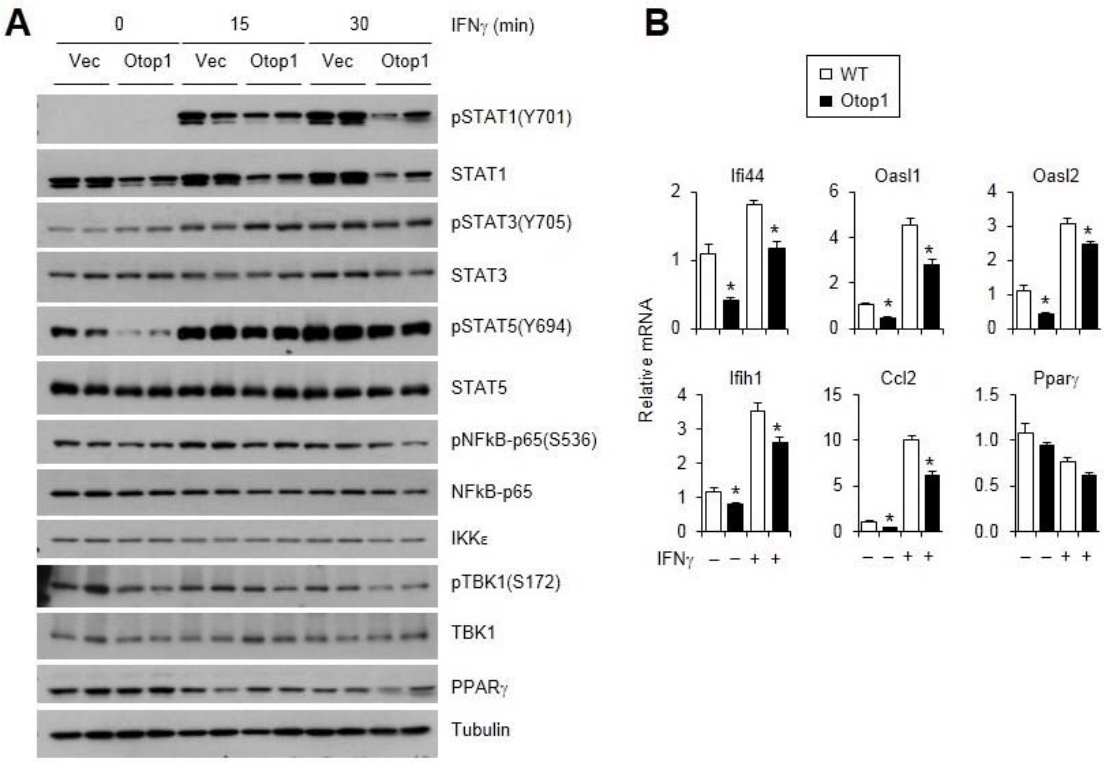

Figure 2.12 Model depicting the role of Otop1 in counteracting obesity-associated inflammation in adipocytes

Otop1 expression is induced by TNFα in white fat during obesity. The induction of Otop1 serves to attenuate proinflammatory cytokine signaling in adipocytes, maintain adipose tissue function, and systemic metabolic homeostasis.

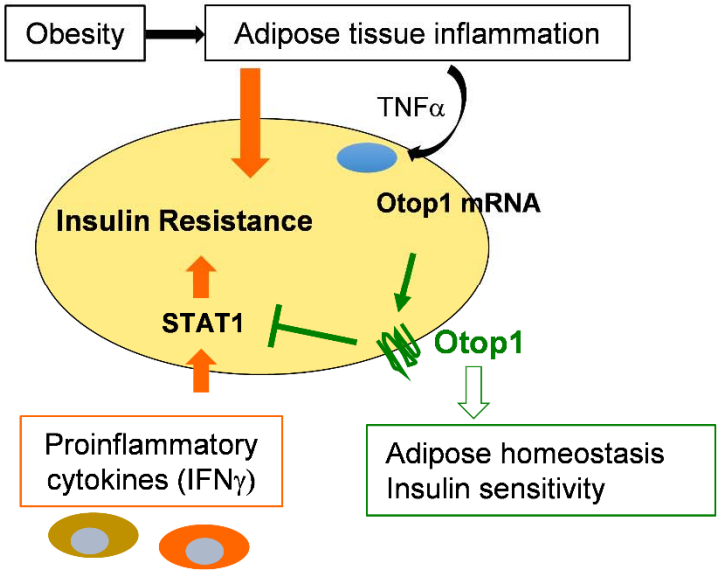

Table 2.S1 List of qPCR primers

Gene name	Forward	Reverse
Otop1	GACAACCCGATGTCTGGACT	GCCAAAGACAATTTCCTCCA
UCP1	GGCATTCAGAGGCAAATCAGCT	CAATGAACACTGCCACACCTC
Dio2	GATGCTCCCAATTCCAGTGT	TGAACCAAAGTTGACCACCA
Prdm16	CGGAAGAGCGTGAGTACAAATG	TCCGTGAACACCTTGACACAGT
PGC1α	AGCCGTGACCACTGACAACGAG	GCTGCATGGTTCTGAGTGCTAAG
Ndufb8	GGCACGTGTTCCCTTCCTAC	CCGCTCCAGGTACAGATTATTGT
COX7B	CGCAGTTCCATCTTCGTCTC	GCATTCCCATATTTGTCATG
CD36	TTAGATGTGGAACCCATAACTGGA	TTGACCAATATGTTGACCTGCAG
AcadL	TGCACACATACAGACGGTGCAG	TCAGATGCCCAGTATTTTGCC
Acadm	GCTGGAGACATTGCCAATCA	GGCGTCCCTCATCAGCTTCT
Leptin	AGCAGTGCCTATCCAGAA	TGCCAGAGTCTGGTCCATCT
iNos	GAGGCCCAGGAGGAGAGAGATCCG	TCCATGCAGACAACCTTGGTGTTG
IL6	AGTTGCCTTCTTGGGACTGA	TCCACGATTTCCCAGAGAAC
CCL5	TGCCCACGTCAAGGAGTATTT	TTCTCTGGGTTGGCACACACT
IFih1	TCCTGGATGTTCTGCGCCAA	GACGAGTTAGCCAAGTCTGTGTT
FSP27	TCGACCTGTACAAGCTGAACCCT	AGGTGCCAAGCAGCATGTGACC
Plin4	GCTCCACCTCCACAAAGGAC	GATGCCAAACACCCCAGAG
Ehhadh	CAGATGAAGCACTCAAGCTTG	ACCTTGGCAATGGCTTCTGCA
Acox1	GCCTGCTGTGTGGGTATGTCATT	GTCATGGGCGGGTGCAT
HMGCS2	GACATCAACTCCCTGTGCCTG	GATGTCAGTGTTGCCTGAATC
CPT1α	GAGAAATACCCTGACTATGTG	TGTGAGTCTGTCTCAGGGCTAG
FGF21	CTGGGGGTCTACCAAGCATA	CACCCAGGATTTGAATGACC
PPARγ	CCGTAGAAGCCGTGCAAGAG	GGAGGCCAGCATCGTGTAGA
SREBP1c	ATCGGCGCGGAAGCTGTCGG	GGGAAGTCACTGTCTTGGTTG
HSL	GAGACACCAGCCAACGGATAC	TTTTGCGGTTAGAAGCCACAT
ATGL	TGGGCCAGCAGATATGTTTG	GAATCCGGACCTGGTGCAT
GyK	GTCAGCAACCAGAGGGAAAC	TGTCAAGGAGCCAACGAAG
FASN	GGTTACACTGTGCTAGGTGTTG	TCCAGGCGCATGAGGCTCAGC
Arg1	ACACGGCAGTGGCTTTAACC	TGGCGCATTCACAGTCACTT
OASL1	TGTGGCAGAAGGCTACAGATG	ATATCGGGTGCTCTCTTCACC
OASL2	TGCCTGGGAGAGAATCGAGA	AGCCTCCCTTCACCACCTTA
IFi44	AGCCCTATGGAGACCTGGTT	AGCTAGACTTCCCAGCTCCA
IFiTM3	CTGAGAAACCGAAACTGCCG	AGTGTGGTTCATGGTGCGGA
IRF1	GCCATTCACACAGGCCGATA	CGATGTCTGGCAGGGAGTTC
CCL2	AGGTCCCTGTCATGCTTCTG	TCTGGACCCATTCCTTCTTG
TNFα	AGCCCCCAGTCTGTATCCTT	CTCCCTTTGCAGAACTCAGG
IFNγ	GCTGATCCTTTGGACCCTCT	GCAAAGCCAAGATGCAGTGT
F4/80	ATCCTTGGCCATCCGGCAGA	GCAAAGCCAGGGTGGCAAGT
Mac2	CAGAGAGCACTACCCAGGAAAAT	TGAGGGTTTGGGTTTCCAGAG
CD68	CTTGTGTTCAGCTCCAAGCC	AACAGATATGCCCCAAGCCC

2.7 References

Aas, V., Larsen, K., and Iversen, J.G. (1998). IFN-gamma induces calcium transients and increases the capacitative calcium entry in human neutrophils. J Interferon Cytokine Res *18*, 197-205.

Arkan, M.C., Hevener, A.L., Greten, F.R., Maeda, S., Li, Z.W., Long, J.M., Wynshaw-Boris, A., Poli, G., Olefsky, J., and Karin, M. (2005). IKK-beta links inflammation to obesity-induced insulin resistance. Nature medicine *11*, 191-198.

Aron-Wisnewsky, J., Tordjman, J., Poitou, C., Darakhshan, F., Hugol, D., Basdevant, A., Aissat, A., Guerre-Millo, M., and Clement, K. (2009). Human adipose tissue macrophages: m1 and m2 cell surface markers in subcutaneous and omental depots and after weight loss. The Journal of clinical endocrinology and metabolism *94*, 4619-4623.

Brakenhielm, E., Cao, R., Gao, B., Angelin, B., Cannon, B., Parini, P., and Cao, Y. (2004). Angiogenesis inhibitor, TNP-470, prevents diet-induced and genetic obesity in mice. Circ Res *94*, 1579-1588.

Cai, D., Yuan, M., Frantz, D.F., Melendez, P.A., Hansen, L., Lee, J., and Shoelson, S.E. (2005). Local and systemic insulin resistance resulting from hepatic activation of IKK-beta and NF-kappaB. Nature medicine *11*, 183-190.

Chang, I., Cho, N., Kim, S., Kim, J.Y., Kim, E., Woo, J.E., Nam, J.H., Kim, S.J., and Lee, M.S. (2004). Role of calcium in pancreatic islet cell death by IFN-gamma/TNF-alpha. J Immunol *172*, 7008-7014.

Chiang, S.H., Bazuine, M., Lumeng, C.N., Geletka, L.M., Mowers, J., White, N.M., Ma, J.T., Zhou, J., Qi, N., Westcott, D.*, et al.* (2009). The protein kinase IKKepsilon regulates energy balance in obese mice. Cell *138*, 961-975.

Feuerer, M., Herrero, L., Cipolletta, D., Naaz, A., Wong, J., Nayer, A., Lee, J., Goldfine, A.B., Benoist, C., Shoelson, S.*, et al.* (2009). Lean, but not obese, fat is enriched for a unique population of regulatory T cells that affect metabolic parameters. Nature medicine *15*, 930-939.

Folick, A., Min, W., and Wang, M.C. (2011). Label-free imaging of lipid dynamics using Coherent Anti-stokes Raman Scattering (CARS) and Stimulated Raman Scattering (SRS) microscopy. Current opinion in genetics & development *21*, 585-590.

Gesta, S., Tseng, Y.H., and Kahn, C.R. (2007). Developmental origin of fat: tracking obesity to its source. Cell *131*, 242-256.

Goldfine, A.B., Silver, R., Aldhahi, W., Cai, D., Tatro, E., Lee, J., and Shoelson, S.E. (2008). Use of salsalate to target inflammation in the treatment of insulin resistance and type 2 diabetes. Clinical and translational science *1*, 36-43.

Gregor, M.F., and Hotamisligil, G.S. (2011). Inflammatory mechanisms in obesity. Annual review of immunology *29*, 415-445.

Hevener, A.L., Olefsky, J.M., Reichart, D., Nguyen, M.T., Bandyopadyhay, G., Leung, H.Y., Watt, M.J., Benner, C., Febbraio, M.A., Nguyen, A.K.*, et al.* (2007). Macrophage PPAR gamma is required for normal skeletal muscle and hepatic insulin sensitivity and full antidiabetic effects of thiazolidinediones. The Journal of clinical investigation *117*, 1658-1669.

Hirosumi, J., Tuncman, G., Chang, L., Gorgun, C.Z., Uysal, K.T., Maeda, K., Karin, M., and Hotamisligil, G.S. (2002). A central role for JNK in obesity and insulin resistance. Nature *420*, 333-336.

Hotamisligil, G.S., Shargill, N.S., and Spiegelman, B.M. (1993). Adipose expression of tumor necrosis factor-alpha: direct role in obesity-linked insulin resistance. Science *259*, 87-91.

Hu, X., Chakravarty, S.D., and Ivashkiv, L.B. (2008). Regulation of interferon and Toll-like receptor signaling during macrophage activation by opposing feedforward and feedback inhibition mechanisms. Immunol Rev *226*, 41-56.

Hu, X., and Ivashkiv, L.B. (2009). Cross-regulation of signaling pathways by interferon-gamma: implications for immune responses and autoimmune diseases. Immunity *31*, 539-550.

Hughes, I., Binkley, J., Hurle, B., Green, E.D., Sidow, A., and Ornitz, D.M. (2008a). Identification of the Otopetrin Domain, a conserved domain in vertebrate otopetrins and invertebrate otopetrin-like family members. BMC Evol Biol *8*, 41.

Hughes, I., Binkley, J., Hurle, B., Green, E.D., Sidow, A., and Ornitz, D.M. (2008b). Identification of the Otopetrin Domain, a conserved domain in vertebrate otopetrins and invertebrate otopetrin-like family members. BMC evolutionary biology *8*, 41.

Hughes, I., Saito, M., Schlesinger, P.H., and Ornitz, D.M. (2007a). Otopetrin 1 activation by purinergic nucleotides regulates intracellular calcium. Proceedings of the National Academy of Sciences of the United States of America *104*, 12023-12028.

Hughes, I., Saito, M., Schlesinger, P.H., and Ornitz, D.M. (2007b). Otopetrin 1 activation by purinergic nucleotides regulates intracellular calcium. Proc Natl Acad Sci U S A *104*, 12023-12028.

Hurle, B., Ignatova, E., Massironi, S.M., Mashimo, T., Rios, X., Thalmann, I., Thalmann, R., and Ornitz, D.M. (2003). Non-syndromic vestibular disorder with otoconial agenesis in tilted/mergulhador mice caused by mutations in otopetrin 1. Hum Mol Genet *12*, 777-789.

Hurle, B., Marques-Bonet, T., Antonacci, F., Hughes, I., Ryan, J.F., Eichler, E.E., Ornitz, D.M., and Green, E.D. (2011). Lineage-specific evolution of the vertebrate Otopetrin gene family revealed by comparative genomic analyses. BMC evolutionary biology *11*, 23.

Kim, E., Hyrc, K.L., Speck, J., Lundberg, Y.W., Salles, F.T., Kachar, B., Goldberg, M.P., Warchol, M.E., and Ornitz, D.M. (2010). Regulation of cellular calcium in vestibular supporting cells by otopetrin 1. Journal of neurophysiology *104*, 3439-3450.

Kim, E., Hyrc, K.L., Speck, J., Salles, F.T., Lundberg, Y.W., Goldberg, M.P., Kachar, B., Warchol, M.E., and Ornitz, D.M. (2011a). Missense mutations in Otopetrin 1 affect subcellular localization and inhibition of purinergic signaling in vestibular supporting cells. Molecular and cellular neurosciences *46*, 655-661.

Kim, E., Hyrc, K.L., Speck, J., Salles, F.T., Lundberg, Y.W., Goldberg, M.P., Kachar, B., Warchol, M.E., and Ornitz, D.M. (2011b). Missense mutations in Otopetrin 1 affect subcellular localization and inhibition of purinergic signaling in vestibular supporting cells. Mol Cell Neurosci *46*, 655-661.

Klein, J., Fasshauer, M., Ito, M., Lowell, B.B., Benito, M., and Kahn, C.R. (1999). beta(3)-adrenergic stimulation differentially inhibits insulin signaling and decreases insulin-induced glucose uptake in brown adipocytes. J Biol Chem *274*, 34795-34802.

Kung, A.W., Lau, K.S., and Wong, N.S. (1995). Interferon-gamma increases intracellular calcium and inositol phosphates in primary human thyroid cell culture. Endocrinology *136*, 5028-5033.

Larsen, C.M., Faulenbach, M., Vaag, A., Volund, A., Ehses, J.A., Seifert, B., Mandrup-Poulsen, T., and Donath, M.Y. (2007). Interleukin-1-receptor antagonist in type 2 diabetes mellitus. The New England journal of medicine *356*, 1517-1526.

Le, T.T., Yue, S., and Cheng, J.X. (2010). Shedding new light on lipid biology with coherent anti-Stokes Raman scattering microscopy. Journal of lipid research *51*, 3091-3102.

Lee, S.K., Lee, J.O., Kim, J.H., Jung, J.H., You, G.Y., Park, S.H., and Kim, H.S. (2010). C-peptide stimulates nitrites generation via the calcium-JAK2/STAT1 pathway in murine macrophage Raw264.7 cells. Life Sci *86*, 863-868.

Li, S., Liu, C., Li, N., Hao, T., Han, T., Hill, D.E., Vidal, M., and Lin, J.D. (2008). Genome-wide coactivation analysis of PGC-1alpha identifies BAF60a as a regulator of hepatic lipid metabolism. Cell metabolism *8*, 105-117.

Lowell, B.B., and Spiegelman, B.M. (2000). Towards a molecular understanding of adaptive thermogenesis. Nature *404*, 652-660.

Lumeng, C.N., Bodzin, J.L., and Saltiel, A.R. (2007a). Obesity induces a phenotypic switch in adipose tissue macrophage polarization. J Clin Invest *117*, 175-184.

Lumeng, C.N., Deyoung, S.M., Bodzin, J.L., and Saltiel, A.R. (2007b). Increased inflammatory properties of adipose tissue macrophages recruited during diet-induced obesity. Diabetes *56*, 16-23.

Lumeng, C.N., and Saltiel, A.R. (2011). Inflammatory links between obesity and metabolic disease. The Journal of clinical investigation *121*, 2111-2117.

McGillicuddy, F.C., Chiquoine, E.H., Hinkle, C.C., Kim, R.J., Shah, R., Roche, H.M., Smyth, E.M., and Reilly, M.P. (2009). Interferon gamma attenuates insulin signaling, lipid storage, and differentiation in human adipocytes via activation of the JAK/STAT pathway. The Journal of biological chemistry *284*, 31936-31944.

Molusky, M.M., Li, S., Ma, D., Yu, L., and Lin, J.D. (2012). Ubiquitin-specific protease 2 regulates hepatic gluconeogenesis and diurnal glucose metabolism through 11beta-hydroxysteroid dehydrogenase 1. Diabetes *61*, 1025-1035.

Nishimura, S., Manabe, I., Nagasaki, M., Eto, K., Yamashita, H., Ohsugi, M., Otsu, M., Hara, K., Ueki, K., Sugiura, S., *et al.* (2009). CD8+ effector T cells contribute to macrophage recruitment and adipose tissue inflammation in obesity. Nature medicine *15*, 914-920.

O'Rourke, R.W., White, A.E., Metcalf, M.D., Winters, B.R., Diggs, B.S., Zhu, X., and Marks, D.L. (2012). Systemic inflammation and insulin sensitivity in obese IFN-gamma knockout mice. Metabolism *61*, 1152-1161.

Odegaard, J.I., and Chawla, A. (2013). Pleiotropic actions of insulin resistance and inflammation in metabolic homeostasis. Science *339*, 172-177.

Oh, D.Y., Talukdar, S., Bae, E.J., Imamura, T., Morinaga, H., Fan, W., Li, P., Lu, W.J., Watkins, S.M., and Olefsky, J.M. (2010). GPR120 is an omega-3 fatty acid receptor mediating potent anti-inflammatory and insulin-sensitizing effects. Cell *142*, 687-698.

Osborn, O., and Olefsky, J.M. (2012). The cellular and signaling networks linking the immune system and metabolism in disease. Nature medicine *18*, 363-374.

Pascual, G., Fong, A.L., Ogawa, S., Gamliel, A., Li, A.C., Perissi, V., Rose, D.W., Willson, T.M., Rosenfeld, M.G., and Glass, C.K. (2005). A SUMOylation-dependent pathway mediates transrepression of inflammatory response genes by PPAR-gamma. Nature *437*, 759-763.

Reilly, S.M., Chiang, S.H., Decker, S.J., Chang, L., Uhm, M., Larsen, M.J., Rubin, J.R., Mowers, J., White, N.M., Hochberg, I., *et al.* (2013). An inhibitor of the protein kinases TBK1 and IKK-varepsilon improves obesity-related metabolic dysfunctions in mice. Nat Med *19*, 313-321.

Rocha, V.Z., Folco, E.J., Sukhova, G., Shimizu, K., Gotsman, I., Vernon, A.H., and Libby, P. (2008). Interferon-gamma, a Th1 cytokine, regulates fat inflammation: a role for adaptive immunity in obesity. Circ Res *103*, 467-476.

Rotter, V., Nagaev, I., and Smith, U. (2003). Interleukin-6 (IL-6) induces insulin resistance in 3T3-L1 adipocytes and is, like IL-8 and tumor necrosis factor-alpha, overexpressed in human fat cells from insulin-resistant subjects. The Journal of biological chemistry *278*, 45777-45784.

Saltiel, A.R. (2012). Insulin resistance in the defense against obesity. Cell metabolism *15*, 798-804.

Stark, G.R., and Darnell, J.E., Jr. (2012). The JAK-STAT pathway at twenty. Immunity *36*, 503-514.

Stienstra, R., Joosten, L.A., Koenen, T., van Tits, B., van Diepen, J.A., van den Berg, S.A., Rensen, P.C., Voshol, P.J., Fantuzzi, G., Hijmans, A., *et al.* (2010). The inflammasome-mediated caspase-1 activation controls adipocyte differentiation and insulin sensitivity. Cell metabolism *12*, 593-605.

Sun, S., Ji, Y., Kersten, S., and Qi, L. (2012). Mechanisms of inflammatory responses in obese adipose tissue. Annu Rev Nutr *32*, 261-286.

Tanaka, T., Soriano, M.A., and Grusby, M.J. (2005). SLIM is a nuclear ubiquitin E3 ligase that negatively regulates STAT signaling. Immunity *22*, 729-736.

Tontonoz, P., and Spiegelman, B.M. (2008). Fat and beyond: the diverse biology of PPARgamma. Annual review of biochemistry *77*, 289-312.

Trujillo, M.E., and Scherer, P.E. (2006). Adipose tissue-derived factors: impact on health and disease. Endocrine reviews *27*, 762-778.

Vandanmagsar, B., Youm, Y.H., Ravussin, A., Galgani, J.E., Stadler, K., Mynatt, R.L., Ravussin, E., Stephens, J.M., and Dixit, V.D. (2011). The NLRP3 inflammasome instigates obesity-induced inflammation and insulin resistance. Nature medicine *17*, 179-188.

Wada, T., Hoshino, M., Kimura, Y., Ojima, M., Nakano, T., Koya, D., Tsuneki, H., and Sasaoka, T. (2011). Both type I and II IFN induce insulin resistance by inducing different isoforms of SOCS expression in 3T3-L1 adipocytes. American journal of physiology Endocrinology and metabolism *300*, E1112-1123.

Wang, L., Tassiulas, I., Park-Min, K.H., Reid, A.C., Gil-Henn, H., Schlessinger, J., Baron, R., Zhang, J.J., and Ivashkiv, L.B. (2008). 'Tuning' of type I interferon-induced Jak-STAT1 signaling by calcium-dependent kinases in macrophages. Nat Immunol *9*, 186-193.

Winer, S., Chan, Y., Paltser, G., Truong, D., Tsui, H., Bahrami, J., Dorfman, R., Wang, Y., Zielenski, J., Mastronardi, F.*, et al.* (2009). Normalization of obesity-associated insulin resistance through immunotherapy. Nature medicine *15*, 921-929.

CHAPTER 3 A BROWN FAT-ENRICHED SECRETED FACTOR PRESERVES METABOLIC HOMEOSTASIS THROUGH ATTENUATING HEPATIC LIPOGENESIS

3.1 Abstract

Brown fat activates uncoupled respiration to defend against cold and also contributes to systemic metabolism. To date, the metabolic action of brown fat has been primarily attributed to adaptive thermogenesis via uncoupling protein 1 (UCP1). Whether brown fat engages other tissues through secreted proteins remains largely unexplored. Here we show that Neuregulin 4 (Nrg4), a member of the EGF family of extracellular ligands, is enriched in brown adipose tissue, highly inducible during brown adipogenesis, and markedly reduced in rodent and human obesity. Gain- and loss-of-function studies in mice demonstrated that Nrg4 protects against diet-induced insulin resistance and hepatic steatosis through attenuating lipogenic signaling in the liver. Mechanistically, Nrg4 stimulates ErbB3/ErbB4 signaling in hepatocytes and negatively regulates *de novo* lipogenesis mediated by LXR/SREBP1c in a cell-autonomous manner. These results establish Nrg4 as a brown fat-enriched adipokine with therapeutic potential for the treatment of type 2 diabetes and non-alcoholic fatty liver disease.

3.2 Introduction

Brown fat defends against cold through mitochondrial uncoupling protein UCP1, which links fuel oxidation to heat generation (Cannon and Nedergaard, 2004; Kozak and Harper, 2000). Brown adipose tissue (BAT) also plays an important role in whole body energy balance and fuel metabolism. Genetic ablation of brown fat via transgenic expression of diphtheria toxin A renders mice prone to the development of obesity (Lowell et al., 1993), whereas activation of BAT thermogenesis by cold has been linked to increased energy expenditure, reduced adiposity, and lower plasma lipids (Bartelt et al., 2011; van der Lans et al., 2013; Yoneshiro et al., 2013). Recent work has demonstrated that metabolically active BAT is present in adult humans (Cypess et al., 2009; Nedergaard et al., 2007; van Marken Lichtenbelt et al., 2009; Virtanen et al., 2009), raising the prospect that augmenting brown fat abundance and/or function may provide an effective avenue for the treatment of obesity and its associated metabolic disorders (Enerback, 2010; Nedergaard and Cannon, 2010). While sharing key molecular and metabolic characteristics with the classical rodent BAT, brown fat in humans appears to contain both classical and brown-like, beige/brite (Petrovic et al., 2010; Wu et al., 2012), adipocytes with distinct molecular signature and developmental origin (Cypess et al., 2013; Jespersen et al., 2013; Seale et al., 2008).

To date, the metabolic action of brown fat has been primarily attributed to UCP1-mediated thermogenesis. Surprisingly, while mice lacking UCP1 had heightened sensitivity to cold (Enerback et al., 1997), they were resistant to diet-induced obesity at ambient temperature and became more prone to weight gain only at thermoneutrality (Feldmann et al., 2009; Liu et al., 2003). The latter is in striking contrast to the obesity-prone phenotype in mice lacking brown fat as a result of transgenic toxin expression in brown adipocytes (Lowell et al., 1993). These

paradoxical findings strongly suggest that brown fat exerts effects on systemic nutrient and energy metabolism through novel mechanisms beyond its intrinsic ability to carry out uncoupled respiration.

Secreted factors are important in mediating metabolic crosstalk among tissues to maintain systemic nutrient and energy homeostasis. Adipose tissue hormones (Kadowaki et al., 2006; Trujillo and Scherer, 2006; Waki and Tontonoz, 2007), gut-derived fibroblast growth factors (Angelin et al., 2012; Potthoff et al., 2012), myokines (Pedersen and Febbraio, 2012), and bone-derived factors (Karsenty and Ferron, 2012) participate in nutrient sensing and coordinate key aspects of metabolic homeostasis. The epidermal growth factor (EGF) family of extracellular ligands has been implicated in the regulation of tissue development and tumorigenesis via the ErbB family of receptor tyrosine kinases (Bublil and Yarden, 2007; Holbro and Hynes, 2004; Schneider and Wolf, 2009). EGFR and ErbB2 are uniquely important in engaging a subset of EGF growth factors in cancer cell growth and survival. Interestingly, a distinct subgroup of growth factors called Neuregulins (Nrg1-4) also contains EGF-like domain and primarily signals through ErbB3 and ErbB4 to regulate diverse biological processes (Schneider and Wolf, 2009). Neuregulins are synthesized as precursor proteins on plasma membrane and undergo proteolysis at sites proximal to the transmembrane domain to release active ligands for receptor binding and signaling. In particular, Nrg1 isoforms have been demonstrated to regulate heart development (Odiete et al., 2012), formation of neuromuscular junction (Falls, 2003), and nervous system development (Birchmeier, 2009). Whether neuregulins are produced by adipose tissues to mediate metabolic crosstalk remains unexplored.

In this study, we tested the hypothesis that brown fat engages UCP1-independent mechanisms to regulate systemic metabolism by globally identifying brown fat-enriched secreted factors. We identified Neuregulin 4 (Nrg4) as a novel secreted factor that binds to the liver and attenuates hepatic lipogenic signaling. Nrg4 expression is markedly downregulated in adipose tissues in murine and human obesity. Using gain- and loss-of-function mouse models, we demonstrated that Nrg4 plays a critical role in preserving insulin sensitivity and alleviating hepatic steatosis in obesity.

3.3 Results

3.3.1 Identification of Nrg4 as a brown fat-enriched secreted protein

To identify BAT-enriched secreted factors, we analyzed the expression profile of the mouse secretome gene set across twelve tissues (GeneAltas MOE430) and during brown adipocyte (BAC) differentiation. The secretome database contains a set of 2,169 mouse genes predicted to encode secreted proteins (Chen et al., 2005), 1,378 of which have probe sets on Affymetrix mouse genome MOE430 chips. Our analysis identified a cluster of 26 genes whose expression is enriched in mouse brown fat and induced during the course of brown adipogenesis (Figure 3.1A). Among these, Neuregulin 4 (Nrg4) exhibited a highly restricted pattern of expression in adipose tissues. Quantitative PCR (qPCR) analysis indicated that Nrg4 mRNA expression was enriched in BAT, *albeit* present at a lower level in WAT (Figure 3.1B). In contrast, its expression in other tissues, including skeletal muscle, liver, brain, and heart, was relatively low. Consistent with microarray data, Nrg4 expression was markedly induced during adipocyte differentiation

(Figure 3.1C), reaching a higher level in mature brown adipocytes than 3T3-L1 adipocytes; the latter more closely resembles white adipocytes.

Nrg4 belongs to a small family of epidermal growth factor-like (EGFL) domain-containing proteins that are synthesized as transmembrane precursors and undergo proteolytic cleavage (Odiete et al., 2012). The released extracellular fragments act on target cells through autocrine, paracrine and endocrine mechanisms. The proteolytic cleavage of Nrg4 near the transmembrane domain is predicted to release a highly conserved N-terminal EGFL peptide (supplementary Figure S3.1) (Harari et al., 1999; Hayes et al., 2008). To map the extracellular cleavage sites, we generated a panel of Alanine mutants (a.a. 51-62) between the EGFL and transmembrane domains. To facilitate detection, full-length wild type and mutant Nrg4 proteins were fused to secreted alkaline phosphatase (SEAP) at the N-terminus. Immunoblotting analysis of conditioned media (CM) from transfected HEK293 cells showed that SEAP-Nrg4 fusion protein was readily detectable in media (Figure 3.2A), indicating that the extracellular fragment of Nrg4 undergoes proteolytic cleavage. Mutants with Ser53-54 or Ser53 replaced with Alanine had markedly reduced SEAP-Nrg4 fusion proteins released into media, despite having similar expression levels in total cell lysates. These results demonstrate that Ser53 is critical for the cleavage of Nrg4 and its subsequent release into the extracellular space.

Neuregulins act through the ErbB family of receptor tyrosine kinases, particularly ErbB3 and ErbB4, but not the EGF receptor (Harari et al., 1999). To determine whether Nrg4 exhibits selectivity toward different ErbB receptors, we transiently transfected HEK293 cells with ErbB2,

ErbB3 and ErbB4 alone or in combinations. As expected, ErbB4 expression resulted in robust phosphorylation at tyrosine residue 1284 (Y1284), likely as a consequence of receptor auto-phosphorylation (Figure 3.2B). Recombinant Nrg4 extracellular fragment (a.a.1-62, GST-$Nrg4^{Ex}$) further increased ErbB4 phosphorylation in cells transfected with an ErbB4 expression vector. Increased ErbB4 phosphorylation was also observed following Nrg4 treatments when ErbB2 or ErbB3 was coexpressed in the cell. Interestingly, Nrg4 treatments enhanced ErbB3 phosphorylation (Y1289) in the presence of ErbB4. Because ErbB3 has an inactive kinase domain, the stimulation of its phosphorylation is most likely caused by Nrg4-induced heterodimerization with ErbB4. In contrast, ErbB2 phosphorylation remained largely unaffected by Nrg4 treatments.

To examine whether native Nrg4 can be released into the extracellular space to activate ErbB4 signaling, we collected CM from HEK293 cells transiently transfected with a vector expressing full-length wild type Nrg4 and treated Min6 cells stably overexpressing ErbB4 (ErbB4-Min6). Compared to control, CM from Nrg4-transfected cells elicited strong tyrosine phosphorylation of ErbB4 (Figure 3.2C). Similarly, biologically active Nrg4 could be detected in culture media from brown adipocytes transduced with a retroviral vector expressing full-length Nrg4. As such, Nrg4 is a BAT-enriched secreted factor that undergoes shedding to release an extracellular ligand capable of activating ErbB3 and ErbB4 receptors.

3.3.2 Nrg4 binding is restricted to the liver

A major function of brown fat is non-shivering thermogenesis. We next examined whether Nrg4 is required for defense against cold in Nrg4 null mice generated using a gene trap method. Unexpectedly, despite its abundant expression in BAT, Nrg4 appears to be dispensable for protection against hypothermia following cold exposure. Rectal body temperature was nearly indistinguishable between wild type (WT) and Nrg4 knockout (KO) mice (Figure 3.3A). Nrg4 mRNA expression was slightly induced in brown fat in response to acute cold exposure (Figure 3.3B). Expression of Ucp1 and deiodinase 2 (Dio2), the latter being an enzyme involved in thermogenic regulation, was induced to similar extent by cold exposure in WT and KO mice. In addition, BAT histology appeared similar between the two groups (Figure 3.3C). These observations raised the possibility that Nrg4 may not directly engage in adaptive thermogenesis. Instead, this factor may act on other tissues following secretion.

To identify the target tissue(s) of Nrg4, we generated a fusion protein between SEAP and the extracellular fragment of Nrg4 (SEAP-Nrg4^{Ex}) and performed binding assays on frozen tissue sections (Muller et al., 1998). The presence of Nrg4 binding sites in tissues can be readily detected by histochemical staining for SEAP enzymatic activity. Compared to vector, CM from HEK293 cells transiently transfected with SEAP-Nrg4^{Ex} expression plasmid robustly stimulated ErbB4 phosphorylation (Figure 3.4A). While SEAP-Nrg4^{Ex} binding was near background levels in BAT, heart, skeletal muscle, and spleen, strong binding as indicated by the presence of SEAP enzymatic staining was detected on the liver section (Figure 3.4B). Binding of Nrg4^{Ex} to hepatocytes was specific as recombinant GST-Nrg4^{Ex}, but not GST, nearly completely abolished the signal (Figure 3.4C). To determine whether ErbB3 and ErbB4 may mediate Nrg4 binding to hepatocytes, we performed competition binding assays in the presence of control CM or CM

containing secreted extracellular fragments of ErbB3 or ErbB4. As shown in Figure 3.4D, extracellular domains of ErbB3 and ErbB4, which contain ligand-binding sites for neuregulins, markedly reduced SEAP-Nrg4^{Ex} binding to the liver. These results illustrate that the liver is a major target tissue of Nrg4 through its direct binding to the ErbB receptors.

3.3.3 Nrg4 deficiency exacerbates diet-induced hepatic steatosis and insulin resistance

Secreted factors released by adipose tissues exert diverse effects on metabolic homeostasis by acting on the central nervous system and peripheral tissues (Kadowaki et al., 2006; Trujillo and Scherer, 2006; Waki and Tontonoz, 2007). Notably, leptin and adiponectin are produced primarily in WAT and play a central role in the regulation of energy balance and glucose and lipid metabolism. To explore the role of Nrg4 in systemic metabolism, we analyzed metabolic parameters of WT and Nrg4-deficient mice fed standard chow or high-fat diet (HFD). Nrg4 KO mice were born at expected Mendelian ratio, had similar food intake, physical activity level and oxygen consumption rate, and gained similar body weight as control when fed standard chow (Figure 3.5A and data not shown). Body composition analysis indicated that percent body fat and percent lean body mass were comparable between the two groups. Upon HFD feeding, Nrg4 null mice gained slightly more weight, accompanied by significantly increased adiposity and reduced percent lean body mass (Figure 3.5A). Compared to control, KO mice had higher fasting blood glucose and plasma insulin levels (Figure 3.5B-C), suggesting that Nrg4 deficiency impairs glucose homeostasis in diet-induced obesity. In support of this, glucose tolerance test (GTT) and insulin tolerance test (ITT) revealed that Nrg4 null mice developed more severe glucose intolerance and insulin resistance than control (Figure 3.5D).

Histological assessment revealed that, while WAT and BAT appeared similar between two groups, Nrg4 null mouse livers developed more pronounced steatotic lesions following HFD feeding (Figure 3.6A). Accordingly, liver triglyceride (TAG) content was significantly elevated in the KO group (Figure 3.6B). Plasma TAG concentrations were also higher in KO mice under fed condition. Because Nrg4 binding was restricted to the liver, we next performed transcriptional profiling on total liver RNA from HFD-fed WT and KO mice to identify metabolic pathways downstream of Nrg4. Among the genes altered by Nrg4 deficiency was a cluster of genes involved in lipid metabolism. Notably, the expression of several key lipogenic genes, including glucose kinase (Gck), malic enzyme (Me1), fatty acid synthase (Fasn), stearoyl-CoA desaturase 1 (Scd1), and ELOVL fatty acid elongase 5 (Elovl5), was significantly elevated in Nrg4 deficient mouse livers (Figure 3.7A). The induction of *de novo* lipogenic genes was further confirmed using qPCR (Figure 3.7B). The expression of Fsp27, a lipid droplet protein associated with hepatic steatosis, was also elevated. In contrast, the expression of genes involved in fatty acid β-oxidation (Ehhadh, Acox1, and Cpt1a), gluconeogenesis (PEPCK, G6Pase), and mitochondrial oxidative metabolism was comparable between two groups (Figure 3.7B and data not shown).

The expression of several transcriptional regulators of hepatic metabolism, including PGC-1α, PGC-1β, ChREBP, and SREBP2, were also similar between control and KO livers. In contrast, mRNA expression of SREBP1c, a key regulator of *de novo* lipogenesis and triglyceride synthesis (Horton et al., 2002), was significantly induced in Nrg4 KO mouse livers. Importantly, protein

levels of precursor SREBP1 (pSREBP1) and the cleaved and transcriptionally active isoform of SREBP1 in the nucleus (nSREBP1) were also elevated (Figure 3.7C). The levels of phospho-AMPK and phospho-AKT (S473) were similar between WT and KO livers. Excess stimulation of SREBP1-mediated lipogenesis has been observed in mouse models of non-alcoholic fatty liver disease (NAFLD) as well as in humans (Horton et al., 2002; Kohjima et al., 2008; Shimomura et al., 1999). Importantly, liver-specific transgenic expression of the transcriptionally active form of SREBP1c increases hepatic lipogenesis, leading to excess adiposity, hepatic steatosis, hypertriglyceridemia, and insulin resistance (Horton et al., 2002; Knebel et al., 2012; Shimano et al., 1997), whereas inhibition of the SREBP pathway had the opposite effects on hepatic fat accumulation and whole body energy metabolism (Moon et al., 2012; Tang et al., 2011). Together, our studies revealed a protective role of Nrg4 in metabolic homeostasis in obesity, at least in part through attenuating the program of hepatic lipogenesis.

3.3.4 Nrg4 cell-autonomously attenuates *de novo* lipogenesis in hepatocytes

As shown above, Nrg4 deficiency resulted in aberrant induction of SREBP1c and its target genes in the liver. To determine whether Nrg4 regulated *de novo* lipogenesis in a cell-autonomous manner, we performed studies in cultured primary mouse hepatocytes. Previous studies have demonstrated that liver expresses all ErbB receptors expect ErbB2 (Carver et al., 2002). However, expression of ErbB4 in hepatocytes is relatively low under culture conditions. To reconstitute ErbB signaling in hepatocytes, we transduced primary hepatocytes with control (GFP) or ErbB4 adenoviral vectors and examined the effects of Nrg4 on receptor activation and downstream signaling. As expected, ErbB4 expression was below detectable range in

hepatocytes transduced with GFP adenovirus (Figure 3.8A). Adenoviral-mediated expression of ErbB4 resulted in auto-phosphorylation that was moderately increased by GST-Nrg4^{Ex}. Interestingly, GST-Nrg4^{Ex} treatment elicited a dose-dependent increase of tyrosine phosphorylation of endogenous ErbB3 and STAT5 proteins without affecting total ErbB3 and STAT5 levels. Because ErbB3 does not have intrinsic kinase activity, increased phosphorylation is likely due to ligand-dependent heterodimerization with ErbB4 in response to Nrg4. Previous studies have demonstrated that ErbB receptor activation stimulates the STAT5 signaling pathway in cultured cells and *in vivo* (Jones et al., 1999; Olayioye et al., 1999). Our results indicate that this signaling pathway is also operational in hepatocytes. Importantly, the stimulation of ErbB3 and STAT5 phosphorylation was completely abolished in the presence of JNJ28871063, a pan-ErbB inhibitor (Figure 3.8B). Further, a kinase-dead mutant of ErbB4 (ErbB4 KD) failed to respond to GST-Nrg4^{Ex} (Figure 3.8C), suggesting that kinase activity of ErbB4 is required for mediating the stimulation of ErbB3 and STAT5 in response to Nrg4.

Hepatic lipogenesis is highly responsive to nutritional and hormonal signals. The induction of lipogenic gene program in the fed state requires transcriptional activation of SREBP1c, which is a direct target of nuclear hormone receptor liver-X receptor (LXR) (Repa et al., 2000; Schultz et al., 2000). We next examined whether Nrg4/ErbB4 activation directly impacts the SREBP1c/lipogenesis axis in hepatocytes in response to LXR activation. Hepatocytes transduced with GFP or ErbB4 adenoviruses were treated with vehicle (DMSO) or T0901317, a potent agonist for liver-X receptor, in the presence of GST or GST-Nrg4^{Ex}. As expected, T0901317 treatment strongly induced mRNA expression of Srebp1c and lipogenic genes such as Fasn and Scd1 in hepatocytes transduced with GFP (Figure 3.9A). Treatment of ErbB4-transduced

hepatocytes with GST-Nrg4^{Ex} significantly lowered the stimulatory effects of T0901317 on these genes. The expression of Abca1, another LXR target gene, was also reduced in response to ErbB4/Nrg4 activation. Consistent with gene expression data, *de novo* lipogenesis as measured by the incorporation of ^{14}C-acetate into lipids was significantly inhibited by Nrg4 in hepatocytes expressing ErbB4 (Figure 3.9B). Activation of STAT5 has been demonstrated to exert inhibitory effects on nuclear hormone receptor signaling (Stocklin et al., 1996). To examine whether STAT5 activation directly modulates the transcriptional activity of LXR, we performed reporter gene assay using a luciferase construct containing LXR responsive element. Cotransfection of LXR/RXR expression plasmids drastically increased reporter luciferase activity in HEK293 cells in the presence of T0901317 (Figure 3.9C). Cotransfection of constitutively active STAT5 significantly inhibited the increase of LXRE reporter gene expression, suggesting that STAT5 activation may transrepress LXR and attenuate its transcriptional activity.

3.3.5 Adipose tissue Nrg4 expression is reduced in murine and human obesity

We next examined whether adipose Nrg4 expression is altered in mouse and human obesity. Compared to lean control, mRNA levels of Nrg4 in epididymal WAT were markedly lower in mice with high-fat diet (HFD)-induced obesity (DIO) or genetic obesity caused by leptin (ob/ob) or leptin receptor (db/db) deficiency (Figure 3.10A). While Nrg4 mRNA expression in brown fat was similar between lean and DIO mice, its levels were significantly lower in BAT from ob/ob and db/db mice, more severe models of obesity. Fractionation studies indicated that Nrg4 mRNA expression was detected nearly exclusively in adipocytes, but not in the stromal vascular fraction, and was significantly lower in the obese group than lean control (Figure 3.10B).

Adiponectin (Adipoq) and nitric oxide synthase 2 (Nos2) were included as control for adipocytes and stromal vascular cells, respectively. Adipose tissue inflammation impairs insulin sensitivity and metabolic homeostasis in part through augmented proinflammatory cytokine signaling (Gregor and Hotamisligil, 2011; Odegaard and Chawla, 2013; Osborn and Olefsky, 2012). To determine whether proinflammatory cytokines contribute to obesity-induced downregulation of Nrg4 in adipocytes, we treated differentiated brown adipocytes and 3T3-L1 adipocytes with TNFα, a prototypical obesity-induced cytokine that has been implicated in adipose tissue dysfunction and insulin resistance (Hotamisligil et al., 1993). We found that Nrg4 mRNA expression was decreased by TNFα treatments in both brown and white adipocytes (Figure 3.10C). Similar inhibition of Nrg4 expression was also observed following interleukin 1β (IL1β) treatments. Thus, the reduction of adipocyte Nrg4 expression is likely a consequence of augmented proinflammatory cytokine signaling in obesity.

To determine whether Nrg4 expression is also reduced in human obesity, we examined its mRNA levels in subcutaneous WAT (scWAT) of a cohort of individuals with a wide range of body fat mass, and found that scWAT NRG4 mRNA levels inversely correlated with log percent body fat mass (Figure 3.11A), and log Homeostatic Model Assessment-Insulin Resistance (HOMA-IR). Similar inverse correlation was also observed between scWAT NRG4 expression and body mass index (BMI), and to a lesser extent, liver fat content (Supplementary Figure S3.2). When assessing NRG4 expression in BMI-matched individuals, we found that NRG4 mRNA levels in both subcutaneous and visceral adipose tissues were significantly lower in individuals with impaired glucose tolerance (IGT) or type 2 diabetes (T2D) compared to those with normal glucose tolerance (NGT) (Figure 3.11B). Together with the observations that Nrg4

deficient mice developed more severe hepatic steatosis and insulin resistance upon HFD feeding, our results strongly suggest that inadequate Nrg4 expression may be causally linked to obesity-associated metabolic disorders.

3.3.6 Transgenic expression of Nrg4 improves diet-induced metabolic disorders

A key prediction of this model is that elevated Nrg4 levels will protect mice from obesity-associated metabolic disorders. To test this, we generated Nrg4 transgenic mice using aP2 promoter/enhancer and chose line #111 that exhibited adipose-selective overexpression for metabolic studies. Nrg4 transgenic mice were indistinguishable from WT littermates when fed standard chow. Upon HFD feeding, transgenic mice gained slightly but significantly less body weight than control (Figure 3.12A). Body composition analyses revealed that percent fat mass was reduced in the transgenic group, whereas percent lean mass remained similar (Figure 3.12B). Plasma TAG levels were lower in the transgenic group (Figure 3.12C). We next measured whole body energy metabolism using Comprehensive Lab Animal Monitoring System (CLAMS). While control and transgenic mice had similar food intake, transgenic mice exhibited significantly elevated oxygen consumption rate (VO_2) as normalized to body weight or lean body mass (Figure 3.13). In contrast to Nrg4 deficiency, Nrg4 transgenic mice had lower blood glucose levels than control under both fed and fasted conditions (Figure 3.14A). Fasting plasma insulin level was also lower in the transgenic group. Accordingly, GTT and ITT studies indicated that Nrg4 transgenic mice had improved glucose tolerance and insulin sensitivity (Figure 3.14B).

Histological analyses and measurements of liver lipid content indicated that transgenic mice had significantly improved hepatic steatosis (Figure 3.15A-B). Adipose tissue histology was similar between two groups. Fatty acid profile analysis of hepatic triglycerides demonstrated that transgenic mice have reduced levels of major fatty acid species, including palmitic acid (C16:0), oleic acid (C18:1), and linolenic acid (C18:2) (Figure 3.15C). Importantly, the desaturation index (C16:1n7/C16:0 and C18:1n9/C18:0), which reflects cellular SCD1 activity, was significantly lower in the transgenic group (Figure 3.15D), suggesting that hepatic lipogenesis is attenuated in aP2-Nrg4 transgenic mice. Accordingly, we found that the levels of SREBP1c mRNA and protein were significantly decreased in transgenic mouse livers (Figure 3.16A-B). The expression of hepatic lipogenic genes, including Gck, Acl, Acc1, Me1, Fasn, and Scd1, was attenuated in response to transgenic expression of Nrg4 in adipose tissues. Further, Fsp27 mRNA expression was also markedly reduced. These results demonstrate that transgenic elevation of Nrg4 levels in brown and white fat is sufficient to ameliorate diet-induced hepatic steatosis and improve systemic metabolic homeostasis.

3.4 Discussion

Brown and beige adipocytes are capable of activating uncoupled respiration through UCP1-mediated proton leak and heat generation. This intrinsic thermogenic function is critical for the defense against cold and contributes to whole body energy balance. However, whether brown fat engages other metabolic tissues via secreted factors remain poorly understood. In this study, we provided evidence for a novel mechanism through which brown fat regulates systemic metabolism independent of its role in thermogenesis. Compared to white fat, Nrg4 mRNA

expression is enriched in brown fat and highly inducible during brown adipocyte differentiation. Nrg4 is secreted into the extracellular space and directly binds to hepatocytes in the liver. While largely dispensable for cold-induced thermogenesis, Nrg4 serves to preserve glucose and lipid metabolism in obesity (Figure 3.17). The levels of Nrg4 mRNA are significantly reduced in adipose tissues in murine and human obesity. Importantly, transgenic rescue of Nrg4 expression in adipose tissues is sufficient to ameliorate obesity-associated insulin resistance and hepatic steatosis, raising the prospect of developing Nrg4 as a therapeutic biologic in treating metabolic disorders.

Among the genes encoding putative secreted factors, Nrg4 mRNA expression exhibited a high degree of restriction to brown fat. Despite this, significant levels of Nrg4 expression were also observed in differentiated 3T3L1 adipocytes and white fat. We cannot rule out the possibility that *bona fide* brown fat-specific adipokines may be excluded from our analyses due to a lack of probesets on Affymetrix chips. However, such factors may not exist given the remarkable similarity in the transcriptional control of gene expression in adipocytes of white, brown, and beige lineages. Nrg4 mRNA expression was markedly reduced in WAT in all three models of mouse obesity (diet-induced obesity, ob/ob, and db/db) and also in BAT in more severe genetic obesity. The inverse association between Nrg4 expression and obesity appears to be conserved between mouse and human. The expression of Nrg4 in brown and white adipocytes was reduced by treatments with proinflammatory cytokines, which contribute to adipose tissue dysfunction in obesity (Gregor and Hotamisligil, 2011; Odegaard and Chawla, 2013; Osborn and Olefsky, 2012). As mass of white fat is significantly more compared to that of brown and beige fats in

individuals, it is likely that Nrg4 derived from different adipose tissues collectively contributes to its regulation of systemic metabolism.

The exacerbation of insulin resistance and hepatic steatosis in Nrg4 null mice strongly suggest that diminished Nrg4 expression may be causally linked to the disruption of metabolic homeostasis in obesity. While Nrg4 null mice were nearly indistinguishable from control when fed standard chow, they developed several characteristics of metabolic syndrome, including insulin resistance, elevated plasma glucose and triglyceride levels, and excess hepatic fat accumulation on HFD. These metabolic perturbations were associated with aberrant induction of SREBP1c and the lipogenic gene program in the liver. Remarkably, transgenic Nrg4 expression in adipocytes attenuated hepatic SREBP1c/lipogenic pathway and significantly improved metabolic parameters following HFD feeding in mice. Together, these in vivo studies revealed a protective role of Nrg4 in metabolic homeostasis during chronic energy excess. In addition, our data strongly suggest that Nrg4 improves metabolic parameters, at least in part, through attenuating the activation of hepatic SREBP1c/lipogenesis in obesity.

Several lines of evidence support the notion that Nrg4 directly acts on the liver and regulates hepatic lipogenesis. First, the extracellular EGF-like domain of Nrg4 exhibited strong binding to hepatocytes when fused to SEAP. Nrg4 binding in the liver was nearly completely abolished when excess GST-Nrg4^{Ex} or CM containing the extracellular domains of ErbB3 and ErbB4 were included as competitors in the binding assays. As such, Nrg4 likely directly binds to ErbB3 and/or ErbB4 on hepatocyte cell surface. Using cultured hepatocytes with reconstituted ErbB4

expression, we found that Nrg4 was capable of triggering dose-dependent activation of endogenous ErbB3 and downstream signaling pathway, most notably phosphorylation of transcription factor STAT5. ErbB3 does not have an active kinase domain but can heterodimerize with ErbB4 in response to ligand binding, resulting in receptor phosphorylation and the activation of downstream effectors. Hepatocytes express very low levels of ErbB2 (Carver et al., 2002). While EGFR is abundantly expressed in the liver, it does not bind to Nrg4 (Harari et al., 1999). Our data are consistent with ErbB3 and ErbB4 serving as major Nrg4 receptors in the liver. Finally, the activation of Nrg4 signaling in hepatocytes resulted in cell-autonomous inhibition of the SREBP1c/lipogenic pathway through transrepression of LXR by STAT5. The inhibitory effects of Nrg4 were consistently observed on lipogenic gene expression and the incorporation of ^{14}C-acetate into newly synthesized lipids.

It was somewhat surprising that, despite high levels of Nrg4 expression in BAT, its deficiency apparently does not impair cold-induced thermogenesis. In fact, core body temperature was nearly indistinguishable between WT and Nrg4 KO mice following acute cold exposure. Histological and gene expression analyses failed to reveal a significant role of Nrg4 in brown adipose tissue development and function. Exposure of animals to cold environment triggers sympathetic nerve activity and stimulates fuel oxidation and heat production in brown fat (Cannon and Nedergaard, 2004; Kozak and Harper, 2000). The activation of cold-induced thermogenesis significantly increases the delivery of glucose and lipid for thermogenesis and is expected to induce metabolic adaptation in other tissues. For example, hepatic fat oxidation and ketone production have been demonstrated to increase during cold acclimation (Hauton et al.,

2006; Iossa et al., 1994). As such, Nrg4 may fine tune metabolic adaptation in the liver to accommodate increased fuel demand by brown and beige fats.

Previous studies have implicated other EGF family of extracellular ligands in glucose metabolism. Nrg1 isoform β1 has been shown to promote glucose uptake in cultured muscle cells (Guma et al., 2010; Suarez et al., 2001), whereas EGF appears to counteract the stimulatory effects of insulin on glycogen synthesis in hepatocytes (Chowdhury and Agius, 1987). Heparin-binding EGF, another member of this ligand family, is inducible by exercise in skeletal muscle and plays a role in facilitating muscle glucose disposal (Fukatsu et al., 2009). While we did not detect significant Nrg4 binding in skeletal muscle, it remains possible that this factor may also target tissues other than the liver once it is released into circulation. Together, our work here has established Nrg4 as a brown fat-enriched adipokine that improves insulin sensitivity and alleviates hepatic steatosis in the context of obesity. Future studies are needed to explore the potential of Nrg4 as a therapeutic biologic for the treatment of type 2 diabetes and non-alcoholic fatty liver disease.

3.5 Future direction

3.5.1 Detecting Nrg4 in circulation

As we propose that Nrg4 is an endocrine hormone secreted from BAT and acts on the liver, it is important to prove its presence in the blood. ELISA mediated detection of Nrg4 is limited by the availability of potent Nrg4 antibody. One possible way to make less sensitive home-made Nrg4

antibody work is enriching low molecular weight plasma proteins through acetonitrile precipitation (Kay et al., 2008). Another possible yet more technically challenging method is parabiosis between Nrg4 transgenic (Tg) and knockout (KO) mice. Restoration of metabolic parameters in knockout mice connected to Tg and unchanged metabolic phenotype in those connected to another KO can provide evidence of Nrg4's presence in circulation.

3.5.2 Role of STAT5 in down-regulating hepatic lipogenesis by Nrg4

Figure 3.8 and 3.9 showed that STAT5 can be phosphorylated in response to Nrg4 in hepacotyes, and constitutively active STAT5 is able to down regulate transcriptional activation of LXR/RXR targets, to which SREBP1c belongs. To find out how important STAT5 is in relaying Nrg4 signal towards lipogenic suppression, we plan to breed AP2-Nrg4 transgenic mice with STAT5 liver specific knockout mice (STAT5-LKO). If transgenic expression of Nrg4 failed to rescue fatty liver on the STAT5-LKO background, it would indicate that STAT5 is an important downstream effector of Nrg4 in terms of liver lipid regulation. Similar experiments can also be done *in vitro*, by isolating hepatocytes from STAT5-floxed mice, and perform gene expression analysis as well as *de novo* lipogenic assay after GST/GST-Nrg4^{Ex} treatment following STAT5 deletion mediated by Cre expressing adenovirus.

3.5.3 Role of ErbB3/ErbB4 in mediating Nrg4's beneficial effect on liver

Figure 3.4 showed that both ErbB3 and ErbB4 can compete off SEAP-Nrg4's binding to the liver, indicating they themselves bind to Nrg4. Moreover, in both HEK293 cells (Figure3.2) and

primary hepatocytes (Figure 3.8), GST-Nrg4^{Ex} treatment led to ErbB3 and ErbB4 tyrosine phosphorylation and activation, indicating ErbB3 and/or ErbB4 may be required for Nrg4's role in suppressing hepatic lipogenesis. For this idea to be testified, we will first perform SEAP-Nrg4 binding assay using liver sections from ErbB3 and ErbB4 KO mice. Abolishment of binding will indicate that Nrg4 binds to liver only through ErbB3/ErbB4, and no other receptors. 2ndly, we will characterize phenotypes of ErbB3/ErbB4 liver specific knockout mice, to see whether they phenocopy the fatty liver phenotype as we see in Nrg4 KO mice. And if they do, whether breeding to AP2-Nrg4 transgenic mice also fail to rescue this phenotype.

3.6 Material and methods

3.6.1 Identification of brown fat-enriched secreted factors

The identification of gene cluster encoding putative brown fat-enriched secreted proteins was based on mouse secretome dataset available at Secreted Protein Database (spd.cbi.pku.edu.cn) (Chen et al., 2005), mouse tissue microarray dataset (GSE9954, GEO database), and brown adipocyte differentiation time course microarray dataset. Among 2,169 high-confident genes predicted to encode secreted proteins, 1,378 of which have annotated Affymetrix probe sets and were included in the analysis. Genes that were induced more than 2-fold in day 7 differentiated brown adipocytes compared to preadipocytes and enriched by more than 2-fold in brown fat were considered as putative brown-fat enriched secreted factors.

3.6.2 Nrg4 knockout and transgenic mice

Nrg4 knockout mice were purchased from the Mutant Mice Regional Resource Center (MMRRC) at the University of California, Davis, and backcrossed for more than ten generations to the C57BL/6J background. The transgenic vector was constructed by placing mouse Nrg4 cDNA that contains part of 5' and 3' UTR between the aP2 enhancer/promoter sequence and human growth hormone polyadenylation signal. Mouse Nrg4 cDNA (including 5'UTR and partial 3'UTR) were TA-cloned into pCR2.1 TOPO vector. The transgenic vector was linearized by using HindIII and ApaI to release the transgenic cassette for microinjecting into fertilized eggs from C57BL/6J mice. Transgenic mice were generated at the Transgenic Animal Model Core at the University of Michigan.

3.6.3 Human studies

In a cross-sectional study, we investigated NRG4 mRNA expression in paired omental and subcutaneous (SC) adipose tissue samples (n=642). Individuals fulfilled the following inclusion criteria: 1) Absence of any acute or chronic inflammatory disease as determined by a leucocyte count > 7000 Gpt/l, C-reactive protein (CrP) > 10.0 mg/dl or clinical signs of infection, 2) Undetectable antibodies against glutamic acid decarboxylase (GAD), 3) No thyroid dysfunction, 4) No alcohol or drug abuse, 5) No pregnancy. All study protocols have been approved by the ethics committee of the University of Leipzig. All participants gave written informed consent before taking part in the study. All subjects had a stable weight, defined as the absence of fluctuations of >2% of body weight for at least 3 months before surgery. Adipose tissue was immediately frozen in liquid nitrogen after explantation. BMI was calculated as weight divided by squared height. Insulin sensitivity was assessed using the HOMA-IR index or with the

euglycemic-hyperinsulinemic clamp method. Human *NRG4* mRNA expression was measured by TaqMan-based qPCR assay. Human *NRG4* mRNA expression was calculated relative to the mRNA expression of *HPRT1*, determined by a premixed assay developed for NRG4 and HPRT1 (Applied Biosystems).

3.6.4 Adipocyte differentiation and treatments

Brown preadipocyte isolation and differentiation were performed as previously described (Klein et al., 2002). SV40 T-large antigen immortalized brown preadipocytes were cultured in DMEM with 10% fetal bovine serum (FBS) for 2 days after reaching confluence (denoted as day 0 of differentiation). BAC differentiation was induced by adding a cocktail containing 0.5mM IBMX, 125μM Indomethacin, 1μM dexamethasone to maintenance media containing 10% FBS, 20nM insulin and 1nM T3. Three days after induction, cells are cultured in the maintenance media alone. Total RNA was isolated at different days during brown adipocyte differentiation for gene expression analysis.

3T3-L1 preadipocytes were cultured in DMEM with 10% bovine growth serum (BGS) until 2 days post confluent (count as d0). Differentiation was induced by adding a cocktail containing 0.5mM IBMX, 1μM dexamethasone and 1μg/mL insulin to DMEM supplemented with 10% FBS. Three days after induction, cells were cultured in DMEM containing 10% FBS plus 1μg/mL of insulin for another 2 days followed by maintenance in DMEM supplemented with

10% FBS. TNFα (10ng/mL) and IL1β (40ng/mL) treatment were carried out in mature adipocytes cultured in the maintenance media.

3.6.5 Adipose tissue fractionation

Epididymal WAT was dissected from lean and HFD-fed obese C57BL/6J mice. The tissues were minced into 2~3mm pieces, digested in Krebs Ringer Bicarbonate HEPES buffer (KRBH, containing 10 mM bicarbonate and 30 mM HEPES, pH 7.4) supplemented with 3% fatty acid free bovine albumin, 500nM adenosine and 3mg/mL collagenase II, and shaked gently at 37ºC for 40min. Digested tissues were filtered through 200μm nylon filters into 50 ml conical tubes followed by centrifugation for at 800rpm for 30sec. The infranatant containing stromal vascular fraction was transferred into another tube using a needle syringe. The top layer containing mature adipocytes was washed again for a total of 3 times with KRBH buffer supplemented with 3% bovine albumin, and used for total RNA isolation. After the final removal of infranatant, the adipocyte fraction was lysed for RNAs. The combined infranatants were centrifuged at 4000rpm for 5min to obtain cell pellets containing stromal vascular fraction.

3.6.6 Min6 cell culture and treatments

Min6 cells stably expressing ErbB4 were a gift from Dr. Peter Dempsey (University of Michigan), and were cultured in DMEM supplemented with 15% FBS, 1.7g/500mL sodium bicarbonate, 2.5uL/500mL β-mercaptoethanol and 1% Pen/Strep. Before conditioned media treatment (for 15min), the cells were starved in serum-free DMEM for 4 hrs.

3.6.7 Nrg4 binding assay

Hormone binding assay was performed as previously described (Lin and Linzer, 1999; Muller et al., 1998). 293T cells were transfected with vectors expressing SEAP or SEAP-Nrg4^{Ex}. 24 hours after transfection, cells were switched to serum-free media for additional 2 days before the media were collected and concentrated using Centricon. Briefly, frozen tissue slices were incubated with SEAP or SEAP-Nrg4^{Ex} conditioned media for 45 min at room temperature before they were washed four times in 0.1% tween-20 containing PBS and fixed in a solution containing 20 mM HEPES (pH 7.4), 60% acetone, and 3% formaldehyde. After inactivating endogenous alkaline phosphatase at 65 °C for 30 min, the enzymatic activity derived from the fusion protein was detected using NBT/BCIP substrate. For competition binding, frozen tissue slices were pre-incubated for 30 min with 4μg/μL GST or GST- Nrg4^{Ex} or 40 fold concentrated conditioned media from HEK293 cells expressing extracellular domain of ErbB3 or ErbB4, followed by one hour of SEAP-Nrg4^{Ex} conditioned media co-incubation with those competitors.

3.6.8 293T transfection

To pinpoint the exact cleavage site of Nrg4, serial alanine mutations encompassing Nrg4's predicted metalloprotease cleavage site were generated through site-directed mutagenesis PCR on top of the WT SEAP-Nrg4 expressing vector. HEK293 cells were transfected with equal amount of plasmids expressing either WT or mutant Nrg4 in the presence of polyethylenimine. The original 10% BGS DMEM were changed to 0.5% FBS DMEM 12 hrs after transfection. 48

more hrs later, both media and total cell lysates were collected for western blotting against SEAP.

For generating extracellular domain (ECD) of ErbB3 and ErbB4, we obtained ErbB3 and ErbB4 ECD expressing plasmids from Dr. Leahy (Leahy et al., 2000). ECDs of ErbB3 and ErbB4 were his tagged and fused to human growth hormone. Conditioned media were collected as above and were concentrated 40 fold using Amicon ultra-centrifugal filter units from Millipore.

3.6.9 Hepatocyte isolation and treatment

Primary hepatocytes were isolated as previously described (Lin et al., 2004) by using collagenase type II (Invitrogen, Carlsbad, CA) from C57BL/6J mice. Hepatocytes were maintained in DMEM medium containing 10% BGS at 37°C and 5% CO2. Adenovirus infection was performed in the same day of isolation. After 24 hrs, cells were treated with GST and GST-Nrg4^{Ex} (10μg/mL) with vehicle (DMSO) or T0901317 (5μmol/L) for 24hrs. For signaling, cells were switched to DMEM supplemented with 0.1% BSA for 12 hrs before GST and GST-Nrg4^{Ex} treatment. Recombinant adenoviruses were generated using AdEasy adenoviral vector (Stratagene, Santa Clara, CA) as previously described (Li et al., 2008a).

3.6.10 Luciferase reporter assay

Hepa 1 cells in 24-well plate were transiently transfected with 4xLXRE-Luc (30 ng/well) in the presence or absence of expression vectors for LXR (30 ng/well), RXR (30 ng/well), and

constitutively active STAT5 (caSTAT5, 100 or 200 ng/well). Twenty four hrs after transfection, the cells were treated with vehicle (DMSO) or T0901317 (10 μM) for an additional 24 hrs before harvesting for luciferase assay. All the reporter assays were repeated at least three times in triplicates.

3.6.11 Gene expression analysis

Total RNA from white adipose tissue was extracted using a commercial kit from Invitrogen. RNAs from other tissues and cultured cells was extracted using TRIzol method. For quantitative real-time PCR (qPCR) analysis, equal amount of RNA was reverse-transcribed using MMLV-RT followed by quantitative PCR reactions using SYBR Green (Life Technologies). Relative abundance of mRNA was normalized to ribosomal protein 36B4. For detecting the coding isoform of Nrg4 using Taqman PCR, we designed sense primer encompassing the junction of exon3 and exon6 (5' CCCAGCCCATTCTGTAGGTG3'), anti-sense primer in exon6 (5'ACCACGAAAGCTG-CCGACAG 3'), and a taqman probe in exon6 but between sense and anti-sense primers (5' 6-FAM-CGGAGCACGCTGCGAAGAGGTT-BHQ 3'). Taqman PCR was carried out using the Taqman Universal PCR Master Mix system (Applied Biosystems). Relative abundance of the Nrg4 coding isoform was normalized to ribosomal protein 36B4.

For microarray study of liver gene expression, total liver RNA isolated from HFD-fed WT and Nrg4 KO mice was used to generate probes for Affymetrix Mouse MG-430 PM array strips. Sample processing and data analyses were performed according to the manufacturer's

instruction. The dataset has been deposited into the NCBI Gene Expression Omnibus (GEO) database with accession number GSE53877.

3.6.12 Immunoblotting analyses

For total lysates livers were homogenized in a lysis buffer containing 50 mM Tris (pH 7.5), 150mM NaCl, 5mM NaF, 25mM β-glycerolphosphate, 1mM sodium orthovanadate, 10% glycerol, 1% tritonX-100, 1 mM dithiothreitol (DTT), and freshly added protease inhibitors. Liver nuclear extracts were prepared as previously described (Calfee-Mason et al., 2002). Briefly, frozen livers were homogenized using a Dounce homogenizer in ice-cold homogenization buffer containing 0.6% NP40, 150mM NaCl, 10mM HEPES (pH=7.9), 1mM EDTA, and protease inhibitor cocktail. The homogenates were briefly centrifuged at 450 rpm at 4ºC to remove tissue debris. The suspension was transferred to a new tube and centrifuged at 3,000 rpm for 5 min at 4ºC. The nuclei pellet was washed with homogenization buffer and resuspended in a low-salt buffer containing 20mM Tris (pH=7.5), 25% glycerol, 1.5mM $MgCl_2$, 200μM EDTA, 20mM KCl, and protease inhibitors. Nuclear proteins were extracted following the addition of a high-salt buffer (½ volume) containing 20mM Tris (pH=7.5), 1.5mM $MgCl_2$, 200μM EDTA, 1.2M KCl, and protease inhibitors at 4ºC for 2hrs. Immunoblotting experiments were performed using specific antibodies against SREBP1 and CHREBP (Santa Cruz Biotechnology), tubulin (Sigma), and Lamin A/C, phospho-ErbB4 (Y1284) and total ErbB4, phospho-ErbB3 (Y1289) and total ErbB3, phospho-ErbB2 (Y1221/1222), phospho-STAT5 (Y694) and total STAT5, phospho-AKT (S473) and total AKT, phosphor-AMPK (Thr172) and total AMPK (Cell signaling).

3.6.13 Metabolic measurements

Plasma concentrations of triglycerides (Sigma) and non-esterified fatty acid (Wako Diagnostics) were measured using commercial assay kits. Liver triglyceride was extracted and measured as previously described (Li et al., 2008b). Plasma insulin was measured using an ELISA assay kit (CrystalChem). Glucose and insulin tolerance tests were performed as previously described (Molusky et al., 2012).

3.6.14 Body composition and metabolic cage studies

Body fat and lean mass were measured using an NMR analyzer (Minispec LF90II, Bruker Optics). Oxygen consumption (VO2) and food intake were measured using the Comprehensive Laboratory Monitoring System (CLAMS, Columbus Instruments), an integrated open-circuit calorimeter equipped with an optical beam activity monitoring device. Mice were individually placed into the sealed chambers (7.9" x 4" x 5") with free access to food and water. The study was carried out in an experimentation room set at 20-23 °C with 12-12 hours (6:00PM~6:00AM) dark-light cycles. The measurements were carried out continuously for 72 hours. During this time, animals were provided with food and water through the equipped feeding and drinking devices located inside the chamber. The amount of food of each animal was monitored through a precision balance attached below the chamber. VO2 in each chamber were sampled sequentially for 5 seconds in a 10 minutes interval.

3.6.15 Quantitative gas chromatography (GC) analysis of TAG

Lipids were extracted by the method of Bligh-Dyer in the presence of an internal standard (T21:0 TAG, 10 nmol/mg protein) and separated on silica gel 60-Å plates that were developed with a nonpolar acidic mobile phase (70:30:1, v/v/v, hexane/ethyl ether/acetic acid), as previously described (Liu et al., 2010; Zhou et al., 2012). Briefly, spots corresponding to TAG were visualized with 0.01% rhodamine 6G and identified with TAG standard. The bands were scraped, extracted, and treated with acidic methanol. Quantitative GC analysis of resulting FA methyl esters was conducted (Hewlett-Packard 5890 GC; Hewlett-Packard, Palo Alto, CA, USA) with a 30-m×0.32 mm Omegawax 250 column (Sigma) coupled with a flame ionization detector.

Figure 3.1 Nrg4 is enriched in brown fat
(A) Clustering analysis of genes encoding secreted proteins that are induced during brown adipocyte (BAC) differentiation and enriched in BAT. (B) qPCR analysis of Nrg4 tissue distribution using pooled RNA samples from three mice. (C) qPCR analysis of Nrg4 mRNA expression during BAC differentiation and in mature BAC and 3T3-L1 adipocytes. Data represent mean ± s.d., *p<0.05.

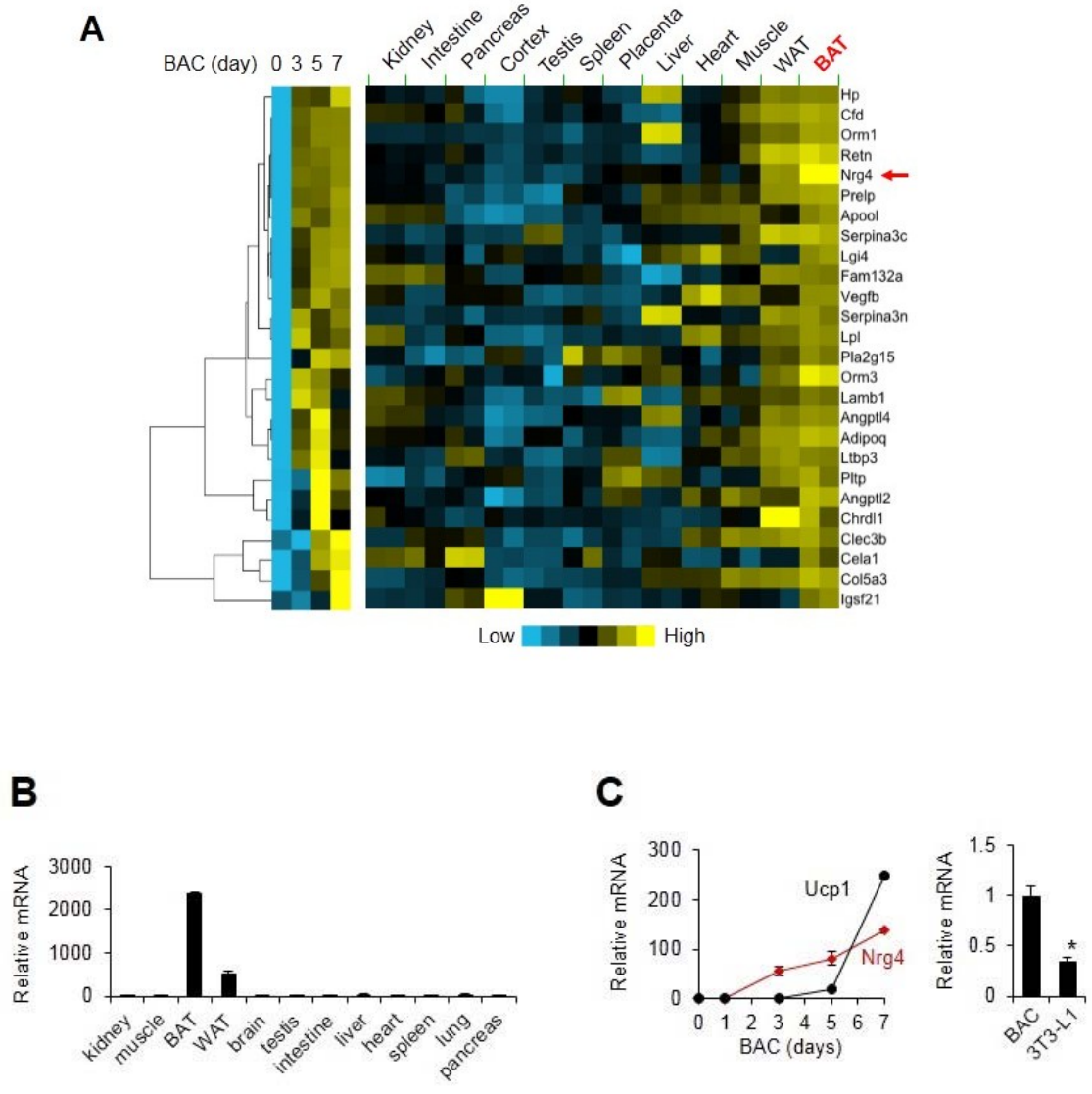

Figure 3.2 Nrg4 is a secreted protein
(A) Immunoblots of media and lysates from HEK293 cells transiently transfected with indicated constructs using anti-SEAP. (B) Stimulation of ErbB receptor phosphorylation by recombinant Nrg4. HEK293 cells transfected with different receptors were treated with GST (-) or GST-Nrg4^{Ex} (+) for 20 min. (C) Secretion of Nrg4 into culture media. Shown are immunoblots of total lysates from ErbB4-Min6 cells treated with DMEM or CM from HEK293 (left) or BAC (right) expressing vector (Vec) or Nrg4.

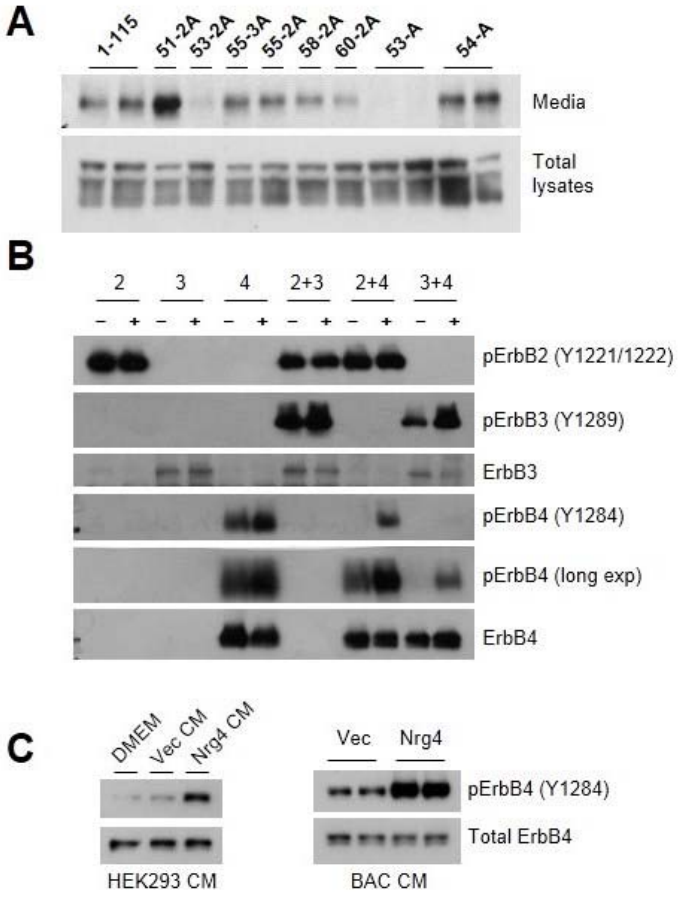

Figure 3.3 Nrg4 is dispensable for defense against cold
(A) Rectal temperature in WT (n=5) and Nrg4 KO (n=7) mice following cold exposure at 4ºC. (B) qPCR analysis of BAT gene expression in mice kept at ambient room temperature (RT; WT, n=5; KO, n=6) or following cold exposure (Cold; WT, n=5; KO, n=6) for 4 hrs. (C) H&E staining of brown fat sections from mice following cold exposure (scale bar=100 μm).

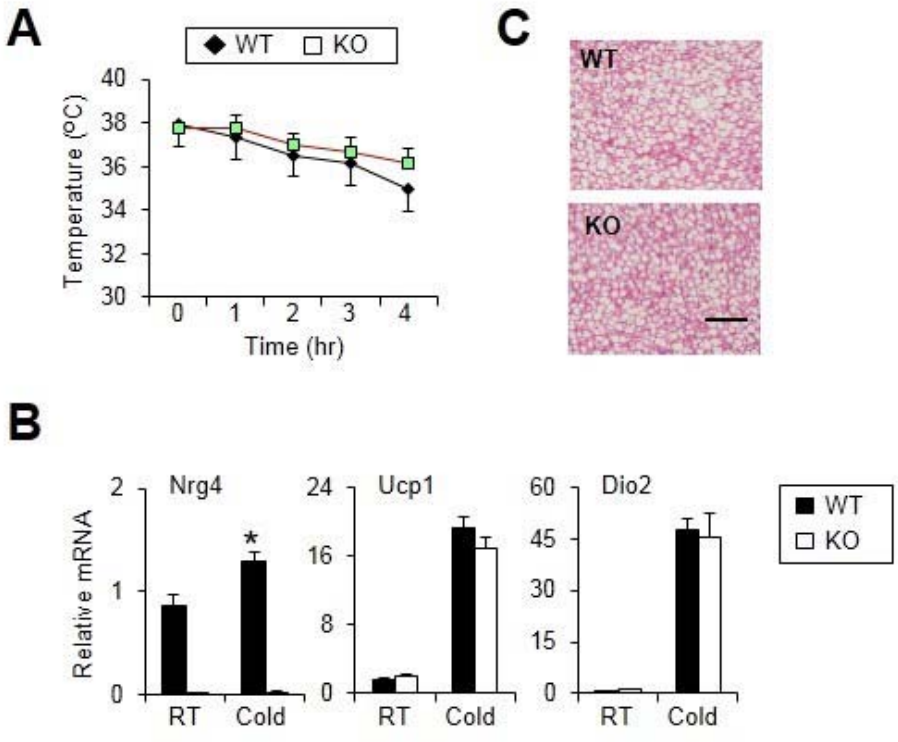

Figure 3.4 Nrg4 binds to hepatocytes
(A) Immunoblots of total lysates from ErbB4-Min6 cells treated with CM containing SEAP or SEAP-Nrg4^{Ex}. (B) Binding assay. Schematic diagrams of SEAP or SEAP-Nrg4^{Ex} fusion proteins were shown on the left. (C) SEAP-Nrg4^{Ex} binding to liver sections in the presence of excess recombinant GST or GST-Nrg4^{Ex}. (D) SEAP-Nrg4^{Ex} binding to liver sections in the presence of control CM or CM containing the extracellular domains of ErbB3 or ErbB4.

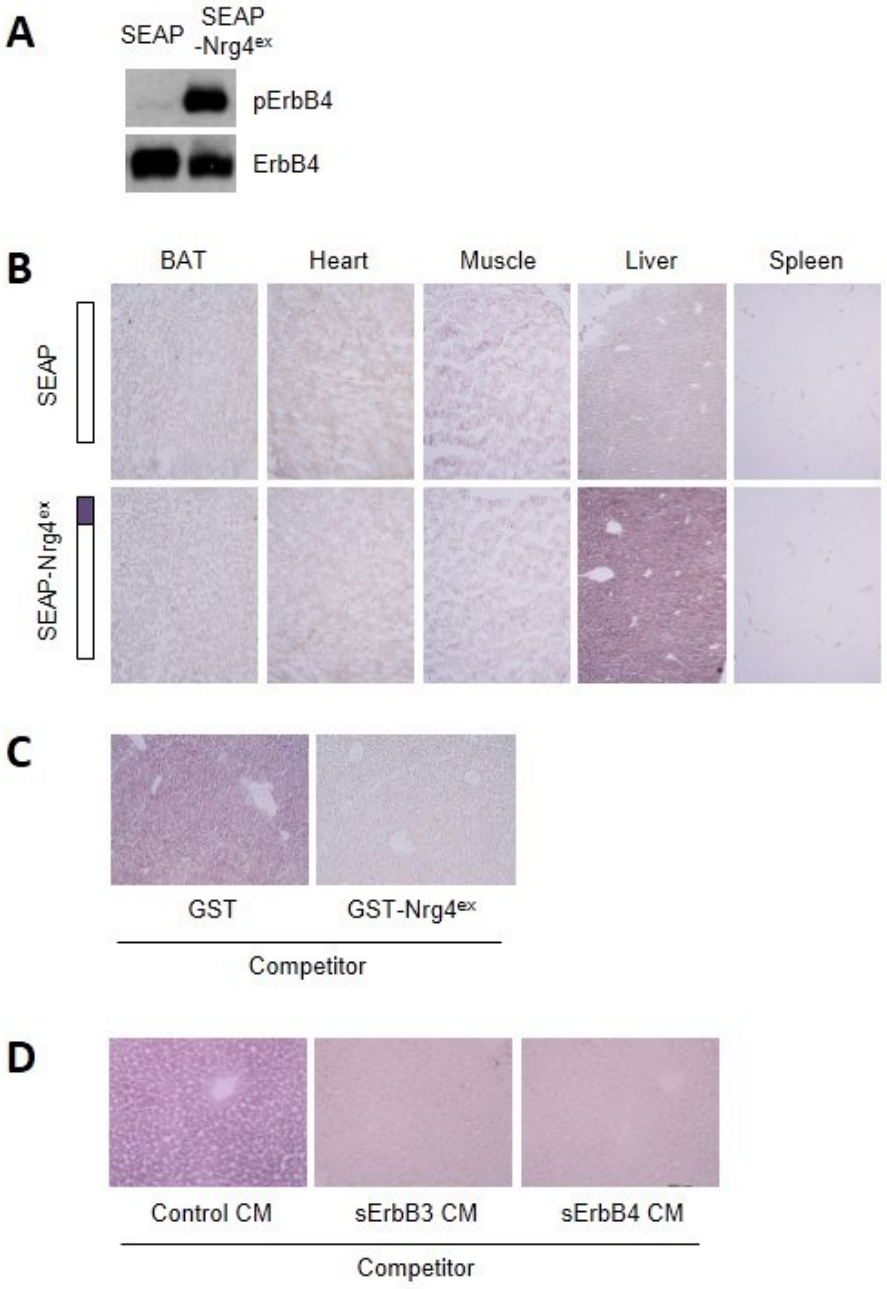

Figure 3.5 Nrg4 deficiency exacerbates diet-induced insulin resistance
(A) Body weight, adiposity, and percent lean body mass in WT (filled, n=8) and Nrg4 KO (open, n=9) mice fed chow or HFD. (B) Fed and fasted blood glucose levels in HFD-fed mice. (C) Fasted plasma insulin levels. (D) Glucose tolerance test (GTT, left) and insulin tolerance test (ITT, right) in HFD-fed WT (filled diamond, n=7) and Nrg4 KO (open square, n=7) mice. Data in A to D represent mean ± s.e.m. *p<0.05, KO vs. WT

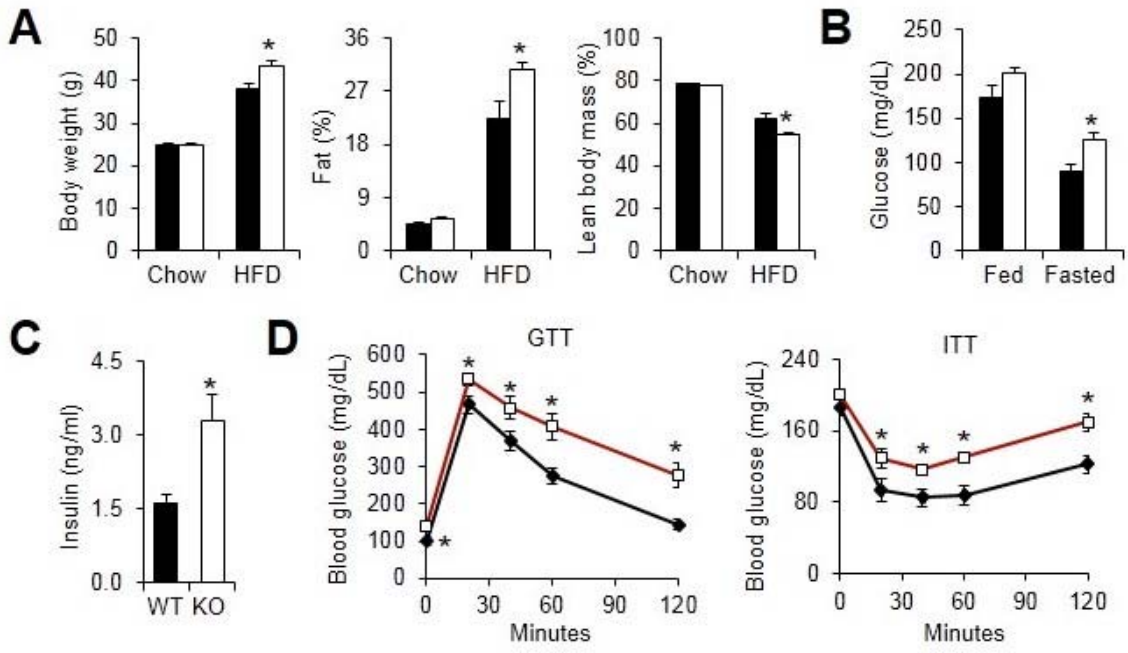

Figure 3.6 Nrg4 deficiency exacerbates diet-induced hepatic steatosis
(A) H&E staining of tissue sections (scale bar=100 μm). (B) Plasma TAG levels (top) and liver fat content (bottom) in HFD-fed WT and Nrg4 KO mice. Data represent mean ± s.e.m. *p<0.05, KO vs. WT

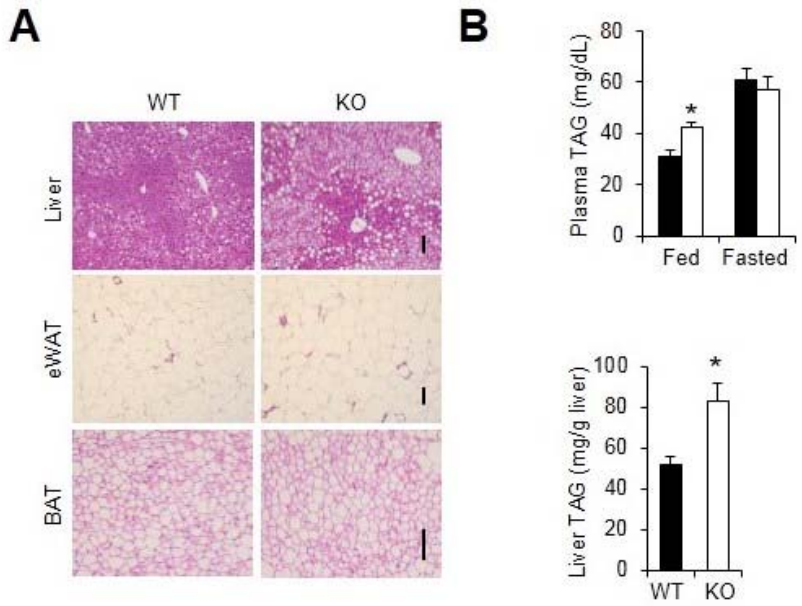

Figure 3.7 Lipogenesis is increased in liver from Nrg4 KO mice
(A) A cluster of differentially expressed genes involved in lipid metabolism. (B) qPCR analysis of hepatic gene expression in HFD-fed WT (filled, n=7) and Nrg4 KO (open, n=9) mice. Data represent mean ± s.e.m. *p<0.05, KO vs. WT. (C) Immunoblots of total liver lysates using indicated antibodies (top); pSREBP1 denotes precursor SREBP1 protein. Immunoblots of nuclear SREBP1 (nSREBP1) using liver nuclear extracts (bottom). Lamin A/C immunoblot was included as loading control.

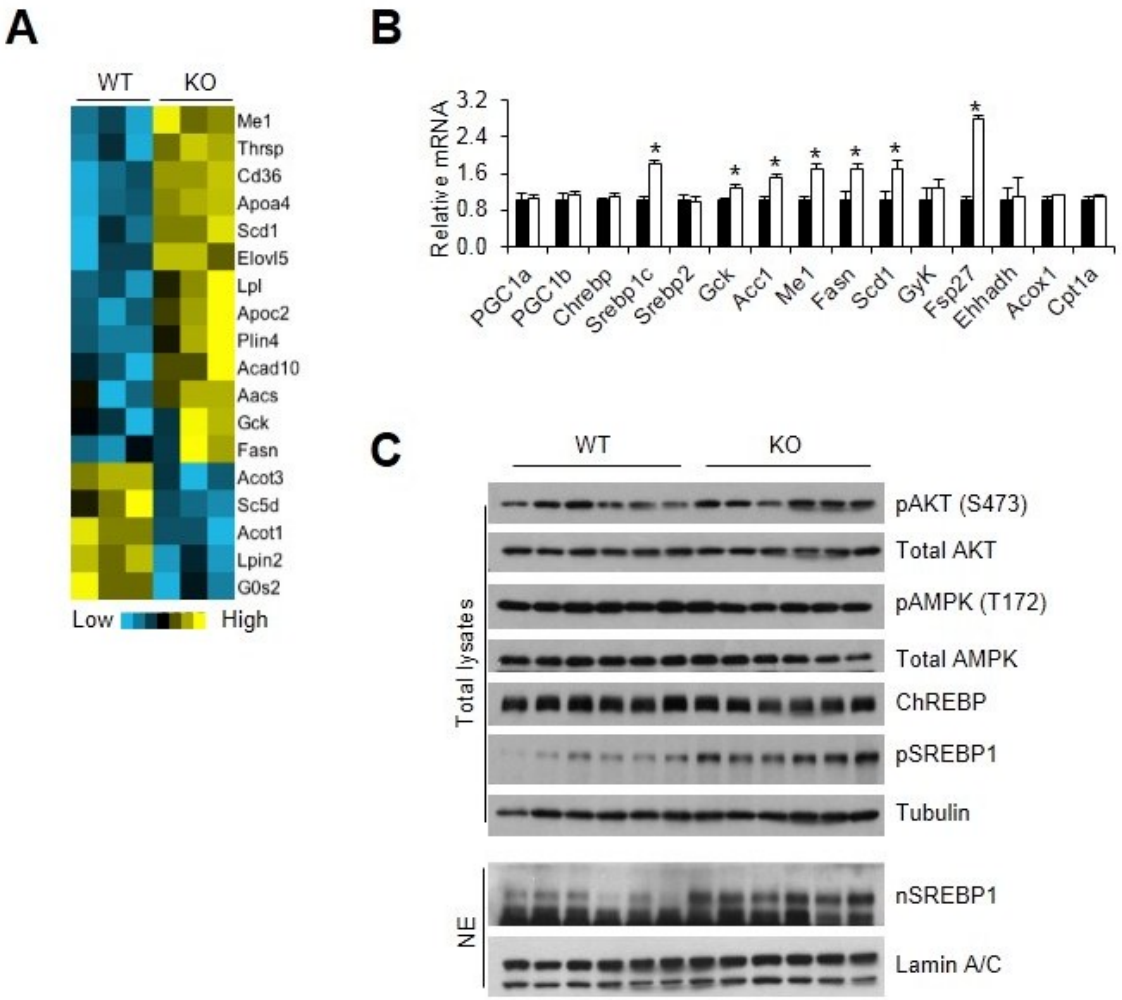

Figure 3.8 Nrg4 signaling in hepatocytes
(A) Immunoblots of hepatocytes transduced with GFP or ErbB4 adenovirus and treated with GST or different doses (2, 10, 20 μg/ml) of GST-Nrg4^{Ex}. (B) Immunoblots of hepatocytes transduced with GFP or ErbB4 adenovirus and treated for 15 min with GST or GST-Nrg4^{Ex} (10 μg/ml) in the presence of vehicle or 10 μM pan-ErbB inhibitor JNJ28871063 (JNJ). (C) Immunoblots of hepatocytes transduced with adenovirus expressing GFP, WT ErbB4, or kinase dead ErbB4 (ErbB4-KD) and treated with GST or GST-Nrg4^{Ex} for 15 min.

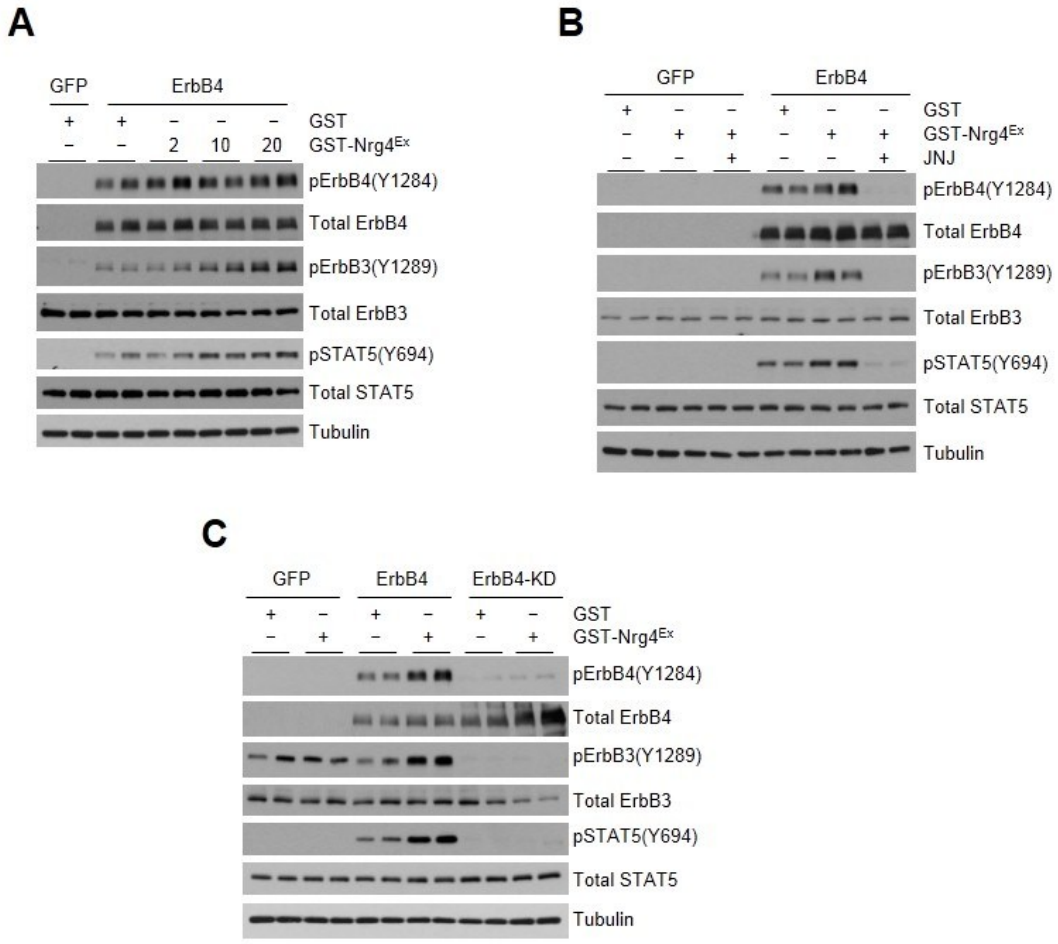

Figure 3.9 Nrg4 cell-autonomously attenuates *de novo* lipogenesis in hepatocytes
(A) qPCR analysis of gene expression in transduced primary hepatocytes treated with vehicle (DMSO) or T0901317 (5 μM) for 24 hrs in the presence of GST or GST-Nrg4^{Ex}. (B) Incorporation of ^{14}C-acetate into lipids in primary hepatocytes treated as in A. (C) Reporter gene assay in Hepa1 cells transiently transfected with 4xLXRE-luc in combination with indicated plasmids. Transfected cells were treated with DMSO or T0901317 (10 μM) for 24 hrs before luciferase assay. Data in A-C represent mean ± s.d. *p<0.05.

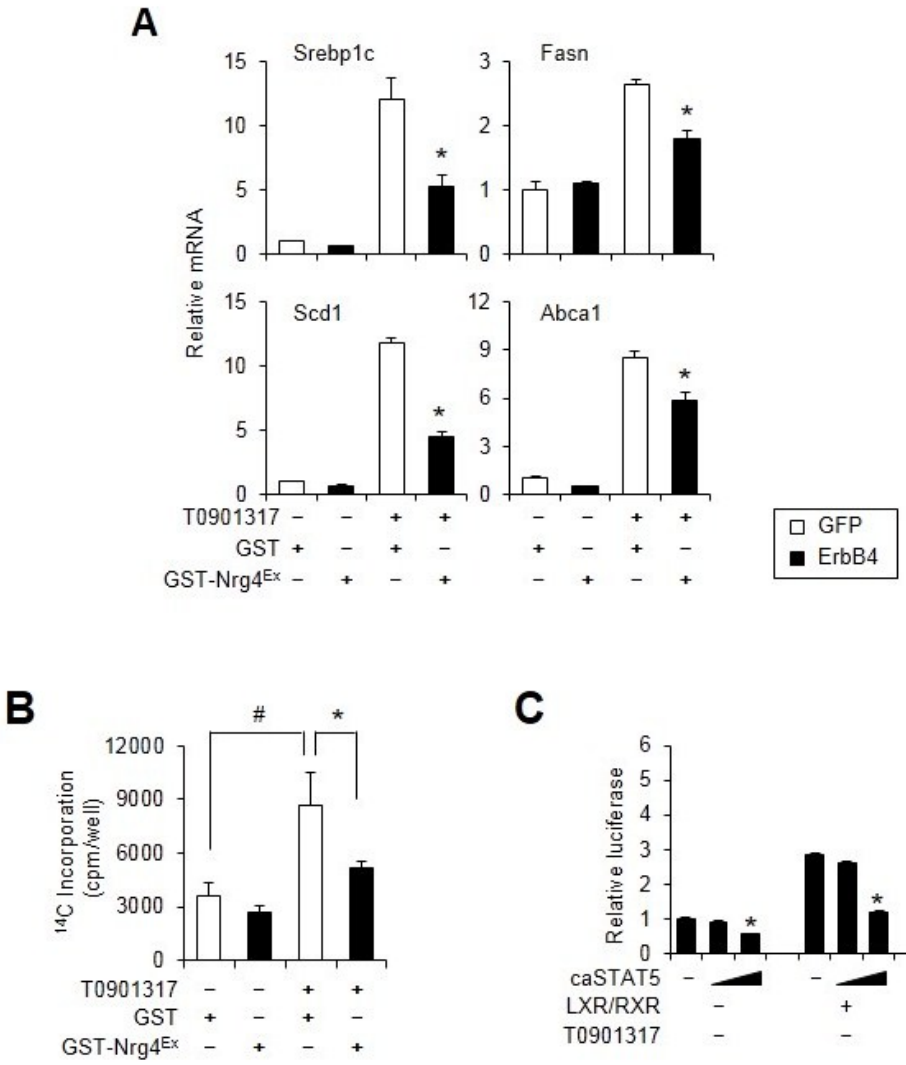

Figure 3.10 Adipose tissue Nrg4 expression is reduced in murine obesity
(A) qPCR analysis of Nrg4 mRNA expression in epididymal white fat (eWAT) and BAT from lean (open) or obese (orange) mice. For DIO, WT male mice were fed standard chow (n=5) or HFD (n=6) for three months. For genetic obesity, a group of WT (n=3) and *ob/ob* (n=4) and a separate group of WT (n=5) and *db/db* (n=6) mice were analyzed. (B) qPCR analysis of Nrg4 mRNA expression in stromal vascular fraction (SVF) and adipocyte fraction (Ad) isolated from eWAT from lean (n=3) or DIO (n=3) mice. Data in A-B represent mean ± s.e.m. *p<0.05. (C) qPCR analysis of Nrg4 mRNA expression in differentiated brown or 3T3-L1 adipocytes following treatments with vehicle (Veh), TNFα (10 ng/ml), or IL1β (40 ng/ml) for 6 hrs. Data represent mean ± s.d. from one representative study performed in triplicates. *p<0.05 vs. Veh.

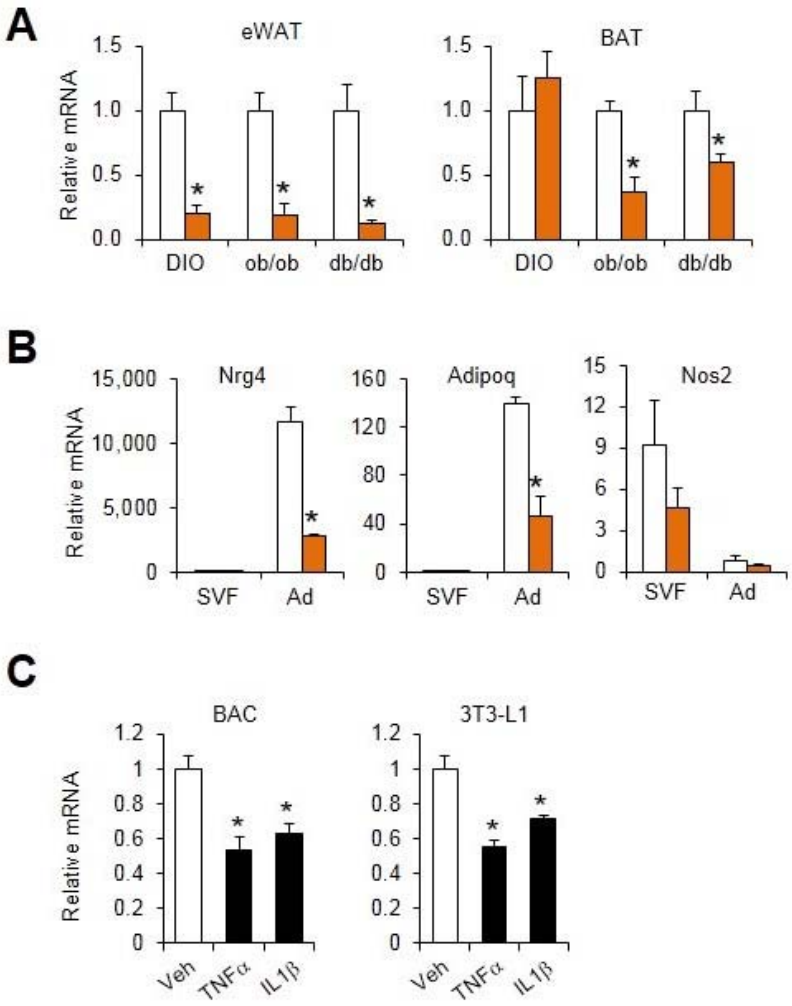

Figure 3.11 Adipose tissue Nrg4 expression is reduced in human obesity
(A) Association between relative scWAT NRG4 mRNA in humans and log HOMA-IR (left) and log percent body fat mass (right). (B) qPCR analysis of NRG4 mRNA expression in scWAT and visceral WAT from individuals with normal glucose tolerance (NGT), impaired glucose tolerance (IGT), and type 2 diabetes (T2D). Data represent mean ± s.e.m. *p<0.05 vs. NGT.

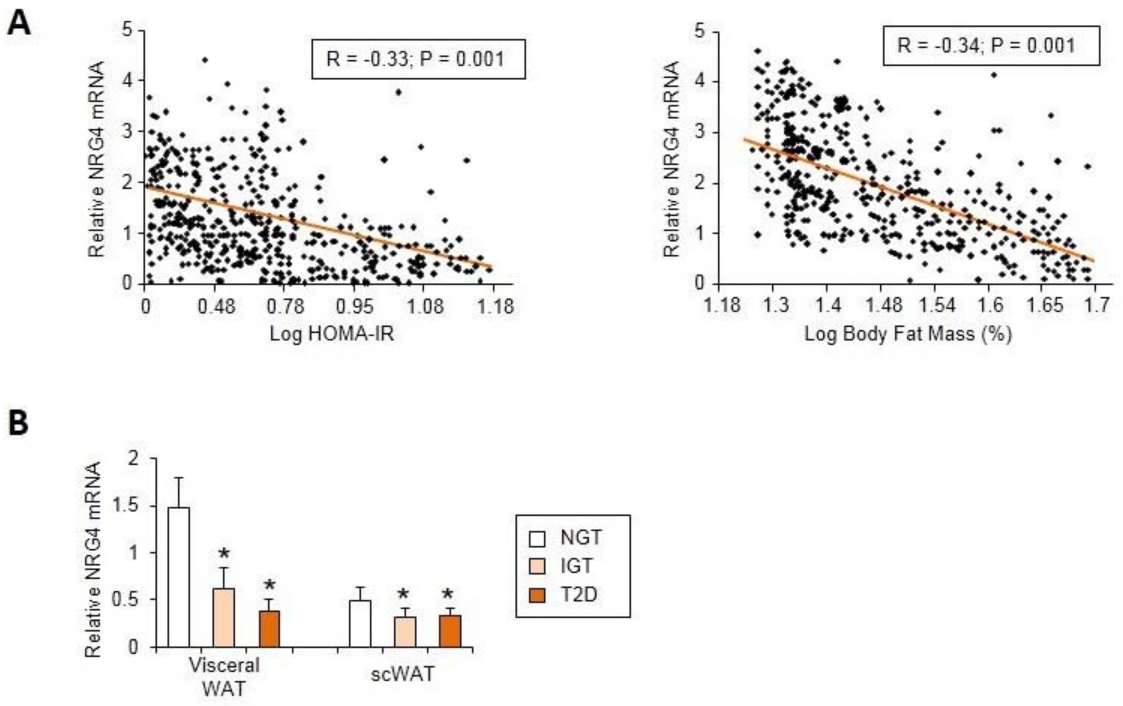

Figure 3.12 Transgenic expression of Nrg4 decreases body weight and plasma triglyceride (TAG) levels

(A) Growth curve of WT (open, n=10) and Tg (gray, n=9) mice before and after 12 weeks of HFD feeding. (B) Body weight (left), percent fat mass (middle), and percent lean body mass (right) in HFD-fed WT (open, n=8) and Tg (gray, n=8) mice. (C) Plasma TAG levels.

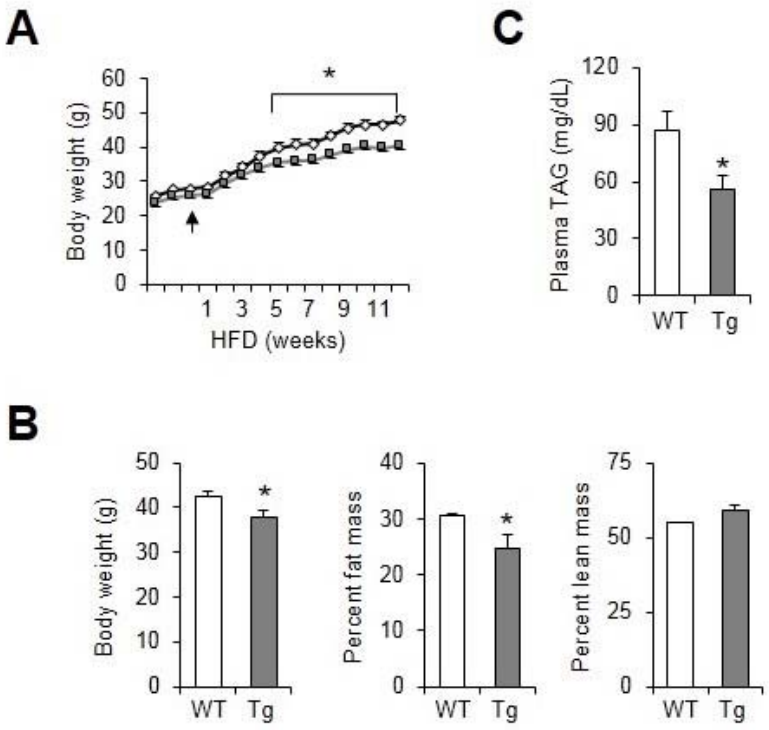

Figure 3.13 Transgenic expression of Nrg4 increases oxygen consumption of the mice
Food intake (top) and oxygen consumption rate in HFD-fed mice. VO_2 was normalized to total body weight (middle) or lean body mass (bottom).

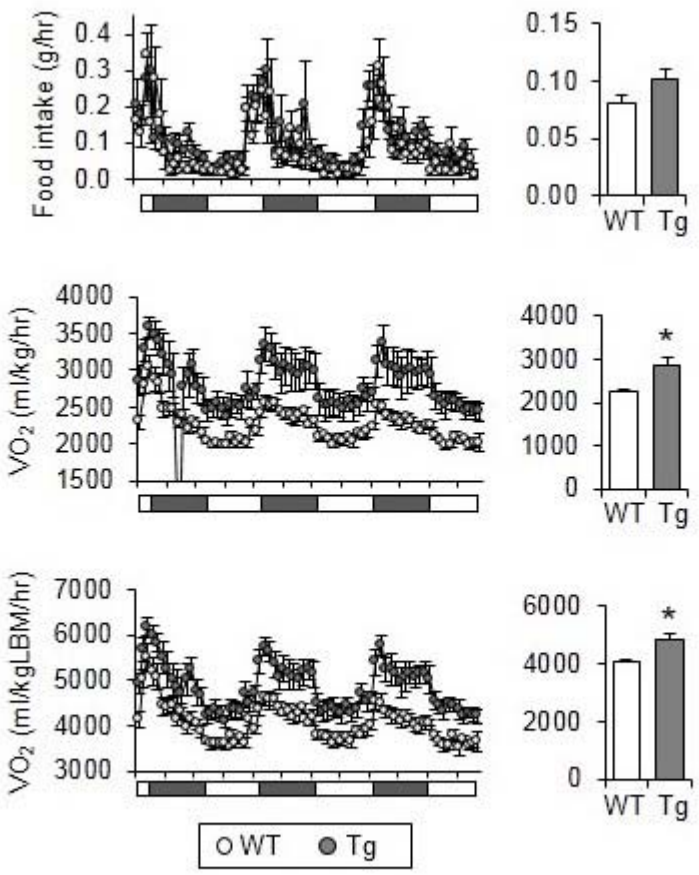

Figure 3.14 Transgenic expression of Nrg4 improves glucose and insulin tolerance in HFD fed mice

(A) Fed and fasted blood glucose (left) and fasted plasma insulin (right) levels in HFD-fed mice. (B) GTT (left) and ITT (right) in HFD-fed WT (black line, n=9) and Tg (gray line, n=8) mice. Data represent mean ± s.e.m. *p<0.05, WT vs. Tg.

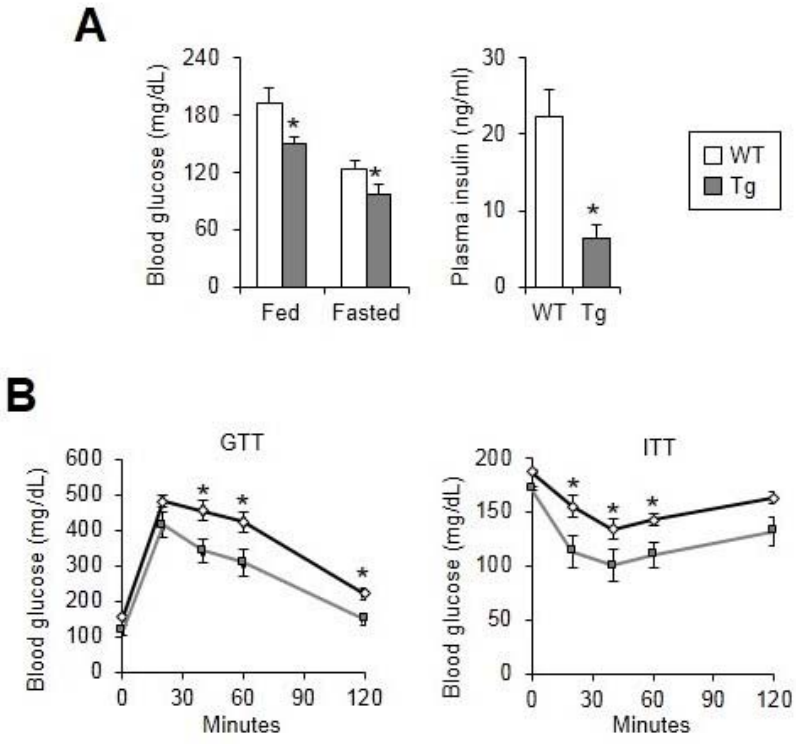

Figure 3.15 Transgenic expression of Nrg4 alleviates diet-induced fatty liver
(A) H&E staining of tissue sections (scale bar=100 μm). (B) Liver TAG content in *ad lib* HFD-fed WT (open, n=8) or Tg (gray, n=9) mice. (C) Fatty acid composition of liver triglycerides from HFD-fed mice. (D) Desaturation index of C16 and C18 fatty acids calculated from data in C. Data in B to D represent mean ± s.e.m. *p<0.05, WT vs. Tg.

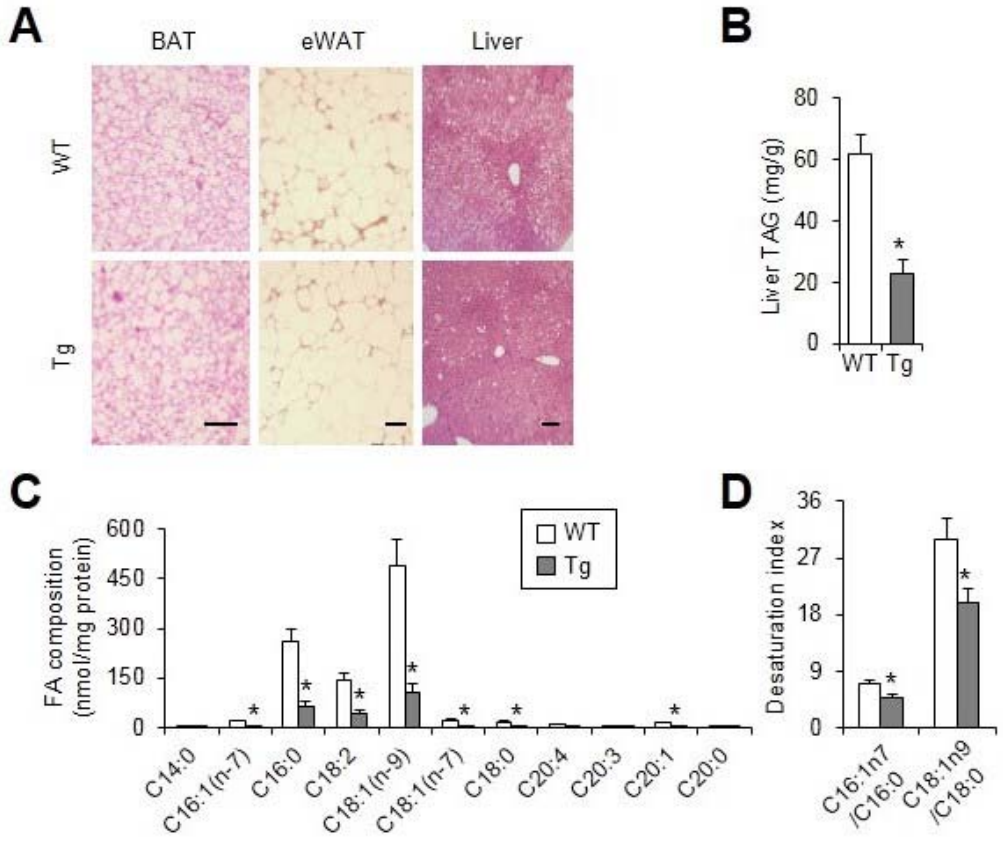

Figure 3.16 Transgenic expression of Nrg4 attenuates lipogenesis in the liver
(A) qPCR analysis of hepatic gene expression. Data represent mean ± s.e.m. *p<0.05, WT vs. Tg. (B) Immunoblots of total liver lysates (top) and nuclear extracts (bottom).

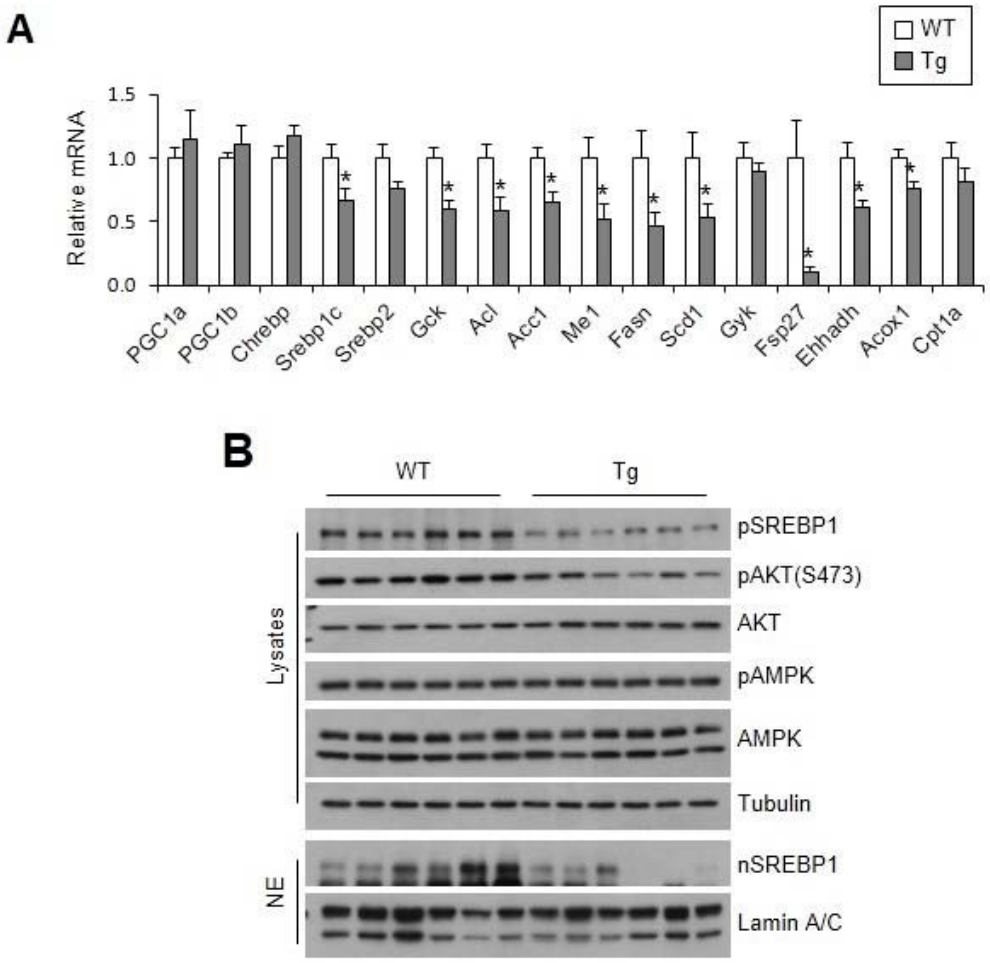

Figure 3.17 Overview of Nrg4 as a brown fat-enriched secreted protein that preserves metabolic homeostasis in diet-induced obesity
Nrg4 binds to the liver and attenuates hepatic lipogenic signaling through ErbB3 and ErbB4.

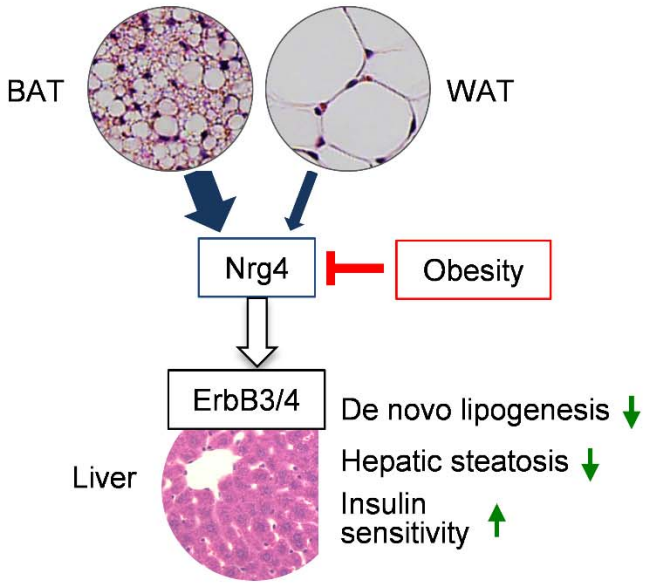

Figure S3.1 Nrg4 is highly conserved among species
(A) Alignment of Nrg4 amino acid sequences. The transmembrane (TM) and EGF-like (EGFL) domains and three disulfide bonds are indicated. (B) Percent amino acid identity between amino acids 1-62 of human Nrg4 and Nrg4 from other species.

A

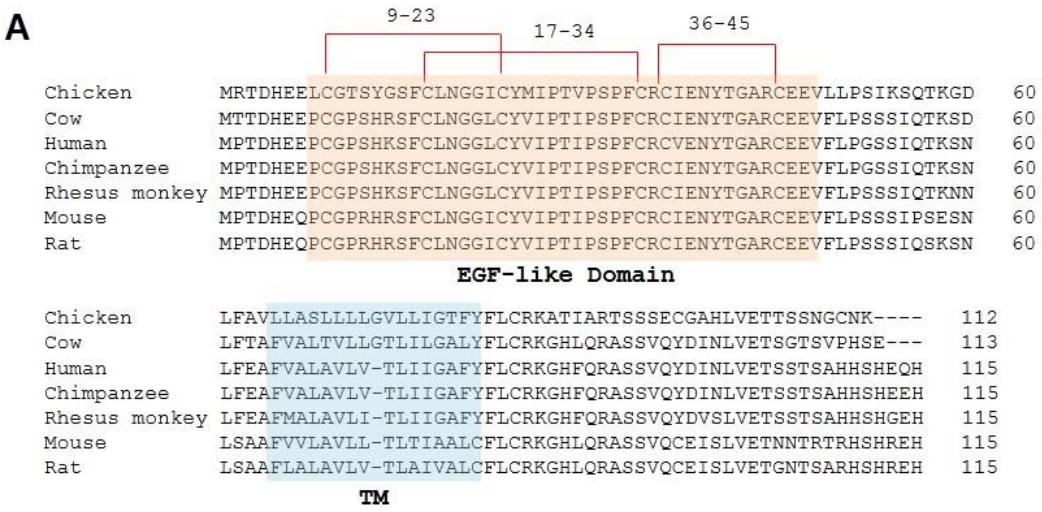

B

	Identity (vs. human Nrg4 a.a. 1-62)
Chicken	44/62 *(71.0%)*
Cow	57/62 *(91.9%)*
Chimpanzee	61/62 *(98.4%)*
Rhesus monkey	58/62 *(93.5%)*
Mouse	52/62 *(83.9%)*
Rat	54/62 *(87.1%)*

Figure S3.2 Association between NRG4 and obesity and hepatic steatosis in humans
Association between relative scWAT NRG4 mRNA and log body mass index (top) and log percent liver fat content (bottom) in humans. The cohort was the same as shown in Figure 3.11.

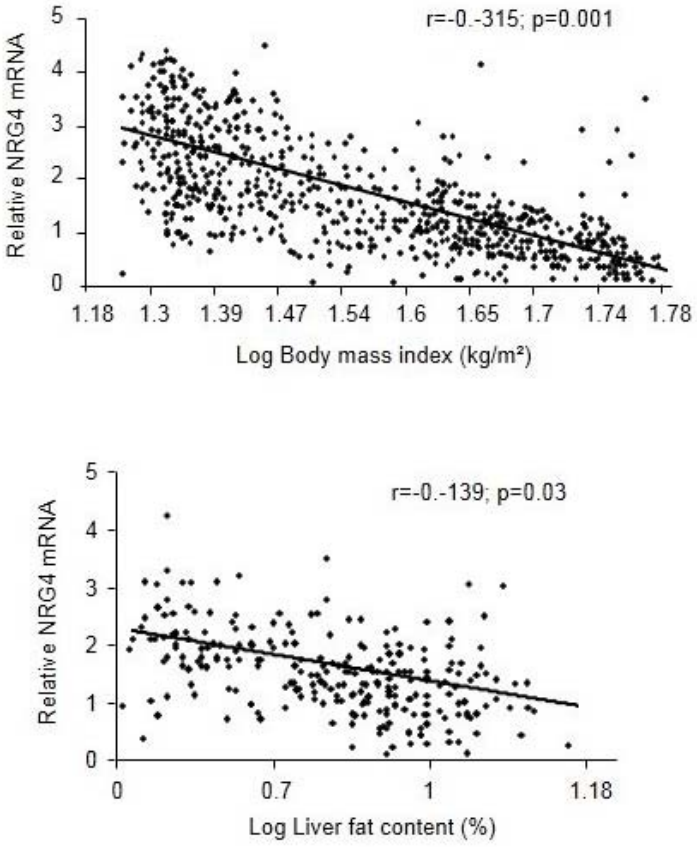

3.7 Refrences

Angelin, B., Larsson, T.E., and Rudling, M. (2012). Circulating fibroblast growth factors as metabolic regulators--a critical appraisal. Cell metabolism *16*, 693-705.

Bartelt, A., Bruns, O.T., Reimer, R., Hohenberg, H., Ittrich, H., Peldschus, K., Kaul, M.G., Tromsdorf, U.I., Weller, H., Waurisch, C., *et al.* (2011). Brown adipose tissue activity controls triglyceride clearance. Nature medicine *17*, 200-205.

Birchmeier, C. (2009). ErbB receptors and the development of the nervous system. Experimental cell research *315*, 611-618.

Bublil, E.M., and Yarden, Y. (2007). The EGF receptor family: spearheading a merger of signaling and therapeutics. Current opinion in cell biology *19*, 124-134.

Calfee-Mason, K.G., Spear, B.T., and Glauert, H.P. (2002). Vitamin E inhibits hepatic NF-kappaB activation in rats administered the hepatic tumor promoter, phenobarbital. The Journal of nutrition *132*, 3178-3185.

Cannon, B., and Nedergaard, J. (2004). Brown adipose tissue: function and physiological significance. Physiological reviews *84*, 277-359.

Carver, R.S., Stevenson, M.C., Scheving, L.A., and Russell, W.E. (2002). Diverse expression of ErbB receptor proteins during rat liver development and regeneration. Gastroenterology *123*, 2017-2027.

Chen, Y., Zhang, Y., Yin, Y., Gao, G., Li, S., Jiang, Y., Gu, X., and Luo, J. (2005). SPD--a web-based secreted protein database. Nucleic acids research *33*, D169-173.

Chowdhury, M.H., and Agius, L. (1987). Epidermal growth factor counteracts the glycogenic effect of insulin in parenchymal hepatocyte cultures. The Biochemical journal *247*, 307-314.

Cypess, A.M., Lehman, S., Williams, G., Tal, I., Rodman, D., Goldfine, A.B., Kuo, F.C., Palmer, E.L., Tseng, Y.H., Doria, A., *et al.* (2009). Identification and importance of brown adipose tissue in adult humans. The New England journal of medicine *360*, 1509-1517.

Cypess, A.M., White, A.P., Vernochet, C., Schulz, T.J., Xue, R., Sass, C.A., Huang, T.L., Roberts-Toler, C., Weiner, L.S., Sze, C., *et al.* (2013). Anatomical localization, gene expression profiling and functional characterization of adult human neck brown fat. Nature medicine *19*, 635-639.

Enerback, S. (2010). Human brown adipose tissue. Cell metabolism *11*, 248-252.

Enerback, S., Jacobsson, A., Simpson, E.M., Guerra, C., Yamashita, H., Harper, M.E., and Kozak, L.P. (1997). Mice lacking mitochondrial uncoupling protein are cold-sensitive but not obese. Nature *387*, 90-94.

Falls, D.L. (2003). Neuregulins and the neuromuscular system: 10 years of answers and questions. Journal of neurocytology *32*, 619-647.

Feldmann, H.M., Golozoubova, V., Cannon, B., and Nedergaard, J. (2009). UCP1 ablation induces obesity and abolishes diet-induced thermogenesis in mice exempt from thermal stress by living at thermoneutrality. Cell metabolism *9*, 203-209.

Fukatsu, Y., Noguchi, T., Hosooka, T., Ogura, T., Kotani, K., Abe, T., Shibakusa, T., Inoue, K., Sakai, M., Tobimatsu, K., *et al.* (2009). Muscle-specific overexpression of heparin-binding epidermal growth factor-like growth factor increases peripheral glucose disposal and insulin sensitivity. Endocrinology *150*, 2683-2691.

Gregor, M.F., and Hotamisligil, G.S. (2011). Inflammatory mechanisms in obesity. Annual review of immunology *29*, 415-445.

Guma, A., Martinez-Redondo, V., Lopez-Soldado, I., Canto, C., and Zorzano, A. (2010). Emerging role of neuregulin as a modulator of muscle metabolism. American journal of physiology Endocrinology and metabolism *298*, E742-750.

Harari, D., Tzahar, E., Romano, J., Shelly, M., Pierce, J.H., Andrews, G.C., and Yarden, Y. (1999). Neuregulin-4: a novel growth factor that acts through the ErbB-4 receptor tyrosine kinase. Oncogene *18*, 2681-2689.

Hauton, D., Richards, S.B., and Egginton, S. (2006). The role of the liver in lipid metabolism during cold acclimation in non-hibernator rodents. Comparative biochemistry and physiology Part B, Biochemistry & molecular biology *144*, 372-381.

Hayes, N.V., Newsam, R.J., Baines, A.J., and Gullick, W.J. (2008). Characterization of the cell membrane-associated products of the Neuregulin 4 gene. Oncogene *27*, 715-720.

Holbro, T., and Hynes, N.E. (2004). ErbB receptors: directing key signaling networks throughout life. Annual review of pharmacology and toxicology *44*, 195-217.

Horton, J.D., Goldstein, J.L., and Brown, M.S. (2002). SREBPs: activators of the complete program of cholesterol and fatty acid synthesis in the liver. The Journal of clinical investigation *109*, 1125-1131.

Hotamisligil, G.S., Shargill, N.S., and Spiegelman, B.M. (1993). Adipose expression of tumor necrosis factor-alpha: direct role in obesity-linked insulin resistance. Science *259*, 87-91.

Iossa, S., Barletta, A., and Liverini, G. (1994). Different effects of cold exposure and cold acclimation on rat liver mitochondrial fatty acid oxidation and ketone bodies production. The International journal of biochemistry *26*, 425-431.

Jespersen, N.Z., Larsen, T.J., Peijs, L., Daugaard, S., Homoe, P., Loft, A., de Jong, J., Mathur, N., Cannon, B., Nedergaard, J., *et al.* (2013). A classical brown adipose tissue mRNA signature partly overlaps with brite in the supraclavicular region of adult humans. Cell metabolism *17*, 798-805.

Jones, F.E., Welte, T., Fu, X.Y., and Stern, D.F. (1999). ErbB4 signaling in the mammary gland is required for lobuloalveolar development and Stat5 activation during lactation. The Journal of cell biology *147*, 77-88.

Kadowaki, T., Yamauchi, T., Kubota, N., Hara, K., Ueki, K., and Tobe, K. (2006). Adiponectin and adiponectin receptors in insulin resistance, diabetes, and the metabolic syndrome. The Journal of clinical investigation *116*, 1784-1792.

Karsenty, G., and Ferron, M. (2012). The contribution of bone to whole-organism physiology. Nature *481*, 314-320.

Kay, R., Barton, C., Ratcliffe, L., Matharoo-Ball, B., Brown, P., Roberts, J., Teale, P., and Creaser, C. (2008). Enrichment of low molecular weight serum proteins using acetonitrile precipitation for mass spectrometry based proteomic analysis. Rapid Commun Mass Spectrom *22*, 3255-3260.

Klein, J., Fasshauer, M., Klein, H.H., Benito, M., and Kahn, C.R. (2002). Novel adipocyte lines from brown fat: a model system for the study of differentiation, energy metabolism, and insulin action. BioEssays : news and reviews in molecular, cellular and developmental biology *24*, 382-388.

Knebel, B., Haas, J., Hartwig, S., Jacob, S., Kollmer, C., Nitzgen, U., Muller-Wieland, D., and Kotzka, J. (2012). Liver-specific expression of transcriptionally active SREBP-1c is associated with fatty liver and increased visceral fat mass. PLoS One *7*, e31812.

Kohjima, M., Higuchi, N., Kato, M., Kotoh, K., Yoshimoto, T., Fujino, T., Yada, M., Yada, R., Harada, N., Enjoji, M., *et al.* (2008). SREBP-1c, regulated by the insulin and AMPK signaling pathways, plays a role in nonalcoholic fatty liver disease. International journal of molecular medicine *21*, 507-511.

Kozak, L.P., and Harper, M.E. (2000). Mitochondrial uncoupling proteins in energy expenditure. Annual review of nutrition *20*, 339-363.

Leahy, D.J., Dann, C.E., 3rd, Longo, P., Perman, B., and Ramyar, K.X. (2000). A mammalian expression vector for expression and purification of secreted proteins for structural studies. Protein Expr Purif *20*, 500-506.

Li, S., Liu, C., Li, N., Hao, T., Han, T., Hill, D.E., Vidal, M., and Lin, J.D. (2008a). Genome-wide coactivation analysis of PGC-1alpha identifies BAF60a as a regulator of hepatic lipid metabolism. Cell Metab *8*, 105-117.

Li, S., Liu, C., Li, N., Hao, T., Han, T., Hill, D.E., Vidal, M., and Lin, J.D. (2008b). Genome-wide coactivation analysis of PGC-1alpha identifies BAF60a as a regulator of hepatic lipid metabolism. Cell metabolism *8*, 105-117.

Lin, J., and Linzer, D.I. (1999). Induction of megakaryocyte differentiation by a novel pregnancy-specific hormone. The Journal of biological chemistry *274*, 21485-21489.

Lin, J., Wu, P.H., Tarr, P.T., Lindenberg, K.S., St-Pierre, J., Zhang, C.Y., Mootha, V.K., Jager, S., Vianna, C.R., Reznick, R.M., *et al.* (2004). Defects in adaptive energy metabolism with CNS-linked hyperactivity in PGC-1alpha null mice. Cell *119*, 121-135.

Liu, X., Rossmeisl, M., McClaine, J., Riachi, M., Harper, M.E., and Kozak, L.P. (2003). Paradoxical resistance to diet-induced obesity in UCP1-deficient mice. The Journal of clinical investigation *111*, 399-407.

Liu, Y., Zhou, D., Abumrad, N.A., and Su, X. (2010). ADP-ribosylation factor 6 modulates adrenergic stimulated lipolysis in adipocytes. American journal of physiology Cell physiology *298*, C921-928.

Lowell, B.B., V, S.S., Hamann, A., Lawitts, J.A., Himms-Hagen, J., Boyer, B.B., Kozak, L.P., and Flier, J.S. (1993). Development of obesity in transgenic mice after genetic ablation of brown adipose tissue. Nature *366*, 740-742.

Molusky, M.M., Li, S., Ma, D., Yu, L., and Lin, J.D. (2012). Ubiquitin-specific protease 2 regulates hepatic gluconeogenesis and diurnal glucose metabolism through 11beta-hydroxysteroid dehydrogenase 1. Diabetes *61*, 1025-1035.

Moon, Y.A., Liang, G., Xie, X., Frank-Kamenetsky, M., Fitzgerald, K., Koteliansky, V., Brown, M.S., Goldstein, J.L., and Horton, J.D. (2012). The Scap/SREBP pathway is essential for developing diabetic fatty liver and carbohydrate-induced hypertriglyceridemia in animals. Cell metabolism *15*, 240-246.

Muller, H., Dai, G., and Soares, M.J. (1998). Placental lactogen-I (PL-I) target tissues identified with an alkaline phosphatase-PL-I fusion protein. The journal of histochemistry and cytochemistry : official journal of the Histochemistry Society *46*, 737-743.

Nedergaard, J., Bengtsson, T., and Cannon, B. (2007). Unexpected evidence for active brown adipose tissue in adult humans. American journal of physiology Endocrinology and metabolism *293*, E444-452.

Nedergaard, J., and Cannon, B. (2010). The changed metabolic world with human brown adipose tissue: therapeutic visions. Cell metabolism *11*, 268-272.

Odegaard, J.I., and Chawla, A. (2013). Pleiotropic actions of insulin resistance and inflammation in metabolic homeostasis. Science *339*, 172-177.

Odiete, O., Hill, M.F., and Sawyer, D.B. (2012). Neuregulin in cardiovascular development and disease. Circulation research *111*, 1376-1385.

Olayioye, M.A., Beuvink, I., Horsch, K., Daly, J.M., and Hynes, N.E. (1999). ErbB receptor-induced activation of stat transcription factors is mediated by Src tyrosine kinases. The Journal of biological chemistry *274*, 17209-17218.

Osborn, O., and Olefsky, J.M. (2012). The cellular and signaling networks linking the immune system and metabolism in disease. Nature medicine *18*, 363-374.

Pedersen, B.K., and Febbraio, M.A. (2012). Muscles, exercise and obesity: skeletal muscle as a secretory organ. Nature reviews Endocrinology *8*, 457-465.

Petrovic, N., Walden, T.B., Shabalina, I.G., Timmons, J.A., Cannon, B., and Nedergaard, J. (2010). Chronic peroxisome proliferator-activated receptor gamma (PPARgamma) activation of epididymally derived white adipocyte cultures reveals a population of thermogenically competent, UCP1-containing adipocytes molecularly distinct from classic brown adipocytes. The Journal of biological chemistry *285*, 7153-7164.

Potthoff, M.J., Kliewer, S.A., and Mangelsdorf, D.J. (2012). Endocrine fibroblast growth factors 15/19 and 21: from feast to famine. Genes & development *26*, 312-324.

Repa, J.J., Liang, G., Ou, J., Bashmakov, Y., Lobaccaro, J.M., Shimomura, I., Shan, B., Brown, M.S., Goldstein, J.L., and Mangelsdorf, D.J. (2000). Regulation of mouse sterol regulatory element-binding protein-1c gene (SREBP-1c) by oxysterol receptors, LXRalpha and LXRbeta. Genes & development *14*, 2819-2830.

Schneider, M.R., and Wolf, E. (2009). The epidermal growth factor receptor ligands at a glance. Journal of cellular physiology *218*, 460-466.

Schultz, J.R., Tu, H., Luk, A., Repa, J.J., Medina, J.C., Li, L., Schwendner, S., Wang, S., Thoolen, M., Mangelsdorf, D.J., *et al.* (2000). Role of LXRs in control of lipogenesis. Genes & development *14*, 2831-2838.

Seale, P., Bjork, B., Yang, W., Kajimura, S., Chin, S., Kuang, S., Scime, A., Devarakonda, S., Conroe, H.M., Erdjument-Bromage, H., *et al.* (2008). PRDM16 controls a brown fat/skeletal muscle switch. Nature *454*, 961-967.

Shimano, H., Horton, J.D., Shimomura, I., Hammer, R.E., Brown, M.S., and Goldstein, J.L. (1997). Isoform 1c of sterol regulatory element binding protein is less active than isoform 1a in livers of transgenic mice and in cultured cells. The Journal of clinical investigation *99*, 846-854.

Shimomura, I., Bashmakov, Y., and Horton, J.D. (1999). Increased levels of nuclear SREBP-1c associated with fatty livers in two mouse models of diabetes mellitus. The Journal of biological chemistry *274*, 30028-30032.

Stocklin, E., Wissler, M., Gouilleux, F., and Groner, B. (1996). Functional interactions between Stat5 and the glucocorticoid receptor. Nature *383*, 726-728.

Suarez, E., Bach, D., Cadefau, J., Palacin, M., Zorzano, A., and Guma, A. (2001). A novel role of neuregulin in skeletal muscle. Neuregulin stimulates glucose uptake, glucose transporter translocation, and transporter expression in muscle cells. The Journal of biological chemistry *276*, 18257-18264.

Tang, J.J., Li, J.G., Qi, W., Qiu, W.W., Li, P.S., Li, B.L., and Song, B.L. (2011). Inhibition of SREBP by a small molecule, betulin, improves hyperlipidemia and insulin resistance and reduces atherosclerotic plaques. Cell metabolism *13*, 44-56.

Trujillo, M.E., and Scherer, P.E. (2006). Adipose tissue-derived factors: impact on health and disease. Endocrine reviews *27*, 762-778.

van der Lans, A.A., Hoeks, J., Brans, B., Vijgen, G.H., Visser, M.G., Vosselman, M.J., Hansen, J., Jorgensen, J.A., Wu, J., Mottaghy, F.M., *et al.* (2013). Cold acclimation recruits human brown fat and increases nonshivering thermogenesis. The Journal of clinical investigation *123*, 3395-3403.

van Marken Lichtenbelt, W.D., Vanhommerig, J.W., Smulders, N.M., Drossaerts, J.M., Kemerink, G.J., Bouvy, N.D., Schrauwen, P., and Teule, G.J. (2009). Cold-activated brown adipose tissue in healthy men. The New England journal of medicine *360*, 1500-1508.

Virtanen, K.A., Lidell, M.E., Orava, J., Heglind, M., Westergren, R., Niemi, T., Taittonen, M., Laine, J., Savisto, N.J., Enerback, S., *et al.* (2009). Functional brown adipose tissue in healthy adults. The New England journal of medicine *360*, 1518-1525.

Waki, H., and Tontonoz, P. (2007). Endocrine functions of adipose tissue. Annual review of pathology *2*, 31-56.

Wu, J., Bostrom, P., Sparks, L.M., Ye, L., Choi, J.H., Giang, A.H., Khandekar, M., Virtanen, K.A., Nuutila, P., Schaart, G., *et al.* (2012). Beige adipocytes are a distinct type of thermogenic fat cell in mouse and human. Cell *150*, 366-376.

Yoneshiro, T., Aita, S., Matsushita, M., Kayahara, T., Kameya, T., Kawai, Y., Iwanaga, T., and Saito, M. (2013). Recruited brown adipose tissue as an antiobesity agent in humans. The Journal of clinical investigation *123*, 3404-3408.

Zhou, D., Samovski, D., Okunade, A.L., Stahl, P.D., Abumrad, N.A., and Su, X. (2012). CD36 level and trafficking are determinants of lipolysis in adipocytes. FASEB journal : official publication of the Federation of American Societies for Experimental Biology *26*, 4733-4742.